THE ASTROPHYSICAL JOURNAL SUPPLEMENT SERIES, 64:269–304, 1987 May

COSMIC-RAY PROPAGATION IN THE GALAXY AND IN THE HELIOSPHERE: THE PATH-LENGTH DISTRIBUTION AT LOW ENERGY

M. GARCIA-MUNOZ AND J. A. SIMPSON[1]
Enrico Fermi Institute, University of Chicago
T. G. GUZIK AND J. P. WEFEL
Department of Physics and Astronomy, Louisiana State University, Baton Rouge
AND
S. H. MARGOLIS[2]
Department of Physics, Washington University, St. Louis
Received 1986 August 25; accepted 1986 November 4

ABSTRACT

A compilation of data from measurements carried out mostly at times of solar minimum modulation and including University of Chicago data from the *IMP 8* satellite at low energy and a collection of data at higher energies has been used to study the energy dependence of secondary-to-primary ratios in Galactic cosmic rays. The data are compared with the results of a fully energy-dependent propagation calculation using the weighted-slab technique in Galactic propagation and a spherically symmetric model of solar modulation in heliospheric propagation. The detailed description of the propagation model and the input parameters is given in the Appendix. From the analysis of the B/C ratio, which is the best-measured secondary-to-primary ratio, it is concluded that the mean free path in Galactic propagation must be fully energy-dependent, with the mean of an exponential path-length distribution increasing with increasing energy below 1 GeV per nucleon and decreasing with increasing energy above 1 GeV per nucleon. Such behavior is consistent with dynamic halo models for the Galaxy, but the detailed fit requires a large velocity for the Galactic wind (≥ 20 km s^{-1}). This energy dependence sets limits on the nature of cosmic-ray diffusion and, at low energies, indicates that diffusion is not the controlling process. The sub-Fe/Fe ratio is sensitive to the relative abundance of short path lengths in the path-length distribution, and simultaneous analysis of both B/C and sub-Fe/Fe reveals that the path-length distribution is not purely exponential but is depleted in short path lengths at low energies. This depletion is shown to be energy-dependent, being largest at low energies and decreasing with increasing energy. This result may be indicative of matter traversed in the vicinity of the cosmic-ray source regions before Galactic propagation. It is seen that at low energies the predominant factor limiting the accuracy in the determination of the cosmic-ray path length is the scarcity of precisely measured cross sections for nuclear fragmentation.

Subject headings: cosmic rays: abundances — particle acceleration

I. INTRODUCTION

The analysis and interpretation of the elemental and isotopic composition and energy spectra of the cosmic-ray nuclei which reach the solar system provide information on the sources and acceleration of cosmic rays, and their propagation through interstellar matter and magnetic fields. A major physical characteristic modifying both the composition and the spectra is the distribution of path lengths of matter traversed by the nuclei between their sources and the observer. This path-length distribution (PLD) determines the relative amounts of nuclear fragmentation and radioactive decay. Therefore, propagation models which satisfy the observational constraints of both the cosmic rays and the interstellar medium are central to reaching an understanding of the origin of the cosmic radiation.

The present paper studies the energy dependence of the path-length distribution of cosmic rays at low energies, below relativistic velocities, and its implications for models of cosmic-ray confinement and propagation in the Galaxy and Galactic halo, including the effects of a possible Galactic wind. This study uses satellite measurements in the interplanetary medium as well as recent, new measurements of nuclear cross sections, and leads to a description of cosmic-ray propagation in terms of an energy-dependent path-length distribution.

The information on the interstellar propagation of cosmic rays began with the discovery that the cosmic radiation contains nuclei heavier than hydrogen, and that the relative abundances of some cosmic-ray elements, in particular those of the "light" (L) elements Li, Be, and B, were far in excess of their solar system abundances (Freier *et al.* 1948; Bradt and Peters 1948). These observed excesses are produced in spallation reactions resulting from the interaction of the propagated cosmic-ray nuclei which originate in the sources (primary

[1]Also Department of Physics; John Simon Guggenheim Fellow, 1985.
[2]Present address: The Aerospace Corporation, Los Angeles, California.

cosmic rays) with interstellar matter, and are called secondary cosmic rays. Cosmic-ray Li, Be, and B result from the spallation of mainly the cosmic-ray "medium" (M) elements C, N, and O. If all cosmic-ray nuclei are assumed to traverse the same amount of interstellar matter, the observed L/M ratio necessitates that they propagate through a slab of material of approximately 6 g cm^{-2} ("slab" PLD). Early models of confinement and propagation assumed this "slab" distribution of path lengths together with a homogeneous distribution of sources (e.g., Hayakawa, Ito, and Terashima 1958; Davis 1960; Ginzburg and Syrovatskii 1964).

As cosmic-ray measurements improved in both resolution and statistical accuracy, other secondary-to-primary ratios, in particular the ratio of the Sc through Mn (sub-Fe) secondaries to Fe, were measured, and it became clear that a single slab of material could not simultaneously reproduce the measured L/M and sub-Fe/Fe ratios (Garcia-Munoz and Simpson 1970; see reviews by Shapiro and Silberberg 1970; Simpson 1983). Simple slab models of propagation could not account for the observations unless there was more than one component in the cosmic radiation at low energies (e.g., Comstock, Fan, and Simpson, 1966; Comstock 1969). The PLD had to be changed from a delta function to a continuous function. Various forms were investigated, including Gaussian (e.g., Balasubrahmanyan, Boldt, and Palmeira 1965) and exponential (e.g., Cowsik *et al.* 1967). An exponential distribution function (Fig. 1*a*) results from propagation models in which the cosmic rays have a small and constant probability of leaking out of the boundaries of the containment region (e.g., a "leaky box"), and in which cosmic-ray production and loss are assumed to be in equilibrium (Davis 1960; Cowsik *et al.* 1968; Gloeckler and Jokipii 1969).

In recent years it has become clear that cosmic-ray propagation is a very complex process. (A description of techniques for modeling cosmic-ray propagation and the required atomic and nuclear data has been given by Letaw, Silberberg, and Tsao 1984.) In addition, it has become apparent recently that the PLD is neither independent of energy nor a pure exponential in form. At energies greater than a few GeV per nucleon the secondary-to-primary ratios decrease with increasing energy (Juliusson, Meyer, and Muller 1972; Smith *et al.* 1973). This fact is interpreted to be the consequence of the decrease with increasing energy of the mean amount of matter traversed by the observed cosmic rays, e.g., decreasing as an inverse power law in total energy or in magnetic rigidity.

Beginning in the early 1960s, the introduction of Earth satellites for measurements in interplanetary space made it possible to extend cosmic-ray measurements to low energies and obtain high-resolution measurements of elemental and isotopic composition.[3] The satellite experiments imposed new constraints on propagation models. For example, the isotopic abundance of radioactive ^{10}Be showed that the low-energy component of the cosmic rays had a confinement lifetime of about 20 million years. This results in an average interstellar matter density of only ~ 0.2 atom cm^{-3} along the propagation paths (e.g., Garcia-Munoz, Mason, and Simpson 1977*a*; Garcia-Munoz, Simpson, and Wefel 1981; Wiedenbeck and Greiner 1980, and references therein). The early investigations showed that solar modulation modifies the intensity and spectra of the low-energy cosmic rays arriving at the orbit of Earth. It was shown that the modulation is heliospheric in origin (e.g., Fan, Meyer, and Simpson 1960) and that a model of heliospheric propagation—including mechanisms of convection, diffusion, and adiabatic deceleration (e.g., Parker 1965; Hsieh 1970)—could explain the observed spectral slopes at low energies (e.g., Fan, Gloeckler, and Simpson 1965, 1966; Hsieh 1970).

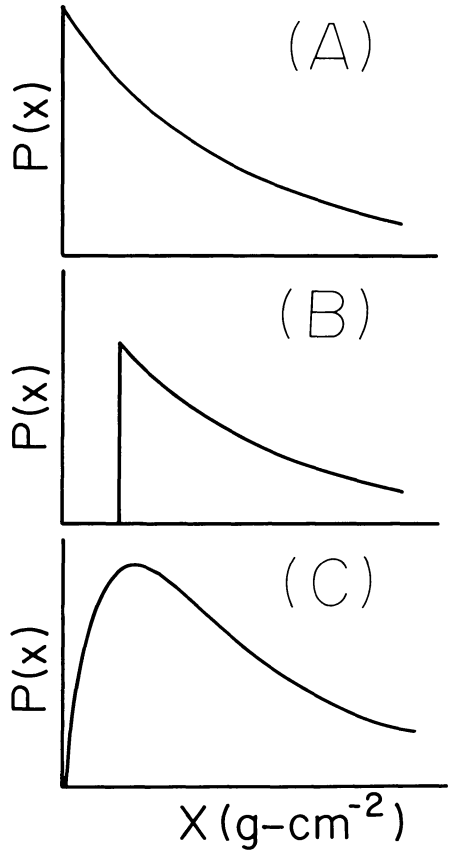

FIG. 1.—Schematic representation of the path-length distributions (PLDs) studied in this paper: (*a*) pure exponential PLD; (*b*) zero-short truncated exponential PLD; and (*c*) double exponential PLD.

Taking into account the effect of solar modulation, Garcia-Munoz *et al.* (1979,1981*a*,1984) in a series of papers showed that at energies below 1 GeV per nucleon, the path-length distribution is also energy-dependent. This conclusion was confirmed by other investigators (Ormes and Protheroe 1983). Using an up-to-date compilation of experimental data and a new propagation algorithm, it is shown in this paper that at low energies the mean path length decreases with decreasing energy.

Claims that the PLD is not a pure exponential started with high-energy data when it was proposed that a depletion of short path lengths in the exponential distribution is needed to

[3]The first spacecraft instrumentation which opened the experimental field of elemental and isotopic measurements was *IMP 1*, launched in 1963, with experiments capable of isotopic separation, by the Goddard Space Flight Center and the University of Chicago.

explain simultaneously both secondary-to-primary ratios L/M and sub-Fe/Fe (e.g., Shapiro and Silberberg 1970). This depletion can be represented by a cutoff of low path lengths at X_c, as illustrated in Figure 1*b*, or by a gradual decrease in the relative abundance of short path lengths as the path length decreases to zero, as in Figure 1*c*.

The presence or absence of short path lengths, or "truncation," in an exponential PLD has been the subject of controversy. The low-energy satellite studies introduced by Garcia-Munoz *et al.* (1979,1981*a*, *b*,1983,1984) indicate that the PLD is deficient in short path lengths at low energy. Using the best set of parameters currently available, this paper confirms this deficiency and furthermore suggests a resolution of the truncation controversy: it is shown that the deficiency of short path lengths is energy-dependent, decreasing in magnitude with increasing energy.

The organization of this paper is as follows. Section II presents the compilation of experimental data on the secondary-to-primary abundance ratios used in this study. Section III deals with the propagation calculations and the input parameters used in these calculations, with special emphasis on the nuclear cross sections. Section IV summarizes our current understanding of solar modulation and presents the modulation model and parameters applied to this analysis. The energy dependence of the PLD under the assumption that the PLD is a pure exponential is presented in § V, where it is concluded that the mean path length decreases with decreasing energy below about 1 GeV per nucleon, and the strength of this conclusion is investigated by considering the sources of error in the calculations. Section VI is devoted to the study of the implications of the above findings for models of confinement and propagation of cosmic rays in the Galaxy. Section VII studies the problem of the relative abundance of short path lengths in the PLD. It is found that at low energies the PLD is deficient in short path lengths and that this deficiency decreases with increasing energy. The functional forms of this depletion are presented in § VIII, and § IX discusses the implications of the truncation for different models of cosmic-ray confinement and transport in the Galaxy. Sections X and XI contain a discussion and the conclusions. The detailed description of the propagation model and the input parameters used in the analysis is relegated to the Appendix.

The results and analysis reported here are part of a continuing program to understand the nature of the cosmic-ray sources and the role of the cosmic rays in our Galaxy. Some aspects of this work have been presented previously (Garcia-Munoz *et al.* 1975, 1979, 1981*a*, *b*; Garcia-Munoz, Simpson, and Wefel 1980; Guzik *et al.* 1980; Dwyer *et al.* 1981; Garcia-Munoz *et al.* 1983, 1984). The present paper focuses on the analysis of the cosmic-ray path-length distribution.

II. SECONDARY-TO-PRIMARY ABUNDANCE RATIOS

This investigation of the cosmic-ray path length distribution utilizes secondary-to-primary ratios as probes of the cosmic-ray confinement and propagation conditions. In particular, we use the B/C and sub-Fe/Fe ratios, since the B/C ratio is predominantly sensitive to the long path lengths and the sub-Fe/Fe ratio is predominantly sensitive to the short path lengths in the PLD. These ratios have been well measured in the cosmic radiation, and the cross sections for the production of their secondaries are relatively well known.

Figure 2 shows a compilation of data for the B/C (*top*) and sub-Fe/Fe (*bottom*) ratios as a function of energy. The points are derived from a large number of different experiments performed mainly in the time period 1974–1978 at energies below about 1 GeV per nucleon. Some of the higher energy points were measured in the 1980s. The 1974–1978 period includes the last solar minimum and was characterized by an approximately constant level of solar modulation (see § IV). Only differential measurements are included in Figure 2. The energy intervals corresponding to each measurement have been suppressed for legibility.

The B/C data in Figure 2 show reasonable consistency over about three decades in energy. At the lowest energies the most precise data are from the University of Chicago experiment on the *IMP 8* satellite (*filled circles*). This data set has been described by Garcia-Munoz and Simpson (1979) and Simpson (1983) and is given for reference in Table 1. The top portion of the table gives the relevant ratios derived for the full energy interval covered by the CsI total-energy detector in the instrument (see Garcia-Munoz, Mason, and Simpson 1977*b*). This interval, defined by range-energy relationships, has the greatest accuracy, and the uncertainties quoted include statistical errors, energy calibration uncertainties, energy interval normalizations, and background uncertainties. The lower part of the table shows, for the B/C and N/O ratios, the results obtained by subdividing the full energy interval using an energy calibration derived from the energy response of the solid state detectors in the instrument. The lower portion of the table contains the data plotted for B/C in Figure 2 and for N/O in Figure 8. For other secondary-to-primary ratios, the full energy interval data on the upper part of the table are used in the data plots.

The results in Table 1 are an update of results reported previously for the *IMP 8* experiment. The B/C, Li/C, and N/O ratios are identical with previous results, but with reduced uncertainty limits. The Be/C, sub-Fe/Fe, Sc/Fe, and V/Fe ratios reported here, for which both statistical and systematic uncertainties are included, are within the uncertainties of the earlier results and represent the most accurate ratios obtained from the University of Chicago *IMP 8* experiment.

There are other secondary-to-primary ratios which could be employed in place of the B/C ratio in this type of analysis, e.g., Li/C, Be/C, F/Ne, but none of these have been measured in the cosmic radiation as well as the B/C ratio. In general, the usefulness of most of the ratios is limited by the relatively low accuracy of the measurements or by the poor knowledge of the cross sections for the production of the secondary species. For example, the beryllium isotope partial production cross sections have been studied extensively (e.g., Raisbeck and Yiou 1975*b*), but the cosmic-ray measurements of beryllium are of significantly poorer quality than those of boron. In addition, two of the beryllium isotopes (^{7}Be, ^{10}Be) are radioactive, and their decay must be included in the analysis. Nevertheless, since beryllium has well-studied partial cross sections, we use the accumulated data for Be/C, along

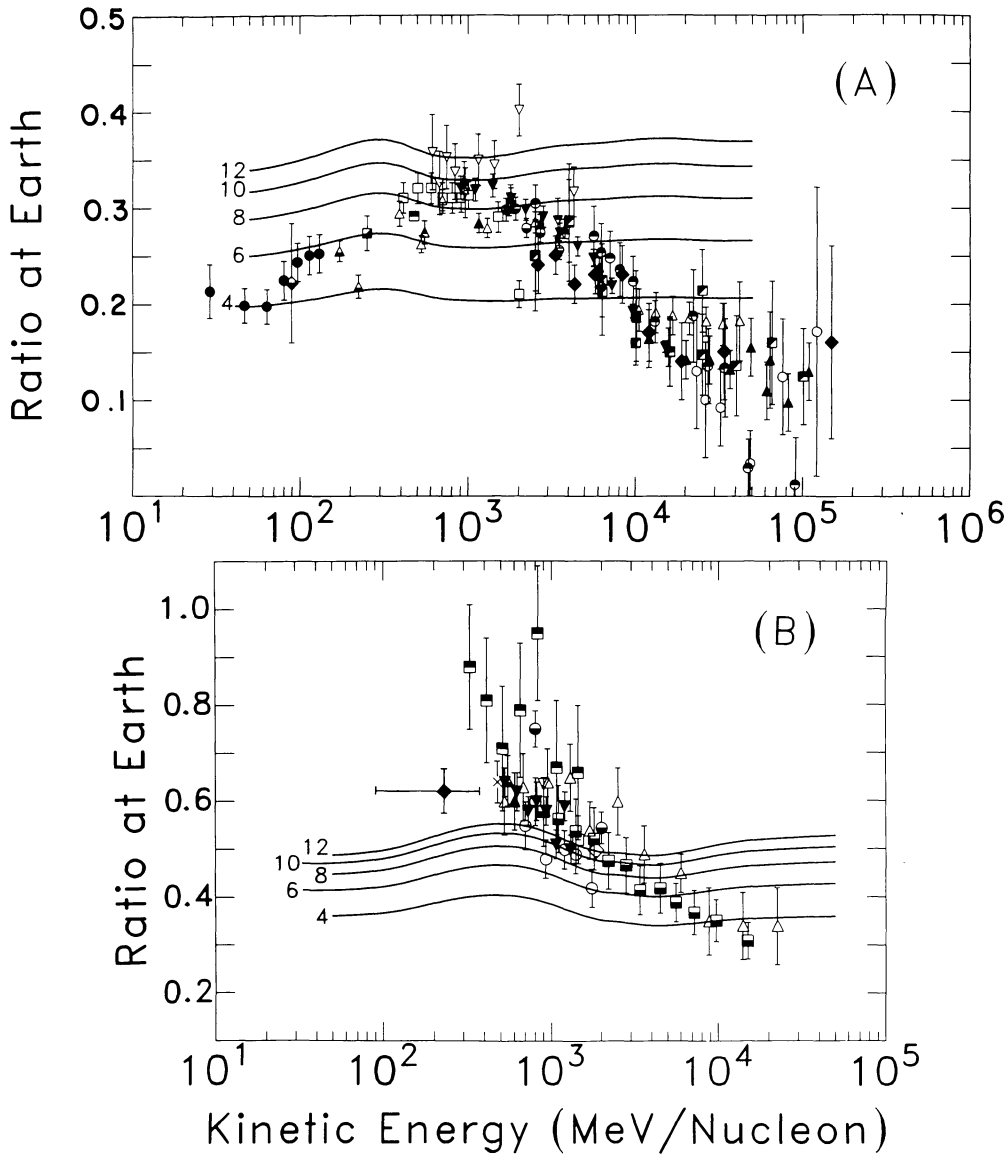

FIG. 2.—Compiled measurements of (*a*) the B/C and (*b*) the Sc+Ti+V+Cr+Mn/Fe ratios, compared with calculated results for energy-independent exponential path-length distributions. (*a*) Measured values are from the following:

- ● Garcia-Munoz and Simpson (1979)
- ◓ Caldwell and Meyer (1977)
- ◒ Dwyer (1978)
- ◑ Dwyer and Meyer (1981)
- ○ Juliusson (1974)
- ◇ Buffington, Orth, and Mast (1978)
- ◈ Mewaldt *et al.* (1981)
- ◆ Orth *et al.* (1978)
- ⬒ Fisher *et al.* (1976)
- ◪ Hagen, Fisher, and Ormes (1977)
- □ Maehl *et al.* (1977)
- ◩ Simon *et al.* (1980)
- ▲ Chappell and Webber (1981)
- △ Lezniak and Webber (1978*a*)
- ⧋ Webber, Damle, and Kish (1972)
- ⧋ Webber *et al.* (1977)
- ◭ Webber (1982)
- ▼ Engelmann *et al.* (1981)
- ▽ Lund *et al.* (1975)
- ⧩ Julliot, Koch, and Petrou (1975)

(*b*) Measurements are from the following:

- ◆ This work (see also Garcia-Munoz and Simpson 1979)
- ◇ Dwyer and Meyer (1981)
- □ Lund *et al.* (1975)
- ⬒ Maehl *et al.* (1977)
- ⬓ Engelmann *et al.* (1981)
- ○ Scarlett, Freier, and Waddington (1978)
- ◒ Young *et al.* (1981)
- x Fisher *et al.* (1976)
- △ Lezniak and Webber (1978*b*)
- ⧋ Webber, Damle, and Kish (1972)
- ▲ Webber, Kish, and Simpson (1979)
- ▽ Israel *et al.* (1979)
- ▼ Benegas *et al.* (1975)

The means of the exponential PLDs range from 4 to 12 g cm^{-2} as indicated on the figure. The calculations include solar modulation with a modulation parameter of 490 MV.

TABLE 1

ELEMENT RATIOS FROM THE UNIVERSITY OF CHICAGO EXPERIMENT ON THE IMP 8 SATELLITE

A. RESULTS FOR FULL INTERVAL

PARAMETER	1974 JANUARY–1978 OCTOBER				1973 OCTOBER–1978 OCTOBER		
	Li/C	Be/C	B/C	N/O	Sc/Fe	V/Fe	Sub-Fe/Fe
Energy interval (MeV/per nucleon).....	29–114	39–151	38–139	49–184	87–366	90–380	87–398
Mean energy (MeV/per nucleon)	72	95	89	117	227	235	236
Ratio	0.12 ± 0.01	0.053 ± 0.01	0.23 ± 0.2	0.25 ± 0.02	0.048 ± 0.009	0.094 ± 0.01	0.62 ± 0.04

B. RESULTS OBTAINED BY SUBDIVIDING INTERVAL

$\bar{E}$ (MeV per nucleon)	ΔE (MeV per nucleon)	Ratio	$\bar{E}$ (MeV per nucleon)	ΔE (MeV per nucleon)	Ratio
B/C			N/O		
29	21–37	0.21 ± 0.03	34.1	25–43	0.28 ± 0.04
46.7.....	38.4–55.1	0.20 ± 0.02	60.2	49.0–71.4	0.26 ± 0.02
63.4.....	55.1–71.8	0.20 ± 0.02	82.7	71.4–94.0	0.24 ± 0.02
80.1.....	71.8–88.5	0.22 ± 0.02	105.2	94.0–116.4	0.24 ± 0.02
96.9.....	88.5–105.4	0.24 ± 0.02	127.9	116.4–139.3	0.24 ± 0.02
113.9.....	105.4–122.4	0.25 ± 0.02	150.6	139.3–161.8	0.27 ± 0.02
130.7.....	122.4–139.0	0.25 ± 0.02	173.0	161.8–184.2	0.27 ± 0.02

with Li/C and N/O (a mixed secondary-plus-primary/primary ratio), as a partially independent check for the results derived from the detailed analysis of the B/C ratio.

The sub-Fe(Sc + Ti + V + Cr + Mn)/Fe ratio is more sensitive than the B/C ratio to the relative abundance of short path lengths in the PLD, since the total inelastic cross section for iron is about 3 times the corresponding cross section for carbon. The collected data for the sub-Fe/Fe ratio (Fig. 2*b*) do not cover as large a range in energy as the B/C data, and there is less agreement among the different measurements. However, the available data do define, reasonably well, the energy dependence of this ratio from ~ 0.5 to about 10 GeV per nucleon. At low energies, only the *IMP 8* point (*filled diamond*; Table 1) has been reported, and this point is plotted showing the energy interval, 87–398 MeV per nucleon of the measurement.

The sub-Fe/Fe ratio has the drawbacks that it is difficult to measure, and that it is not a pure secondary-to-primary ratio. There may well be source components of Mn, Cr, and Ti, which, if they have the relative abundance of the solar system (about 3%; Cameron 1981), make a contribution to the calculated results. The isotope ^{54}Mn has an allowed decay channel to ^{54}Fe for which the half-life is very poorly known (see Appendix and Koch *et al.* 1981*a*). The partial production cross sections from iron spallation have been studied and used to analyze cosmic-ray data, but often with conflicting results (e.g., Perron 1976; Dwyer *et al.* 1981; Perron and Koch 1981; Westfall *et al.* 1979*a*; Webber *et al.* 1983; Raisbeck *et al.* 1979). The most reliable heavy secondary-to-primary ratios would be Sc/Fe and V/Fe, since a solar system source abundance for these elements produces a negligible contribution to the final calculated ratio. The main difficulty with the Sc/Fe and V/Fe ratios is the quality of the compiled cosmic-ray data for which the systematic uncertainties are still large. Nonetheless, we will use the Sc/Fe and V/Fe ratios both as a guide and as a check on the results derived from our analysis of the sub-Fe/Fe data.

III. PROPAGATION CALCULATIONS

For the investigation of the cosmic-ray path length distribution, we use the weighted-slab technique (Fichtel and Reames 1968) in which the PLD is an input parameter in the propagation calculation. Starting with a set of relative abundances of elements and isotopes at the source and assuming a common source energy spectrum, the different isotopic species are propagated through slabs of interstellar matter and integrated over an assumed PLD to obtain the particle densities in local interstellar space outside the heliosphere. These densities are then modified by solar modulation in the heliosphere (using a model of solar modulation; see § IV) to calculate the ratios at the orbit of Earth. The results of these calculations are then compared with the experimental data. The procedure is repeated with different PLDs until a good fit to the data is obtained. The details of the calculational technique and the input parameters to the code are described in the Appendix to this paper.

The most important parameters for the study of secondary-to-primary ratios in Galactic propagation are the nuclear cross sections and their energy dependence, and also, at low energies, the ionization energy loss. Accurate propagation calculations require knowledge of both the partial cross sections for the production of the secondary nuclei and the total inelastic cross sections. Figure 3 shows an example of the excitation function for the production of the boron isotopes, and their radioactive progenitors, from ^{12}C fragmentation. Experimental data reported in the literature are shown along with two excitation functions. The dashed curves have been traced through the experimental points and are the excitation

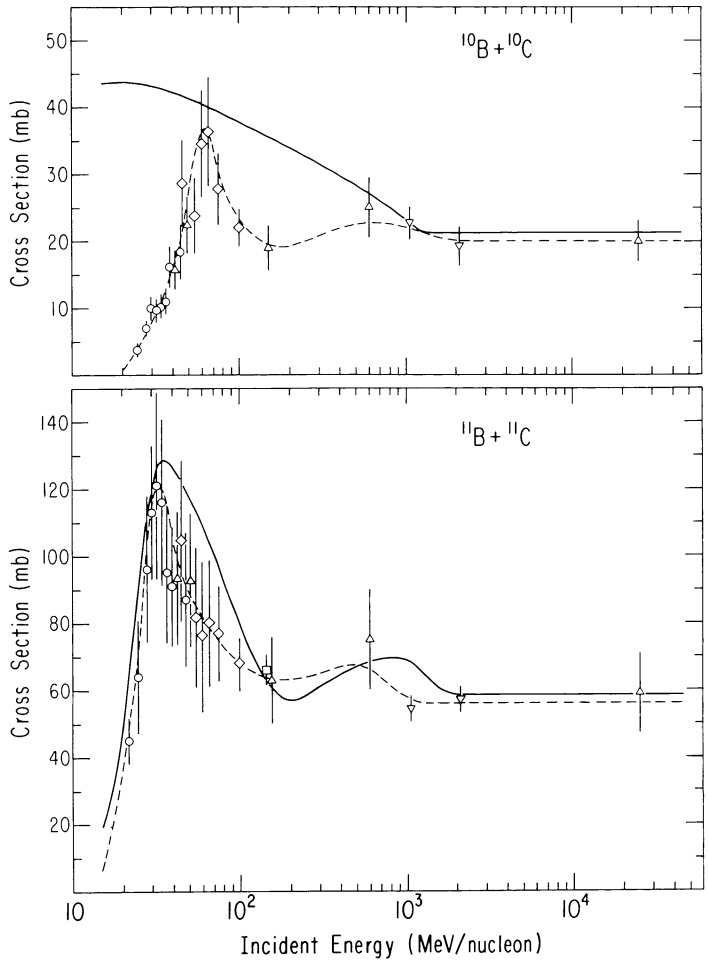

FIG. 3.—Partial production cross section for the isotopes of boron (plus radioactive progenitors) in $p + ^{12}C$ interactions. Data points are the following: *circles*, Davids, Laumer, and Austin (1970); *diamonds*, Roche *et al.* (1976); *triangles*, Fontes (1977); *inverted triangles*, Lindstrom *et al.* (1975*a*); *squares*, Silberberg and Tsao (1973*a*). The solid curve gives the results of the semiempirical calculations (Silberberg and Tsao 1973*b*), and the dashed curve shows the excitation function adopted for the present analysis.

functions adopted for use in this analysis. For comparison the solid curves are the excitation functions given by the semiempirical formulae of Silberberg and Tsao (1973*a*, *b*). For ^{11}B production the curves are very similar, differing mainly in the energy interval 0.6–2 GeV per nucleon. For ^{10}B, however, the cross sections are quite different below 1 GeV per nucleon, with the difference increasing with decreasing energy.

Most of the needed excitation functions are much more poorly measured than the ones in the example of Figure 3. Curves similar to the dashed line in Figure 3 have been generated for all reactions for which reliable data exist in the literature. When experimental data are unavailable, semiempirical excitation functions have been used. A similar approach has been adopted for the total inelastic cross sections (Guzik *et al.* 1980), and this aspect of the problem is addressed in the Appendix.

The curves shown in Figure 2 give the results of propagation calculations for an exponential PLD whose mean X_0 is energy-independent. The numbers on the curves give the values of X_0 in g cm^{-2} of interstellar matter (93% H, 7% He by number). Two conclusions are immediately evident from Figure 2. First, no single constant value of X_0 can reproduce the experimental data over the full energy range covered by the measurements. Second, in any energy interval below about 5 GeV per nucleon, the value of X_0 needed to reproduce the B/C observation does not, simultaneously, explain the sub-Fe/Fe ratio.

Figure 2 illustrates the dual problem investigated in the remainder of this paper: (1) the energy dependence of an exponential PLD over the entire energy range shown, and (2) the shape of the PLD, as a function of energy, needed to reproduce both of the ratios shown on Figure 2. To accomplish these objectives, an iterative procedure is adopted: (*a*) establish the best values for all of the input parameters in the propagation calculation (this is the subject of the Appendix and § IV), (*b*) adopt an energy dependence of X_0 in order to reproduce the B/C observations, (*c*) compare the results with the sub-Fe/Fe data and with the ratios Sc/Fe and V/Fe, and (*d*) modify the shape of the PLD to satisfy all the ratios. Finally, the set of best values for the input parameters is varied, within the uncertainty limits for the individual parameters, to assess the overall uncertainty in the derived PLD.

IV. SOLAR MODULATION

We discuss in this section the modification introduced in the interstellar secondary-to-primary ratios by solar modulation at energies below several GeV per nucleon, and its effects on the interpretation of the propagation calculations. It is shown that a propagation calculation in which the mean path length is constant below 1 GeV per nucleon fails to agree with the experimental data if the propagation calculation assumes the modulation level characteristic of the 1974–1978 period around the solar minimum. A stronger modulation level will lead to even larger disagreement.

It is well known (see reviews by Jokipii 1971 and Fisk 1979) that at energies below a few GeV per nucleon the intensity and the spectral shape of the cosmic rays arriving at the orbit of Earth are significantly modified by solar modulation. The cosmic rays diffuse into the heliosphere against the outward-flowing solar wind, carrying the frozen-in interplanetary magnetic field, which tends to convect the cosmic rays out of the heliosphere. In this process, the cosmic rays lose energy to the expanding field (adiabatic deceleration), and their energy spectrum is modified.

A spherically symmetric model of solar modulation has been developed (Parker 1965; Jokipii 1971; Urch and Gleeson 1972; Fisk 1979) which explains most of the gross features of the modulation process. This model includes the effects of diffusion, convection, and adiabatic deceleration (but not drifts due to the gradient and curvature of the magnetic field) and assumes that these three physical processes are in equilibrium in the heliosphere. Quantitatively these effects are represented by a Fokker-Planck equation in which the parameters are the solar wind velocity, the diffusion coefficient and the radius of the heliosphere, with the cosmic-ray differential energy spectrum in local interstellar space as a boundary condition.

Recently Evenson *et al.* (1983) (see, for more details, Garcia-Munoz *et al.* 1986), solving this equation numerically, have analyzed the simultaneous modulation of electrons, protons, and helium nuclei over the 1965–1979 period involving more than one solar cycle. They find that in general the model fits the data well.

In this model the depth of modulation at the heliospheric radius r is given by the modulation parameter

$$\phi(r) = \frac{1}{3}\int_r^R \frac{V(r')}{K(r')}\,dr', \qquad (1)$$

where $V(r')$ is the solar wind velocity, $K(r')$ is the radial part of the diffusion coefficient, and R is the radius of the heliosphere. An insight into the physical meaning of ϕ is obtained, noting that in the "force-field" approximation (Gleeson and Axford 1968) this modulation parameter corresponds to a "potential energy" Φ that in the particular case in which the diffusion coefficient is proportional to particle rigidity takes the simple form

$$\Phi = |Ze|\phi(r), \qquad (2)$$

where Ze is the particle charge. This potential energy has been identified as the mean energy loss that the particles experience in penetrating the heliosphere to a radius r. Thus Φ in units of kinetic energy per nucleon is equal to ϕ in units of rigidity times the ratio A/Z of the particle.

The modulated nucleonic differential energy spectra obtained by the numerical solution of the Fokker-Planck equation are almost completely determined by the value of the modulation parameter ϕ. Combinations of the parameters R, r, $V(r)$, and $K(r)$ giving the same value of ϕ will lead to modulated nucleonic spectra which will be very closely equal to each other (Urch and Gleeson 1972). Therefore, we have used values of the modulation parameter ϕ to specify different levels of modulation.

Figure 4 shows the time dependence of the modulation parameter used by Evenson *et al.* (1983) for 1973–1980, compared with the time dependence of the Climax Neutron Monitor count rate (given as the percent decrease below the 1954 solar minimum level). The period 1974–1978 corresponding to the data used in this paper is characterized by a nearly constant level of solar modulation for which the average value of the modulation parameter is approximately $\phi =$ 490 MV, or $\Phi = 245$ MeV per nucleon for $A/Z = 2$ particles.

We have used the model and techniques of Evenson *et al.* (1983) to calculate the effect of solar modulation on the ratio B/C at the orbit of Earth. We have solved numerically the complete Fokker-Planck equation using the computer code developed by Fisk (1971), and we have labeled the solutions with the corresponding value of the modulation parameter ϕ, or the corresponding "potential energy" Φ. Figure 5 demonstrates the effect of modulation for different values of Φ. The curves are the results of calculations of interstellar propagation followed by solar modulation. The propagation calculation for Figure 5 used an exponential PLD in which the mean path length X_0 was constant below 1 GeV per nucleon and varied at higher energies as $X_0 \propto E^{-0.6}$. The B/C ratio has been calculated at different levels of modulation indicated in the figure by values of the parameter Φ of equation (2), expressed in units of MeV per nucleon. The essential point demonstrated on Figure 5 is that the calculation agrees with the data only for modulation levels less than about $\Phi =$ 75 MeV per nucleon. However, since we have shown above (Fig. 4) that the average value of Φ for the 1974–1978 period is 245 MeV per nucleon, models in which the mean path length is a constant at energies below about 1 GeV per nucleon cannot fit the experimental data.

V. ENERGY DEPENDENCE OF THE PLD

Figure 2 shows the energy dependence of the secondary-to-primary ratios B/C and sub-Fe/Fe over a wide energy interval. The decrease in the ratios with energy above a few GeV per nucleon (e.g., Juliusson, Meyer, and Muller 1972) can be modeled in propagation calculations using an exponential path-length distribution in which the mean path length decreases with increasing energy as a power law in total energy or rigidity with an exponent in the range -0.4 to -0.7. Here a dependence $E^{-0.6}$ is adopted. The new investigation reported in this paper is the energy dependence of the ratios below ~ 1 GeV per nucleon, and it will be shown that an explanation of the data requires that in this energy interval the mean path length decreases with decreasing energy.

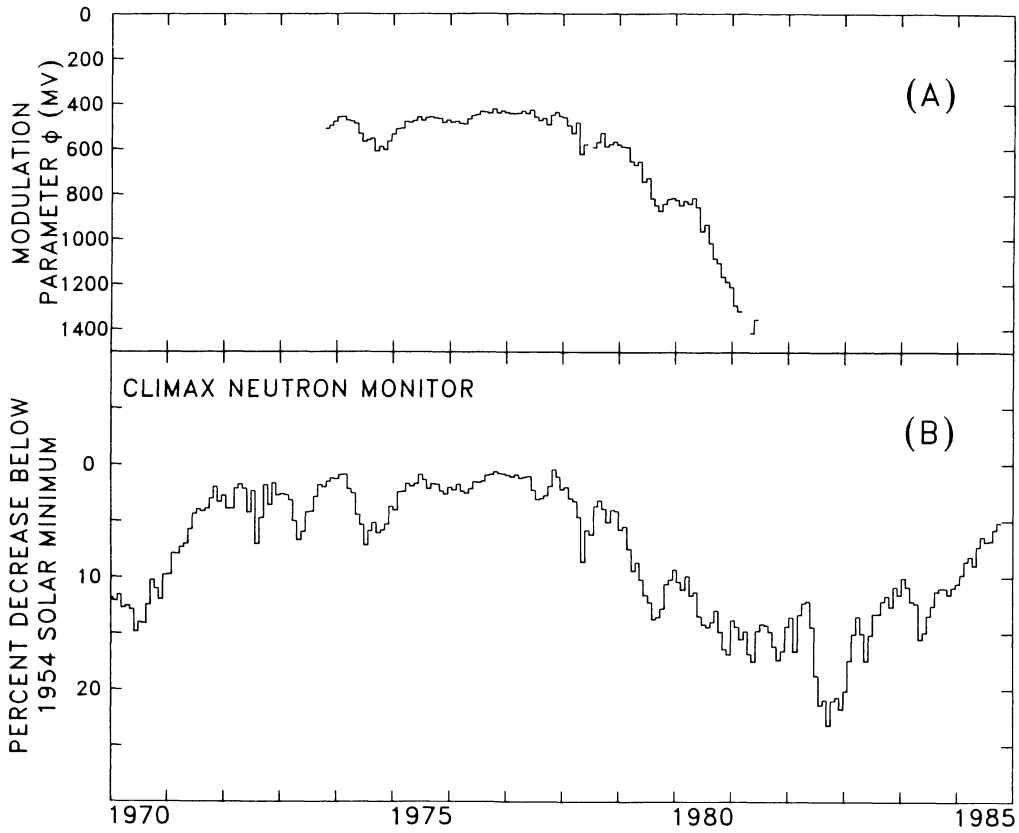

FIG. 4.—Time dependence of solar modulation in the heliosphere. (*a*) Modulation parameter ϕ(MV) as derived by Evenson *et al.* (1983) from the measured flux of 70–95 MeV per nucleon cosmic-ray helium for the period 1973–1980. (*b*) The Climax Neutron Monitor 27 day average count rate for the period 1967–1985 (J. A. Simpson 1985, private communication).

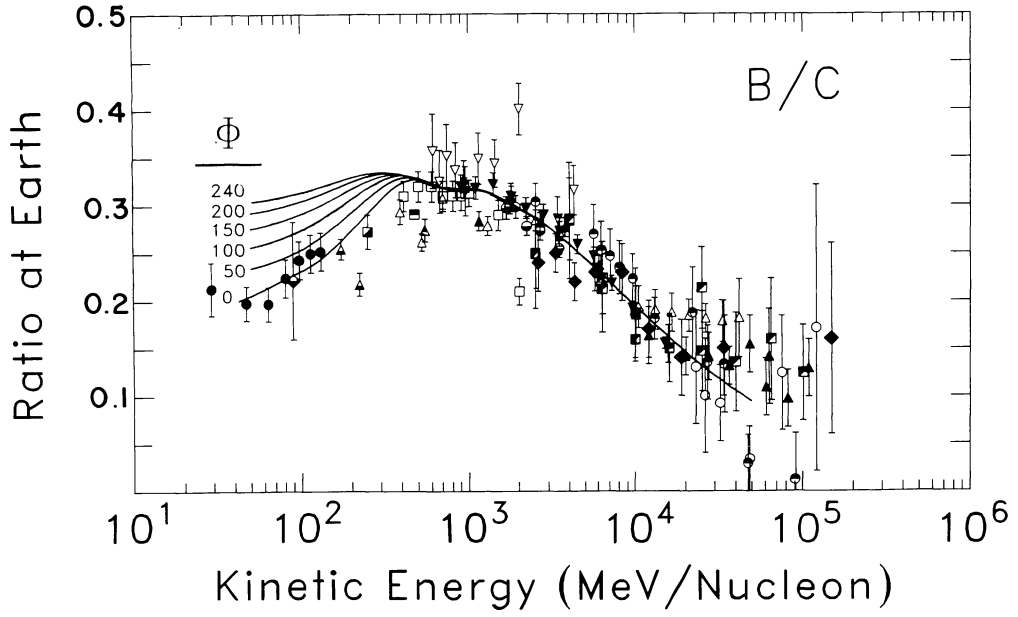

FIG. 5.—Calculated B/C ratio using different levels of solar modulation. The PLD used is an exponential with $X_0 \propto E^{-0.6}$ for $T > 1$ GeV per nucleon and X_0 constant for $T < 1$ GeV per nucleon. The constant value of $X_0 = 9.25$ g cm^{-2} adopted for $T < 1$ GeV per nucleon is determined by requiring that the calculated ratio reproduce the weighted mean of the B/C observations in the interval ~ 0.5–2 GeV per nucleon. Different levels of solar modulation are indicated by the value of the modulation parameter Φ expressed as mean adiabatic deceleration in MeV per nucleon for $A/Z = 2.0$ particles. (Data references as in Fig. 2*a*).

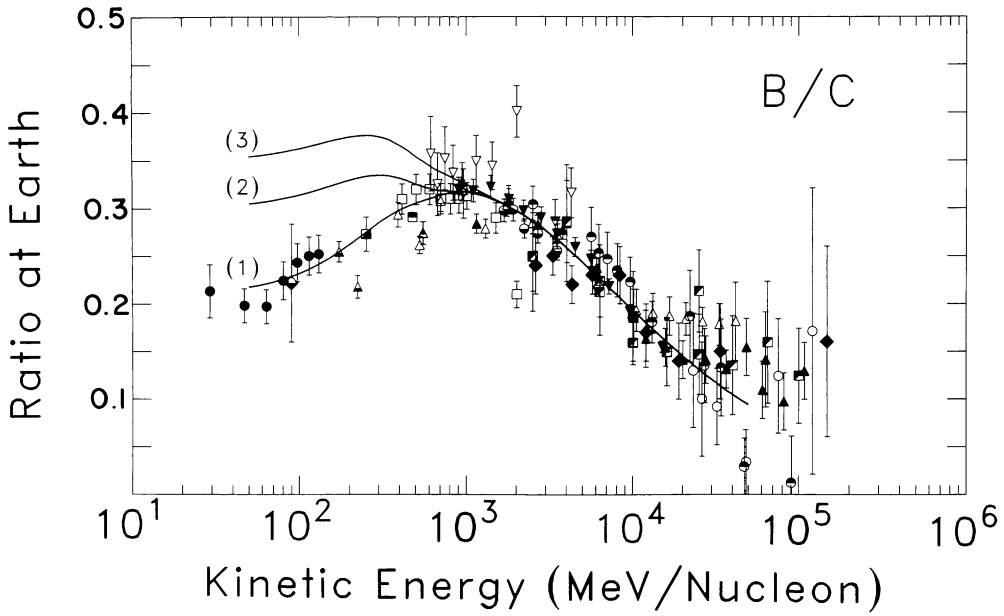

FIG. 6.—Comparison of the compiled data for the B/C ratio (data references as in Fig. 2*a*) with calculations involving three different assumptions for the energy dependence at low energy of the mean X_0 of an exponential PLD. In all cases, for energies above ~1 GeV per nucleon, $X_0 \propto E^{-0.6}$. Below 1 GeV per nucleon: curve 1 is for $X_0 \propto E^2$; curve 2 is for X_0 = constant = 9.25 g cm^{-2}; and curve 3 is for $X_0 \propto E^{-0.6}$, where E is the total particle energy per nucleon. Solar modulation for $\phi = 490$ MV has been included for all curves.

a) Low-Energy Analysis

Various energy dependences for the mean, X_0, of an exponential PLD have been suggested at energies below a few GeV per nucleon. The most frequent assumption is that X_0 is a constant in this energy interval. Figure 6 compares the experimental B/C data with the calculated ratio after Galactic propagation and solar modulation for three different energy dependences of X_0 at low energy.

1. X_0 decreasing with decreasing energy below ~1 GeV per nucleon, $X_0 \propto E^2$.
2. X_0 constant (9.25 g cm^{-2}) below ~1 GeV per nucleon (this is the form used in most interpretations of cosmic-ray data, e.g., Ormes and Freier 1978; Protheroe, Ormes, and Comstock 1981).
3. X_0 increasing with decreasing energy. This is an extension of the energy dependence at high energy, $X_0 \propto E^{-0.6}$, to the low-energy region which has been employed by several authors (Westergaard 1979; Koch *et al.* 1981*b*; Perron *et al.* 1981).

The flattening of the curves at low energy is due to the combined effects of ionization energy loss and solar modulation. Of the three dependences, only curve 1 is an adequate representation of the experimental data.

The results of the calculations are only mildly sensitive to the form of the energy spectrum at the cosmic-ray source. The source spectrum used in our calculations is very similar to a source spectrum in rigidity. As shown in the Appendix, a source spectrum in total energy gives the largest difference with the measured low-energy B/C ratios.

The variation of X_0 with energy employed for curve 1 is given by the empirical formula

$$X_0(E) = A\left(\frac{T+T_0}{850+T_0}\right)^{\beta}\left[1-0.2\exp\left(-\frac{T-850}{300}\right)\right], \quad (3)$$

where A is a normalization constant (=11.0 g cm^{-2}) of interstellar matter, E is total energy per nucleon, T is kinetic energy per nucleon in MeV, T_0 is the nucleon rest energy = 931 MeV, and $\beta = -0.6$ for $T > 850$ MeV per nucleon and $\beta = 2.0$ for $T < 850$ MeV per nucleon. The third factor, in square brackets, is chosen to smooth the function across the energy $T = 850$ MeV per nucleon, where the value of β is changed discontinuously. At 1 GeV per nucleon the value of X_0 given by equation (3) is 9.2 g cm^{-2} of interstellar matter, and X_0 decreases to 3.6 g cm^{-2} at 100 MeV per nucleon. Further discussion of this energy dependence is contained in § VI, following the analysis of the uncertainties in the derivation of the energy dependence of the PLD.

b) Uncertainties in the Derived Energy Dependence

The energy dependence for the mean, X_0, of the exponential path length distribution given by equation (3) is an empirical, analytic representation. The numerical values of X_0 as a function of energy were determined using the best set of input parameters to the propagation code and requiring that the calculations reproduce the average of the B/C measurements, e.g., 0.32 ± 0.01 at 1 GeV per nucleon and 0.23 ± 0.02 at 100 MeV per nucleon (see Table 1). The uncertainty to be assigned to these derived values of X_0 results from uncertainties in the input parameters, principally from the nuclear cross sections, and from the dispersion in the B/C measurements. The uncertainty in $X_0(E)$ was determined in two steps. First, the uncertainty in X_0 due to the nuclear cross section uncertainties was found. Then, the uncertainty in X_0 due to the spread in the B/C measurements was evaluated. Finally, these two uncertainties were combined, assuming uncorrelated errors, to give the final uncertainty limits.

The partial cross section uncertainties were estimated from the dispersion in the experimental data in plots such as Figure

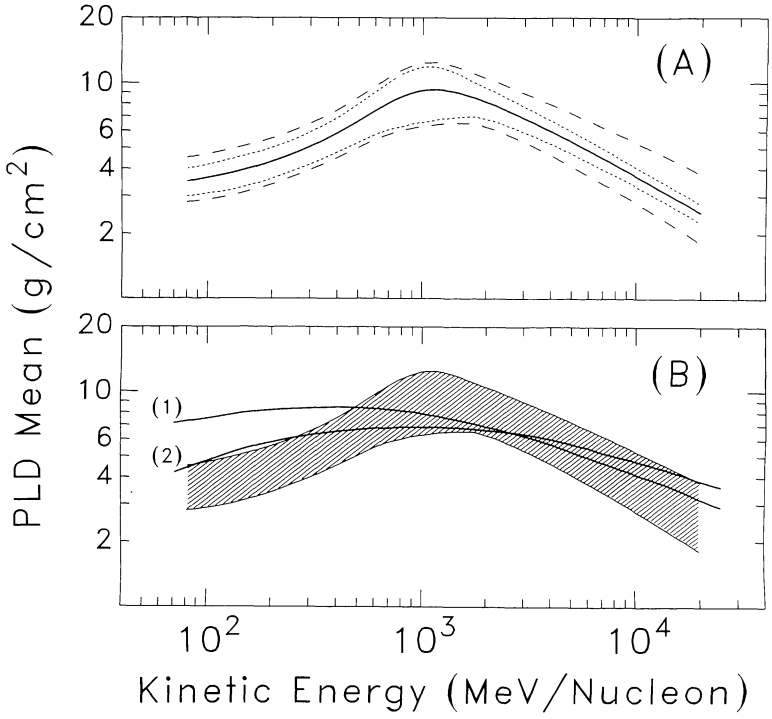

FIG. 7.—Mean of the exponential PLD used to fit the B/C data as a function of energy, (*a*) showing the uncertainties in X_0 and (*b*) comparing the results with theoretical calculations for the dynamical halo model. In (*a*) the actual value of X_0 used to fit the B/C ratio is shown by the heavy line, while the uncertainty due to cross section error is shown by the dotted lines. The outer dashed lines include the uncertainty in the B/C measurements, and this outer uncertainty envelope is reproduced as the hatched region in (*b*) and compared with the results of the dynamic halo model for convection velocities of 9 km s^{-1} (curve 1) and 17 km s^{-1} (curve 2).

3 or Figure 17. This provided experimental uncertainties for boron production cross sections from interactions of cosmic-ray ^{12}C, ^{13}C, ^{14}N, and ^{16}O. These uncertainties ranged from ~10% at energies of a few hundred MeV per nucleon to 15%–20% at a few GeV per nucleon for the best case, and from about 15% to 30% for the less well measured reactions. For other cross sections, a uniform 15% error was assigned at all energies. This value is somewhat low compared with the 30% uncertainty usually quoted for the semiempirical cross sections (Stone and Wiedenbeck 1979; Perron and Koch 1981; but see also Letaw, Silberberg, and Tsao 1985), but these unmeasured cross sections were found to contribute little to the overall uncertainty in X_0, which is dominated by the errors in the measured partial cross sections for the spallation of the primary CNO nuclei.

The uncertainty in X_0 due to the cross section errors was determined with a simple propagation code (leaky box model without ionization energy loss) which included all of the nuclear reactions and in which all the cross sections were assigned an uncertainty as a function of energy. The main contributions to this error in X_0 were found to be, in order of importance, the uncertainty in the partial cross sections for carbon spallation, oxygen spallation, total inelastic cross sections, and nitrogen spallation. The uncertainty contributed by cross sections for elements heavier than oxygen (e.g., ^{20}Ne, ^{24}Mg, ^{28}Si, ^{56}Fe) was negligible.

Figure 7*a* shows the energy dependence of X_0. The heavy line in the center gives the energy dependence evaluated from equation (3). The cross section–induced uncertainties, just discussed, produce the error band shown as the inner dotted curves. The outer dashed band gives the overall uncertainty after folding in the errors in the cosmic-ray measurements.

In order to assess the uncertainty due to errors in the measurements of the B/C ratio, curves were drawn on Figure 2 corresponding to an upper and a lower envelope of the data points, following approximately the 2σ level from the weighted mean of the observations. For example, at 1 GeV per nucleon the upper and lower limits were B/C = 0.34 and 0.30, respectively. These envelopes were then assumed to represent the boundaries of the data, and an energy-dependent X_0 was fitted to each limit. These upper and lower bounds for $X_0(E)$ were then compared with the best fit given by equation (3), and the difference used to determine an uncertainty due to the errors in the experimental data. This uncertainty was folded with the cross section uncertainty, as a function of energy, to give the total uncertainty in X_0, which is shown as the dashed curves in Figure 7*a* and also as the shaded region in Figure 7*b*. Below several GeV per nucleon the overall uncertainty in X_0 (~30%) is dominated by the cross section uncertainties, but at higher energies the spread in the experimental measurements provides the largest contribution to the total error (~50%). Improved cosmic-ray data can reduce the uncertainty in X_0 at high energies, but more accurate nuclear cross section measurements are required to reduce the error in X_0 at lower energies.

The cross sections and the experimental data are the biggest contributors to the uncertainty in X_0. Additional sources of uncertainty are the ionization energy loss relation (mea-

sured to an accuracy of $\leq 3\%$), the cosmic-ray source energy spectrum ($\leq 5\%$; see Appendix), and the level of solar modulation employed in the calculations ($\Delta\Phi \leq 40$ MeV per nucleon for $A/Z = 2$ particles). Inclusion of these additional uncorrelated errors does not significantly alter the overall error in X_0 show in Figure 7. The important conclusion to be drawn from this analysis is that even with all of the uncertainties included, (1) X_0 is not energy-independent below ~ 1 GeV per nucleon, and (2) it must decrease with decreasing energy.

c) *Other Secondary-to-Primary Ratios*

Figure 8 shows compiled data for the N/O, Be/C, and Li/C ratios compared with the results of the propagation calculations which produced curve 1 in Figure 6, i.e., using the energy dependence given by equation (3). The N/O is a mixed ratio, secondary-plus-primary to primary, since there are both a source component of ^{14}N and large secondary components of both ^{14}N and ^{15}N. Our calculated N/O ratio is in reasonable agreement with the compiled experimental data in Figure 8, but appears to fall somewhat below the mean of the measurements at all energies. However, slightly increasing the source ratio ^{14}N/O will move the entire curve upward. Thus, the N/O ratio provides a test for the shape of the calculated curve rather than for the absolute normalization, and the results shown in Figure 8*a* reproduce well the shape of the experimental data.

In the case of the Be/C ratio (for which good experimental cross section data exist, as discussed in the Appendix), the calculations agree with the data at low energy and with the high statistics *HEAO* C-2 data (Engelmann *et al.* 1981) at higher energy. It should be noted that the *HEAO* C-2 data were collected in 1979–1980 under heliospheric conditions approaching solar maximum. The solar modulation used in the calculation of the curve applies strictly to the 1974–1978 time period. The larger level of modulation would have the effect of increasing, slightly, the calculated Be/C ratio at the *HEAO* C-2 energies, thereby bringing the calculations into better agreement with that data set.

For the Li/C ratio the cosmic-ray data are scarce and show little self-consistency. No conclusions can be drawn from this comparison, except to point to the need for better measurements of cosmic-ray lithium.

The above comparisons between calculations (using measured cross sections wherever possible) and the up-to-date compilations of the light elements and N/O argue that the propagation process is the same for all these species and that some previous interpretations in the literature drawing conflicting conclusions originate mainly from the quality of the experimental data or the cross sections used. Figures 8*b* and 8*c* suggest that significantly improved measurements of Be/C and Li/C will be necessary before these two ratios can be employed as detailed tracers of the propagation process of the cosmic rays.

VI. IMPLICATIONS OF THE ENERGY DEPENDENCE FOR COSMIC-RAY CONFINEMENT AND PROPAGATION IN THE GALAXY

We show in Figure 6 a comparison of experimental data with calculations assuming three possible dependences of the mean X_0 of an exponential PLD on energy below about 1 GeV per nucleon. In curve 3, X_0 follows the same energy dependence proportional to $E^{-0.6}$ at all energies. This case has been explored by a number of workers, since if cosmic-ray escape from the confinement region is controlled by the interaction of the particles with interstellar hydromagnetic waves, then the energy (rigidity) dependence of X_0 is expected to be a power-law function of rigidity with a spectral index that is related to the power spectrum of the waves (Jokipii and Higdon 1979; Cesarsky 1980). However, we have shown that at low energies curve 3 does not give an acceptable fit to the experimental data. This implies that the rigidity (energy) dependence of the trapping/scattering mechanism must change at energies below a few GeV per nucleon or be overwhelmed by another physical effect. For example, the interstellar hydromagnetic waves might show a break in their power-law spectrum at low rigidity or become inefficient in controlling particle escape from the confinement region.

An alternate approach, represented by curve 2 on Figure 6, involves models in which the escape is independent of rigidity below a few GeV per nucleon. If the low-energy particles produce hydromagnetic waves and are, in turn, scattered by these waves, the process may become self-limiting, and the cosmic rays are constrained to stream at about the Alfvén velocity (Holmes 1974). This argument leads directly to an escape length which is constant with energy (rigidity) in the region of low particle energy. However, such a constant escape length below a few GeV per nucleon also does not give a good fit to the low-energy B/C observations, suggesting either that such self-limiting confinement does not operate in the Galactic disk (although it may be effective in the low-density halo region) or that another mechanism is more important at low particle energies.

The experimental data discussed above show that the value of X_0 must decrease with decreasing energy below about 1 GeV per nucleon. Such behavior is predicted by dynamical halo models involving a Galactic wind energized by the cosmic rays themselves (Johnson and Axford 1971; Ipavich 1975; Jokipii 1976; Jones 1979*b*; Freedman *et al.* 1980). In these models the cosmic rays, which are coupled to the gas by hydromagnetic waves, drive gas and magnetic field out of the disk in a Galactic wind forming a dynamical Galactic halo, where they diffuse while being convected by the Galactic wind. If convection dominates diffusion, the lowest energy particles will be removed most effectively by the convection process, leading to a smaller effective value of X_0 and a decrease of X_0 with decreasing energy.

Kota and Owens (1980), following the work of Jokipii (1976) and Jones (1979*b*), have performed detailed integrations of the equations for a dynamical halo model including energy-dependent diffusion coefficients, obtaining predictions for the energy dependence of the mean amount of matter traversed by the cosmic rays for different values of the Galactic wind speed and dimensions of the Galactic halo. Figure 7*b* shows the results of two of these calculations—curve 1 for a wind velocity of 9 km s^{-1} and curve 2 for a wind velocity of 17 km s^{-1}—compared with the energy dependence of X_0 derived from the B/C data (*shaded region*). A wind velocity of 17 km s^{-1} appears to be marginally consistent with the shaded region, but the lower wind velocity predicts too little

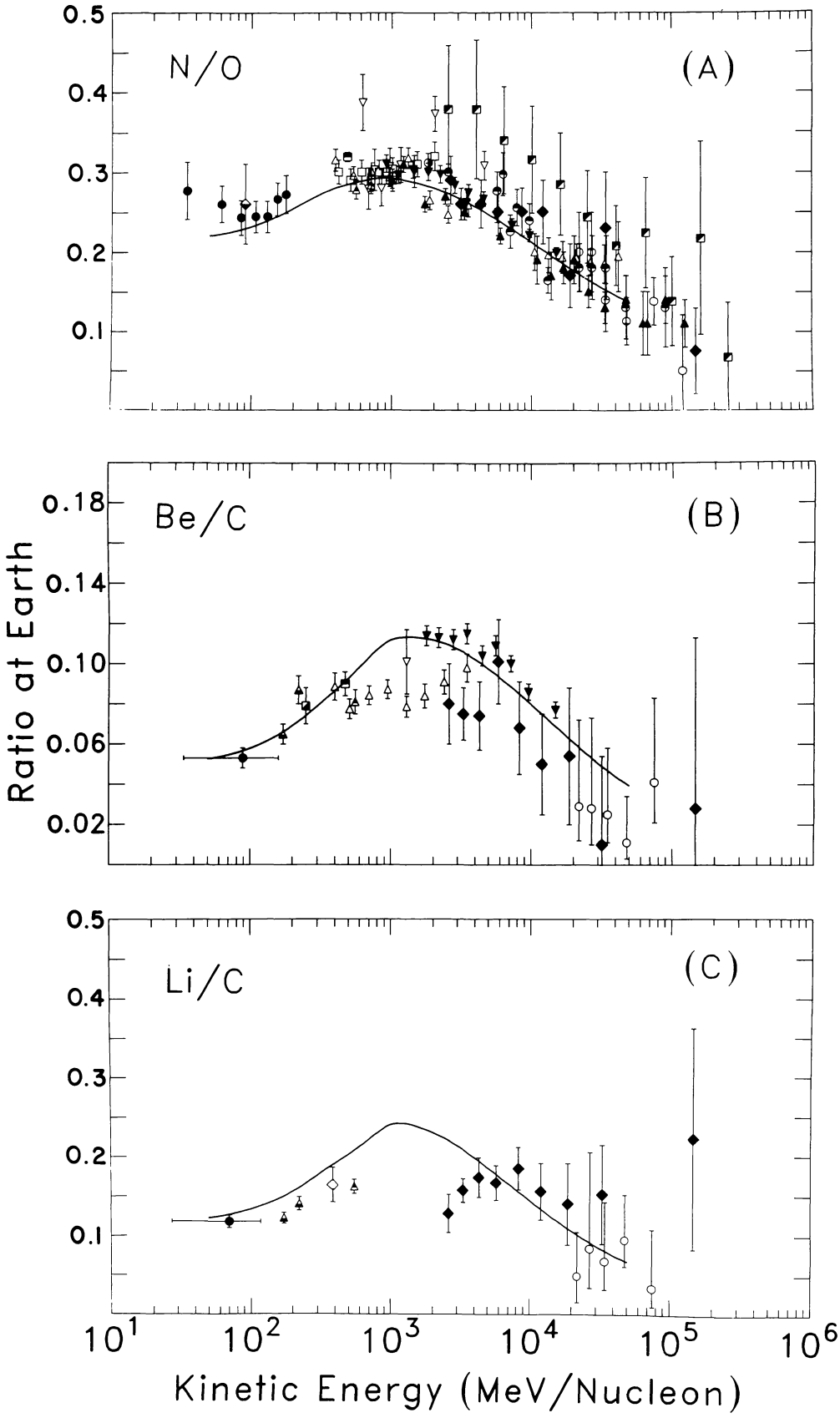

FIG. 8.—Comparison of the calculated ratios (using the "best-fit" energy-dependent exponential PLD, curve 1 of Fig. 6) with the compiled experimental data for the ratios: (*a*) N/O, (*b*) Be/C, and (*c*) Li/C. (Data references as in Fig. 2*a*.) See text for details.

variation with energy. Also, the experimental form of $X_0(E)$ below 1 GeV per nucleon appears to decrease faster with decreasing energy than the theoretical predictions. Extrapolating crudely from these curves, the variation in X_0 deduced from the B/C measurements would imply wind velocities in excess of 25 km s^{-1}. Note also that the rigidity dependence assumed at high energy by Kota and Owens (1980) appears to be somewhat flatter than the observations.

The cosmic-ray age or mean confinement time is a parameter in the dynamical halo model. Therefore, the cosmic-ray age derived from the surviving fraction of a radioactive species such as ^{10}Be (Garcia-Munoz, Mason, and Simpson 1977*b*; Wiedenbeck and Greiner 1980; Garcia-Munoz, Simpson, and Wefel 1981) can be used, along with the mean amount of matter traversed at the equivalent energy, to compute limits on the wind velocity, the size of the halo, and the diffusion coefficient. Freedman *et al.* (1980) adopted this approach and derived an upper limit of 16 km s^{-1} for the Galactic wind velocity assuming a surviving fraction of ^{10}Be less than $\frac{1}{3}$, and $X_0 = 6$ g cm^{-2} of interstellar matter at 300 MeV per nucleon. However, if X_0 is less than 6 g cm^{-2} (as is the case for our curve 1 in Fig. 6), the upper limit for the wind velocity is increased.

Jones (1979*b*) took the approach of assuming a wind velocity of 8 km s^{-1} and using the measurements of the surviving fraction of ^{10}Be to place limits on the effective size of the halo and the diffusion coefficient. He concluded that the spread in measured values for the ^{10}Be/^{9}Be ratio was too large to permit definite conclusions and did not investigate other values for the velocity of the Galactic wind.

It is concluded that the energy dependence of X_0 derived from the cosmic-ray B/C observations when interpreted in the frame of current dynamical halo models indicates convective velocities for the Galactic wind of ≥ 20 km s^{-1}.

If we examine the fundamental question of the dominant mechanism for particle loss from the confinement region, we see that particle escape driven by a convective Galactic wind can be made consistent with the data, but other mechanisms may be involved. Parker (1969,1976) assumed that at the upper and lower edges of the Galactic disk the cosmic rays inflate the magnetic field, leading to the formation of magnetic "bubbles" which extend far above the Galactic disk into the Galactic halo, where they may rupture, releasing the trapped cosmic rays. Blandford and Ostriker (1980) argue that, if such a mechanism is principally responsible for the loss of low-energy particles, then the probability of escape per unit time should become constant at low energies (rigidities), which implies that the mean amount of matter traversed by the particles becomes proportional to the particle velocity. Such a prediction can be tested against the results in Figure 7 by fitting the values of X_0 derived at various energies to a power law in particle velocity ($X_0 \propto \beta^n$). An index for such a power law of $n = 0.98 \pm 0.15$ is obtained, showing that the results described here are consistent with the simple picture in which the low-energy cosmic rays are lost via magnetic "bubbles" produced by inflation of the field.

An alternative explanation for the energy dependence of B/C data may lie in particle acceleration theories. Shock waves have been shown to provide an efficient acceleration mechanism for cosmic rays (Bell 1978; Axford, Leer, and Skadron 1977; Blandford and Ostriker 1978; see also the review in Axford, 1981) at the energies studied here. In such models, the observed cosmic-ray spectrum might be the result of acceleration by a single shock or from the accumulated effects of many passes through different shocks. For the latter case, the acceleration and propagation process are interspersed, leading to reacceleration after the production of the secondary species. Blandford and Ostriker (1980) presented the details of such a model.

It is then conceivable that the cosmic rays may result from a near-equilibrium, within the cosmic-ray lifetime, between a continuum shock acceleration process in the interstellar medium and particle energy loss by ionization, fragmentation, deceleration, and escape. The difficulty here, as pointed out by Eichler (1980), Cowsik (1980), and Fransson and Epstein (1980), is that one would expect secondary-to-primary ratios to increase with increasing energy as lower energy particles are moved to higher energies by the repeated reaccelerations. Although this is the trend observed in the data up to ~ 1 GeV per nucleon, at higher energies the ratio decreases with increasing energy, in disagreement with the model predictions. However, Lerche and Schlickeiser (1985) claim that such an objection to the continuous acceleration model is invalid and arises solely from the incorrect assumption of equality, for primaries and secondaries, of the reciprocal sum of spallation and escape lifetimes.

Several works discuss the predictions, for the variation of the B/C ratio, of models in which the cosmic rays obtain most of their energy from an initial acceleration (possibly in or near the source) and experience minor reacceleration during propagation in the Galaxy (Silberberg *et al.* 1983, 1985; Simon, Heinrich, and Mathis 1985, 1986). However, the variations at low energy have not been considered in detail.

VII. DEPLETION OF SHORT PATH LENGTHS IN THE PLD

We turn now to the second problem discussed in § I, the shape of the cosmic-ray path length distribution. Figure 2 illustrates the problem: at energies below several GeV per nucleon a propagation calculation which reproduces the B/C ratio does not simultaneously reproduce the measured sub-Fe/Fe ratio. The sub-Fe/Fe ratio is important for determining the relative abundance of short path lengths in the PLD, since the larger total inelastic cross section for iron, compared with that of C or O (see Appendix), makes the sub-Fe/Fe ratio sensitive to small amounts of matter traversed. Figure 9 shows a comparison of the compiled data for the sub-Fe/Fe ratio with the curve giving the prediction for the energy-dependent exponential PLD discussed in § V. Note that the curve is in agreement with the data at high energy, but the agreement becomes progressively worse toward the lower energies, indicating a need for more iron fragmentation at low energies. This can be accomplished by reducing the number of short path lengths in the PLD (truncation—cf. distributions B and C in Fig. 1), which causes more iron to interact, while producing only a small effect on the calculated B/C ratio. However, as we reported earlier (Garcia-Munoz *et al.* 1984),

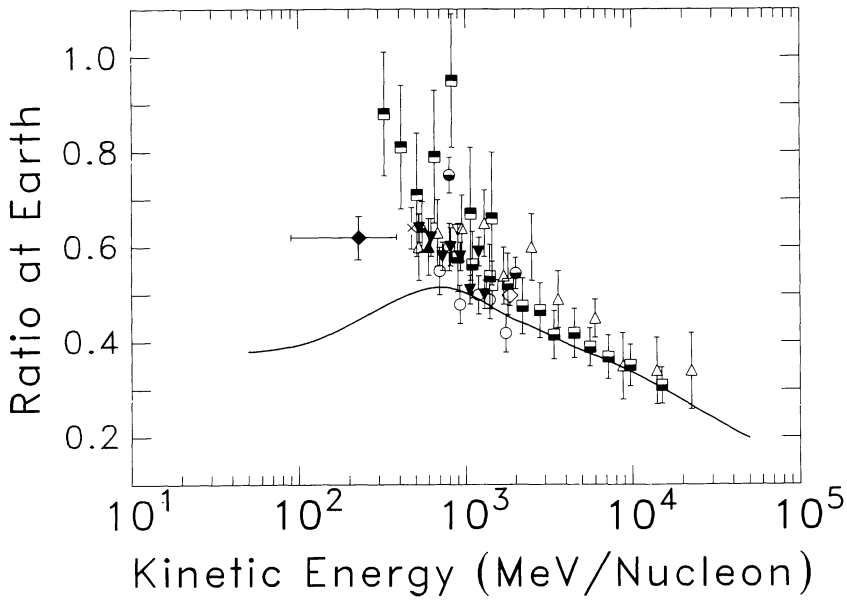

FIG. 9.—Calculated sub-Fe/Fe (Sc+Ti+V+Cr+Mn/Fe) ratio using the energy-dependent exponential PLD (see Fig. 8) compared with the compiled experimental data. (Data references as in Fig. 2*b*.)

to explain the data over the full energy range of Figure 9, it is necessary to remove short path lengths *as a function of energy*, with the largest truncation occurring at the lowest energies. Figure 10 shows an example of calculated ratios for such a truncated PLD where the calculations fit *both* the B/C and the sub-Fe/Fe ratio.

The Sc/Fe and V/Fe ratios are preferable to the sub-Fe/Fe ratio as tracers of the abundance of short path lengths, and Figure 11 shows the available experimental data for these ratios. The most precise data are the *HEAO* results measured above 1 GeV per nucleon (*half-filled squares*). At low energy only the *IMP 8* point is available. The two sets of curves correspond to the results of propagation calculations for (*a*) the energy-dependent exponential PLD of § V (cf. Figs. 7 and 9) and (*b*) the energy-dependent *truncated* PLD used in the calculations of Figure 10. Overall, curves *b* give a better fit to the data, especially at low energy. The calculations appear to underestimate, slightly, the high-energy V/Fe ratio from the *HEAO* data. This can be explained by a small increase in the vanadium partial production cross section, or may indicate the need for some truncation in the PLD at high energy. The latter is favored by Margolis (1986), who employed a parametrized analysis of the PLD, neglecting ionization energy loss, to show that a nonzero truncation is most consistent with the high-energy data. In order to provide a more stringent test for the depletion of short path lengths, better Sc/Fe and V/Fe measurements (~10% uncertainty) are needed at energies below several GeV per nucleon.

We next consider whether alterations in the adopted parameters in the propagation model eliminate the need for energy-dependent truncation of the PLD. Garcia-Munoz *et al.* (1981*b*) investigated this question at a single energy of 1 GeV per nucleon. In this analysis we study the sensitivity to the parameters as a function of energy. The results are shown in Figure 12. Starting with the energy-dependent exponential PLD from Figure 9 (curve *a* in Fig. 12), each of the curves labeled 1–4 shows the effect of a parameter change *added to* the effects of all preceding changes.

Curve 1.—Inclusion of source abundances in solar system proportion for the sub-Fe elements.

Curve 2.—Use of the energy-independent total inelastic cross sections from Protheroe, Ormes, and Comstock (1981).

Curve 3.—Increase of all partial production cross sections by 15%.

Curve 4.—Adoption of a total energy source spectrum with $T_0 = 931$ MeV per nucleon and $\gamma = -2.3$ (the main effect here is due to the change in T_0, not to the different power-law index).

Curve 4 gives reasonable agreement with the sub-Fe/Fe ratio and demonstrates that it is possible to conclude that no truncation is necessary in the PLD, but *only* if one accepts, simultaneously, all of the above alterations in the input parameters.

The available experimental evidence favors a cosmic-ray source spectrum in rigidity which is close to our $(T+400)^{-\gamma}$ form, as shown in the Appendix. Also, Figure 16 in the Appendix shows that the total cross section excitation functions are definitely energy-dependent (Garcia-Munoz, Simpson, and Wefel 1980; Letaw, Silberberg, and Tsao 1983). Alteration 3 above is unlikely, although uncertainties remain in the partial production cross sections, and, finally, the inclusion of sub-Fe abundances at the source alone cannot give agreement. Thus, the experimental evidence points to an *energy-dependent truncation* in the PLD (curve *b* in Fig. 12) as the best explanation for the cosmic-ray data.

VIII. FUNCTIONAL FORMS FOR THE DEPLETION

To analyze the truncation of the PLD quantitatively, two forms of truncation have been studied: a "zero-short" (ZS) PLD and a "double exponential" (DE) PLD. The ZS PLD is

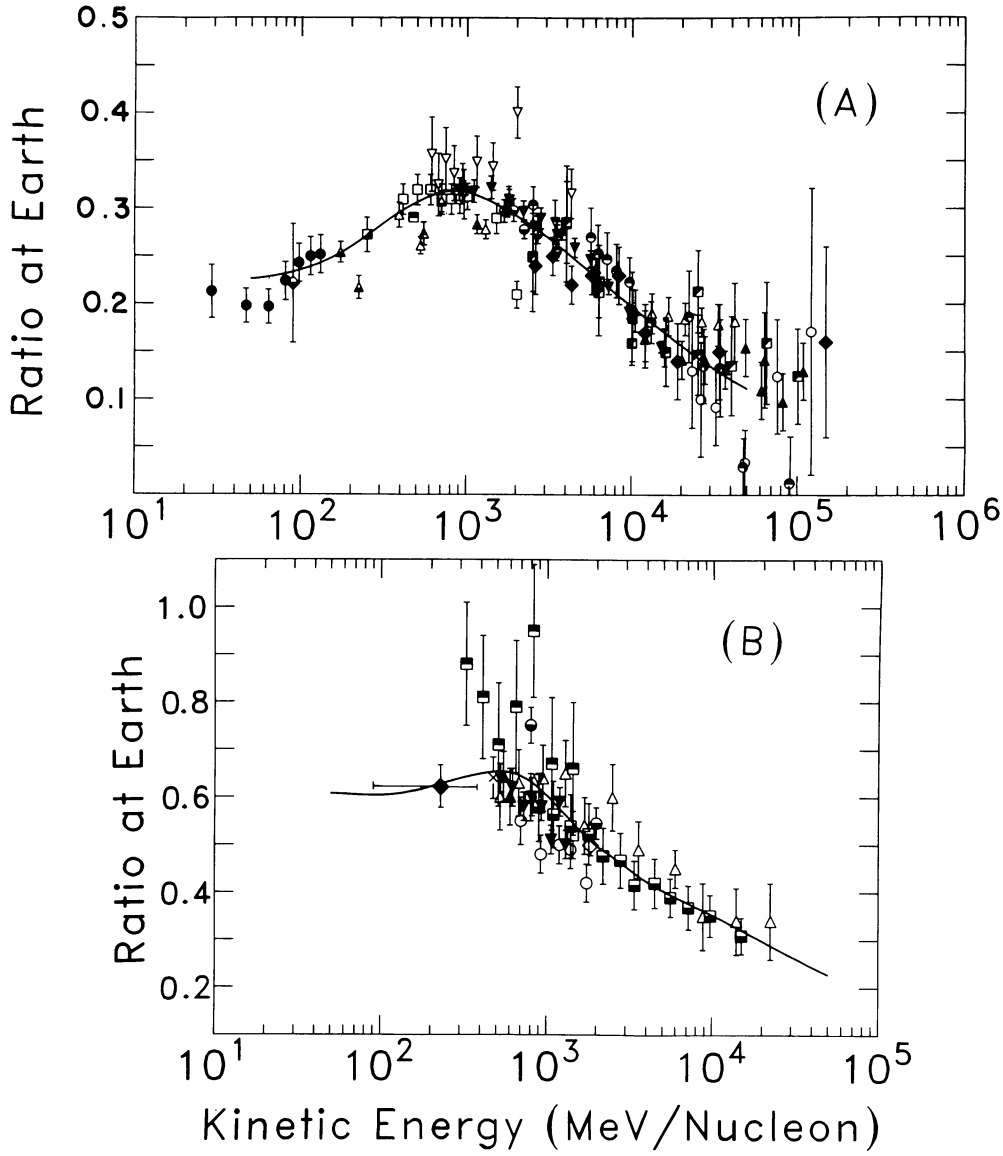

FIG. 10.—The ratios (*a*) B/C and (*b*) sub-Fe/Fe of Fig. 2 compared with the results of a propagation calculation using a path-length distribution that includes an energy-dependent deficiency of short path lengths as well as an energy-dependent mean for the exponential part of the distribution. (See text for details.)

given by

$$P(x) = \begin{cases} 0 & \text{for } x < X_c, \\ (1/X_0)\exp(-x/X_0) & \text{for } x \geq X_c, \end{cases} \quad (4)$$

where $P(x)$ is the (normalized) probability distribution and X_c and X_0 are parameters determined, as a function of energy, from the data. Equation (4) may be interpreted as cosmic rays passing through a slab of matter before propagation in the Galaxy, as might be realized from a shell of matter surrounding the cosmic-ray source regions (e.g., Garcia-Munoz and Simpson 1970; Cowsik and Wilson 1975). The parameter X_c determines the thickness of the matter shell. The shape of the ZS PLD is shown in Figure 1*b*.

The DE PLD is represented by

$$P(x) = \begin{cases} \dfrac{\exp(-x/X_1) - \exp(x/X_2)}{X_1 - X_2} & \text{for } X_1 \neq X_2, \\ \dfrac{x\exp(-x/X_1)}{X_1^2} & \text{for } X_1 = X_2, \end{cases} \quad (5)$$

where X_1 and X_2 are parameters determined from the data. Equation (5) is the PLD resulting from the "nested leaky box" model (Cowsik and Wilson 1973, 1975; Simon 1977), with energy-dependent escape lengths. A sketch of the shape of the DE PLD is shown in Figure 1*c*.

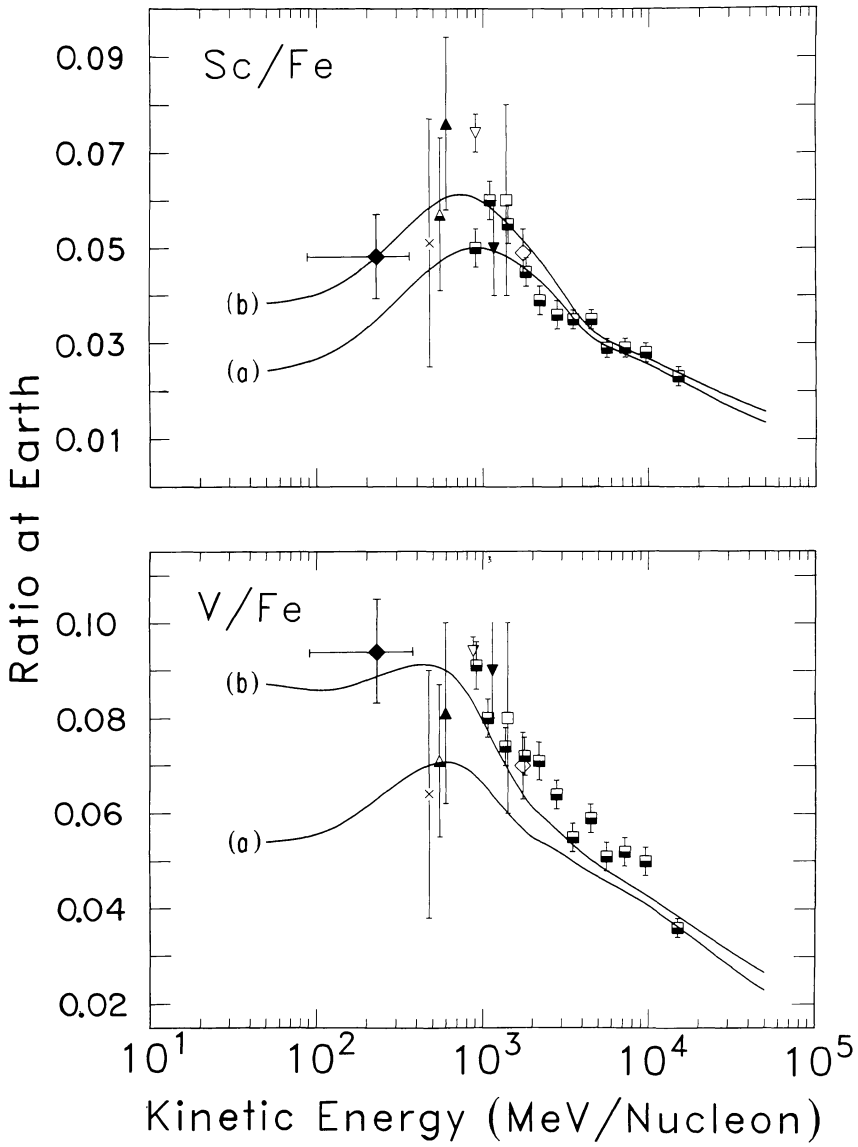

FIG. 11.—Measurements of the ratios Sc/Fe (*top*) and V/Fe (*bottom*) compared with a calculation using a PLD with no truncation (curves *a*) and with an energy-dependent truncation (curves *b*). (Data references as in Fig. 2*b*.)

The parameters X_0, X_c, or X_1, X_2, are evaluated, as a function of energy, by requiring that the calculations fit, simultaneously, both the B/C and the sub-Fe/Fe ratios over the full energy range of the experimental data. The derived energy dependence of the parameters is shown in Figure 13 for the ZS PLD (*a*) and the DE PLD (*b*). The mean path length, $\langle X \rangle$, as a function of energy is also shown on both plots. The principal exponential component, X_0 or X_1, shows a behavior identical with the energy-dependent exponential PLD discussed earlier (and shown in Fig. 7). This component is identified with Galactic propagation, and the interpretation of the energy dependence discussed in § VI applies to this component.

The new feature of the ZS and DE PLD models is the energy-dependent depletion of short path lengths characterized respectively by the parameters X_c and X_2. These parameters are largest at low energy and decrease with increasing energy to become negligible at 3–5 GeV per nucleon. (A small constant value for X_c or X_2 at high energy cannot be ruled out with current experimental data.)

It should be noted that the energy scale in Figure 13 refers to energies outside the heliosphere in local interstellar space. Considering solar modulation, the region actually studied by the available data corresponds to energies ≥ 300 MeV per nucleon.

IX. IMPLICATIONS OF THE TRUNCATION OF THE PLD

The truncation components, X_c and X_2, are most easily interpreted as properties of the cosmic-ray source regions. In the simplest model, the ZS PLD would correspond to a shell of material around the source regions with the energy dependence of X_c produced by trapping that increases with decreasing particle energy or magnetic rigidity. In the DE PLD

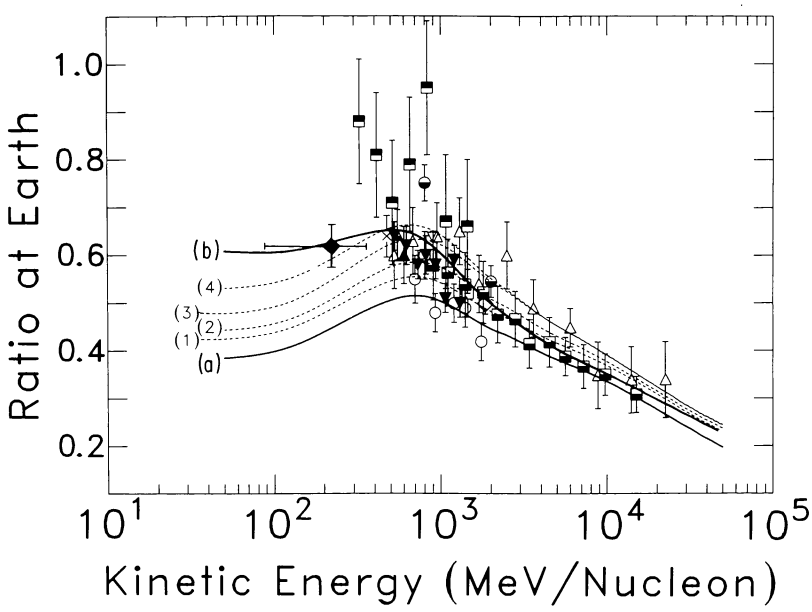

FIG. 12.—The experimental sub-Fe/Fe ratios, compared with calculations using the energy-dependent truncated PLD (curve *b*), and calculations using a PLD with no truncation and different input parameters. Curve *a* (reproduced from Fig. 9) and curves 1–4 have been calculated using energy-dependent exponential PLDs which fit the B/C measurements over the full energy range. The different curves result from cumulative additions in the input parameters: curve 1, sub-Fe element abundances at the source; curve 2, effect of energy-independent total inelastic cross sections; curve 3, effect of increasing all partial cross sections by 15%; curve 4, effect of adopting a source spectrum in total energy with $\gamma = -2.3$ (see text for details). (Data references as in Fig. 2*b*.)

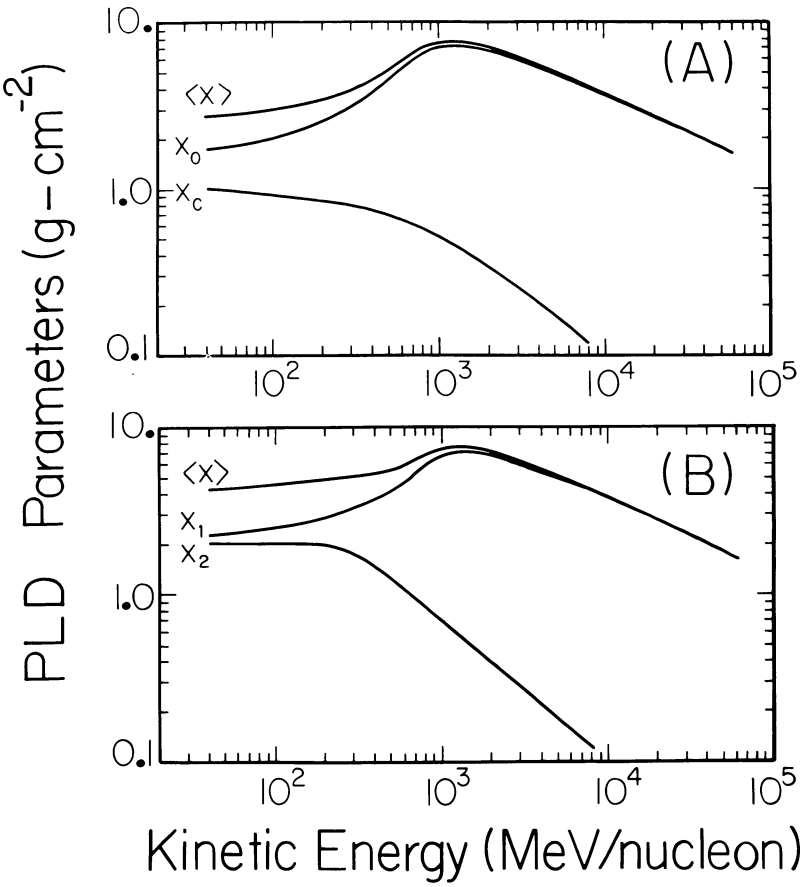

FIG. 13.—Energy dependence of the parameters in the models involving a depletion of short path lengths. (*a*) Derived energy dependence of the parameters X_c and X_0 in the ZS PLD of eq. (4) and of the mean amount of matter traversed. A sketch of the shape of the ZS PLD is given on Fig. 1*b*. (*b*) Derived energy dependence of the parameters X_1 and X_2 in the DE PLD of eq. (5) and of the mean amount of matter traversed. A sketch of the shape of the DE PLD is given in Fig. 1*c*.

model, X_2 corresponds to the mean of the distribution of matter traversed by the particles in leaving the source regions. The energy dependence of X_2 implies that the particles leak out of the source region in an energy-dependent fashion with, effectively, no trapping for particles above ~ 5 GeV per nucleon. In both cases it is assumed that the particles are first accelerated and then propagate in the vicinity of the sources before being released into the Galaxy.

An alternative explanation for X_c or X_2 may involve interstellar acceleration. If the cosmic rays are accelerated by interstellar shock waves, then the matter traversal could reside in the shocks. The energy dependence of X_c or X_2 argues against such an interpretation, since, for shock acceleration, the higher the particle energy, the more passes across the shock are needed. This would imply larger matter traversals with increasing energy, just opposite to the energy dependence found experimentally for X_c and X_2 in Figure 13.

Shock acceleration may indeed be responsible for energizing the cosmic rays, but the constraint implied by the energy dependence of the truncation parameters argues for localized sources of high-energy particles. Such a configuration might be realized within a supernova remnant (e.g., Wefel 1981) or within an OB association with intense stellar evolution activity (e.g., Reeves 1981; Olive and Schramm 1982). Such possible "source" regions have been mentioned recently in connection with the heavy-isotope overabundances observed in cosmic-ray source matter (e.g., Mewaldt 1983; Simpson 1983).

A final possibility for explaining the observed energy-dependent truncation involves particle transport in an inhomogeneous interstellar medium (Bretthorst and Margolis 1985), in particular, the penetration/trapping of cosmic rays in large clouds (column densities 0.1–0.2 g cm^{-2}) in the interstellar medium (Volk 1983; Morfill, Meyer, and Lust 1985). At high cosmic-ray energies, the interstellar clouds are relatively transparent to the particles, but at lower energy there can be some scattering/diffusion. For large clouds that are undergoing accretion of matter from the interstellar medium, the cosmic rays are convected into the cloud where compression occurs. The magnetic field irregularities in such clouds scatter the particles, with the largest effects at low particle energy. Thus, the cosmic rays which find themselves in one of these clouds would undergo energy-dependent trapping, with the lowest energy particles residing the longest times and thereby passing through the largest amount of matter. Qualitatively, such a scenario could produce the energy dependence observed for the truncation parameters X_c and X_2.

X. DISCUSSION

The results on the shape and the energy dependence of the PLD discussed above rely on compiled cosmic-ray data and on the nuclear excitation functions. For the latter we have used a combination of compiled experimental data and semiempirical calculations. Recently, new cross section data measured at the LBL Bevalac have become available (Webber 1985; Webber and Kish 1985) which indicate that the cross sections for the production of the element boron in ^{12}C interactions may be smaller than the values reported in earlier experiments. A similar trend was reported for iron fragmentation.

In the cosmic-ray problem, the production of boron involves principally the cross sections for production of ^{10,11}B and radioactive ^{10,11}C, which decay to boron. At 415 MeV per nucleon, Webber and Kish (1985) report values for ^{10}B + ^{10}C and ^{11}B + ^{11}C production which are 32% and 13%, respectively, below the values employed in this analysis (cf. Fig. 3). These reduced values fall within our uncertainty limits for the boron cross sections (§ V*b*) and have the effect of decreasing the calculated B/C ratio. Should these smaller cross section results be verified, then, in the present analysis, the PLD would decrease less strongly with decreasing energy below 1 GeV per nucleon, bringing the empirically determined PLD into better agreement with Galactic wind calculations (Fig. 7*b*) for wind velocities ≤ 20 km s^{-1}. Webber *et al.* (1985) and Soutoul *et al.* (1985) have employed these new cross sections in an analysis of *HEAO* C-2, balloon, and satellite data (such as our compiled data in Fig. 2) in a leaky box model and have found that at energies below 1 GeV per nucleon an escape length proportional to particle velocity reproduces the experimental data, confirming the conclusion reached in § VI.

The changes in the cross sections for iron fragmentation suggested by Webber (1985; but see also Lau, Mewaldt, and Stone 1985) lead to a reduced production of sub-Fe elements, particularly at energies below several GeV per nucleon. Use of these cross sections gives a large discrepancy in the values of the escape length needed, in a leaky box model, to reproduce separately the experimental B/C and sub-Fe/Fe ratios (Soutoul *et al.* 1985). Investigating the effect of including intestellar helium in the calculations (which has already been done in all the calculations reported in this paper), Ferrando, Goret, and Soutoul (1985) showed that the discrepancy in escape lengths became even larger. These papers verified the conclusion presented by Garcia-Munoz *et al.* (1984), and developed in detail in this paper, that an energy-dependent depletion of short path lengths in the PLD is needed to reproduce simultaneously the measured B/C and sub-Fe/Fe ratios. The detailed effect of these new iron fragmentation cross sections is to increase slightly the value of X_c or X_2 at low energy (Fig. 13) and to extend to higher energy the range over which the X_c or X_2 component is important.

A unique test for the energy-dependent depletion of short path lengths in the PLD involves the ultraheavy (UH; $Z > 30$) cosmic rays whose total inelastic cross sections are larger than that of iron, thereby making the UH cosmic rays more sensitive to the short path lengths in the PLD. Unfortunately, there have been no reliable studies of low-energy UH cosmic rays, but at higher energies the two existing satellite experiments *HEAO* C-3 (Binns *et al.* 1981, 1984) and *Ariel 6* (Fowler *et al.* 1985*a*, *b*) do provide data at different energies owing to the differences in their orbits. The mean energy for the *Ariel* data set is lower than that for the *HEAO* data set and might therefore be expected to show more effects due to the depletion of short path lengths. Klarmann *et al.* (1985) have analyzed two secondary-to-primary ratios, $(70 \leq Z \leq 73)/(74 \leq Z \leq 86)$ and $(62 \leq Z \leq 69)/(74 \leq Z \leq 86)$, and find that the *Ariel* ratios are significantly larger than the *HEAO* ratios. Further, the *HEAO* ratios are in agreement with calculations using a rigidity-dependent escape length at these high energies. Qualitatively, these observations are expected from the energy-dependent truncation discussed in § VII. At

the *HEAO* energies, the PLD is effectively exponential with a rigidity (energy) dependent mean. At the lower *Ariel* energies, there is still an important contribution from the truncation, which would increase the amount of spallation and, consequently, the secondary-to-primary ratios, as observed in the data. Thus, the UH cosmic rays can provide a test for the energy-dependent depletion effect in the PLD once UH secondary-to-primary ratios can be measured over a large energy range including low energies (so far not accessible to low-altitude non–polar-orbiting satellites).

XI. CONCLUSIONS

Using compiled cosmic-ray data as a function of energy and a complete Galactic propagation plus solar modulation model, we have studied the cosmic-ray path-length distribution at low energy and find the following:

1. The mean of the PLD varies with the energy over the full range of energies investigated (0.1–50 GeV per nucleon).
2. The PLD can be represented by an exponential distribution in which there is a depletion of short path lengths which decreases with increasing energy.

The energy dependence of the Galactic confinement/propagation is consistent with dynamical halo models involving Galactic winds with velocities in excess of 20 km s^{-1} and also with particle loss from the Galaxy via "magnetic bubbles" inflated by the cosmic rays. The rigidity-dependent loss of cosmic rays from the confinement region observed at high energies does not continue to be dominant at low particle energies. The short path length depletion may be the result of a two-stage propagation, first in the source/acceleration region and then in interstellar space.

The source/acceleration region is characterized by an energy-dependent trapping of the low-energy cosmic rays, with the lowest energy particles constrained to pass through the largest amount of material. The new factor introduced by the two confinement regions and the energy-dependent particle confinement can explain the existing body of cosmic-ray data and provides new constraints for models of the cosmic-ray source/acceleration process.

We would like to thank S. Hayakawa, H. Volk, R. Mewaldt, and M. Wiedenbeck for useful discussions, and V. Zuell, G. Sutton, and M. Prouty for help in manuscript preparation. This work was supported in part by NASA grant NGL-14-001-006, contract NAS 5-25731, and NSF grant ATM 84-12382 at the University of Chicago; in part by NASA grant NAGW-550 and the Department of Physics and Astronomy at Louisiana State University; and in part by NASA grant NAG-8848 and The McDonnell Center at Washington University. J. A. Simpson would like to thank the John Simon Guggenheim Foundation for a fellowship in 1984–1985.

APPENDIX

THE GALACTIC PROPAGATION MODEL AND THE INPUT PARAMETERS

Cosmic-ray propagation calculations by different groups have often produced conflicting results, even when the same experimental data set is employed. These differences have been the subject of much recent debate (highlighted in Freier 1981), the principal conclusion being that the differences can be traced directly to (1) varying levels of sophistication in the propagation computer codes and (2), most important, differences in the adopted input parameters, particularly the nuclear fragmentation cross sections. Therefore, in this Appendix we present a discussion of our Galactic propagation code and the input parameters selected for the problem. The following subsections describe, in detail, (1) the calculation technique, (2) the reaction list and the radioactive decays, (3) the total inelastic cross sections, (4) the fragmentation partial cross sections, (5) electron capture and loss cross sections, (6) ionization energy loss, (7) the interstellar medium, and (8) the cosmic-ray source abundances and source energy spectrum. In each subsection, the results presented are those relevant to the analysis of the shape and the energy dependence of the cosmic-ray path-length distribution discussed in the body of this paper.

I. CALCULATIONAL TECHNIQUE

We employ the weighted-slab technique of cosmic-ray propagation (e.g., Ginzburg and Syrovatskii 1964; Fichtel and Reames 1968; Garcia-Munoz, Mason, and Simpson 1977*a*; Lezniak 1979) using a Lagrangian computer algorithm written by one of us (S. H. M.). The basic idea is to solve the slab propagation equation,

$$\frac{dN_i(E,x)}{dx} = \frac{\partial}{\partial E}\left(\left.\frac{dE}{dx}\right|_i N_i\right) - \frac{N_0}{\bar{A}}\sigma_i N_i + \sum_{j\neq i}\frac{N_0}{\bar{A}}\sigma_{ij}N_j - \frac{N_i}{\gamma\beta cn\bar{A}T_i} + \sum_{j\neq i}\frac{N_j}{\gamma\beta cn\bar{A}T_j}, \tag{A1}$$

for many small increments (usually $\Delta x = 0.1$ g cm^{-2}) from $x = 0$ to $x = x_{max}$ and to store the results $[N_i(E,x)]$ of each incremental step. In equation (A1), $N_i(E,x)$ is the number density of species i at energy E after traversing a distance x, in g cm^{-2} of interstellar matter; n is the density (in atoms cm^{-3}) of the interstellar medium; $\bar{A}$ is the mean atomic weight of an average atom of interstellar gas; β is the particle velocity in units of the velocity of light; γ is the particle Lorentz factor; σ_i is the total inelastic cross section for the interaction of species i (i.e., the mass changing $\Delta A \geq 1$ cross section); σ_{ij} is the partial cross section for the production of species i from interactions of species j; T_i is the mean lifetime of species i for radioactive decay; T_j is the mean lifetime for the production of species i as a daughter nucleus in the radioactive decay of species j; and $(dE/dx)|_i$ is the ionization energy loss rate for species i. Thus, equation (A1) is actually a coupled set of first-order differential equations which

must be solved simultaneously for all species i. Currently, we consider 96 isotopic "species" (see Appendix §§ II and V) ranging from ^{4}He through the isotopes of the element nickel.

Once the set of equations (A1) have been solved, the number density of species i at the boundary of the heliosphere is obtained by numerical integration as

$$n_i = \int_0^\infty P(x, E)\, N_i(E, x)\, dx \tag{A2}$$

for each energy point of interest. $P(x, E)$ is the path-length distribution (PLD), a probability distribution for particles observed at energy E to have passed through an amount of material x, and $N_i(E, x)$ are the intermediate slab distributions. In practice, the upper limit of integration in equation (A2) is replaced with $x_{\max}$, which is selected so that the integral between $x_{\max}$ and infinity contributes less than 1% to the total integral. All of the PLDs investigated in this paper are based upon an exponential function for which, at 1 GeV per nucleon, the mean of the exponential is in the range 8–9.5 g cm^{-2}, and we have adopted $x_{\max} =$ 30 g cm^{-2} as the operational upper limit.

The weighted-slab method, as used here, is an exact solution of the diffusion equation when ionization energy loss is neglected (Ginzburg and Syrovatskii 1964). However, in the presence of energy loss, Lezniak (1979) has shown that the weighted-slab technique does not yield an exact solution to the diffusion equation unless several correction terms are included. At high energies, where ionization energy loss is less important, these correction terms are negligible. At lower energies, it can be shown that the magnitude of the corrections, evaluated in terms of the secondary-to-primary ratios discussed here, are smaller than the other uncertainties in the calculations—for example, the cross section uncertainties. The PLDs used in this paper are similar to PLDs which have been discussed in the literature, allowing our results to be compared directly with previous work. A fuller description of the mathematical form of an energy-dependent PLD derived from the diffusion equations will be presented elsewhere.

Below several GeV per nucleon, the ionization energy loss causes the largest change in particle number during propagation. In the calculations reported here, the numerical solutions of equations (A1) are tailored to this condition. A set of energy bins is established initially, consistent with a resolution parameter, $\Delta E/E$, which is set externally. The size of $\Delta E/E$ determines the width of each energy bin and the number of bins required to cover the region of the energy spectrum of interest. Each energy bin is filled with particles as determined by the source relative abundances and the source energy spectrum. The calculation then proceeds in small steps Δx, with the size of Δx determined by the ratio of the grid spacing ΔE to the maximum energy loss rate. The overall speed of the calculation is determined by the species of highest charge at the lowest energies. For each step, the boundaries of the energy bins are permitted to move in energy space; the lower boundary moves faster than the upper boundary because of the increasing ionization energy loss with decreasing particle energy. For each step, the number of particles of species i in each energy bin is varied according to losses by nuclear interactions and radioactive decay and to gains due to interactions or decay of all species j affecting species i, assuming $\Delta\beta = 0$ for secondary particle production in nuclear interactions (Heckman *et al.* 1972). Fragmentation and decay products generated within each step are permitted to decay through the network of isotopes. Accuracy is maintained by using analytic solutions for the calculation of such products within each step. Cross sections for each species are calculated at the energy corresponding to the bin center (in energy) from an analytic expression for the total inelastic cross sections (see Appendix § III) and by interpolation in a large matrix for the fragmentation partial cross sections. The time for radioactive decay corresponding to a step Δx is calculated assuming a uniform density and composition of the propagation medium. Species decaying by electron capture present a special problem and are discussed in Appendix § V.

Two consequences of this technique are that the energy bins continue to grow in width and that the lowest energy bin moves below the lower energy limit as the calculation progresses. The latter problem is handled by collecting the lowest energy particles in a single bin below the lower energy limit of the calculation. In addition, the code includes an automatic "rezoning" procedure which subdivides energy bins which have become too wide (as determined by the $\Delta E/E$ criterion). The code resembles others employing a Lagrangian formulation of hydrodynamics (Richtmyer and Morton 1967) in that particles are evolved along characteristics of the energy-loss relation. This technique maintains an accurate energy dependence for the number densities of both primary (i.e., source-produced) and secondary (i.e., produced by nuclear interactions during propagation) particle species.

Another technique to solve equations (A1), developed a number of years ago at the University of Chicago by J. D. Anglin (Garcia-Munoz, Mason, and Simpson 1977*a*; Blake *et al.* 1978; see also Jones 1979*a* for a similar solution technique employing residual range) and used in much of our previous work, involves inverting the transformation matrix formed for propagation through a step Δx, accounting for fragmentation, radioactive decay, and energy loss, and then interpolating to correct the fluxes back to a fixed energy grid. The accuracy of this technique is limited, again, by the step size Δx and the number of points in the fixed energy grid. Using identical sets of input parameters, we have compared the results of both codes and found them to be in agreement to within a few percent, with the largest deviations occurring, as expected, at the lowest energy points. The level of agreement can be improved by reducing $\Delta E/E$ and the step size Δx in both codes, but at a cost of a prohibitively large amount of computer storage and CPU time. As a practical matter, it is necessary to adjust $\Delta E/E$ and/or the step Δx to fit a given calculation and a finite computer budget.

For an energy-independent exponential PLD, $P(x) = (1/x_0) \exp(-x/x_0)$, where x_0 is the "mean" of the PLD, the results of this technique are equivalent to a leaky box model in which the escape length λ_e equals x_0 (Cowsik *et al.* 1967). In the case of no energy loss, the leaky box equations can be solved analytically and compared with the computer calculations, giving in our case agreement to better than 2%. A pseudo–energy loss (constant dE/dx) can be included and still permit an analytic solution to the

leaky box equations, and in this test case the analytical result compares equally well with the full computer calculation. Finally, the computer results can be compared with the calculations of other groups, using a predetermined set of input parameters, and again our code is in good agreement with the results from other groups for cases both with and without energy loss (Freier 1981; Wiedenbeck 1981; Ormes 1981).

II. REACTION LIST AND RADIOACTIVE DECAY

The species actually followed in the propagation calculations consist of all the stable isotopes between ^{4}He and ^{64}Ni plus the long-lived radioactive isotopes (β-unstable) and electron capture isotopes. Figures 14 and 15 present a "cosmic-ray progenitor" chart of the nuclides. The stable isotopes are shown as shaded squares, and the radioactive species as squares which are open or with shading in the upper right and lower left corners. Radioactive isotopes must have half-lives $T \geq T_{\rm limit}$ to be included in the propagation calculation. For the results reported here, and displayed in Figures 14 and 15, $T_{\rm limit}$ is 10^5 years.

Isotopes with $T < T_{\rm limit}$ (in Figs. 14 and 15, *unshaded squares*) are included in the calculation of the cross section data file by assuming decay immediately upon formation as an interaction product. The cross section for the production of species j from an interaction of species i, then, is computed as the sum of the cross section for the direct production of species j ($i \rightarrow j$) plus the cross sections for all of the radioactive progenitors of species j. All of the known nuclides were considered as progenitors (Lederer and Shirley 1978; Ajzenberg-Selove 1977, 1978, 1979, 1980, 1981; Endt and van der Leun 1978) including many newly discovered nuclei off the valley of β stability (Arthukh *et al.* 1969, 1970*a*, *b*, 1971; Auger *et al.* 1979; Butler *et al.* 1977; Detrax *et al.* 1979; Fintz *et al.* 1976; Poskanzer *et al.* 1966, 1968; Roeckl *et al.* 1974; Symons *et al.* 1979; Thomas *et al.* 1968; Westfall *et al.* 1979*a*). Decay by β-particle emission was assumed unless energy level data or decay studies (Freedman *et al.* 1978; Gronemeyer *et al.* 1980; Hardy *et al.* 1980; Alburger, Millener, and Wilkinson 1981; Aysto *et al.* 1981; Benenson *et al.* 1978; Bogatin *et al.* 1980; Eskola *et al.* 1980; Ewan *et al.* 1980; Kekelis *et al.* 1978; Norman, Davids, and Moss 1978) indicated otherwise. Known branches

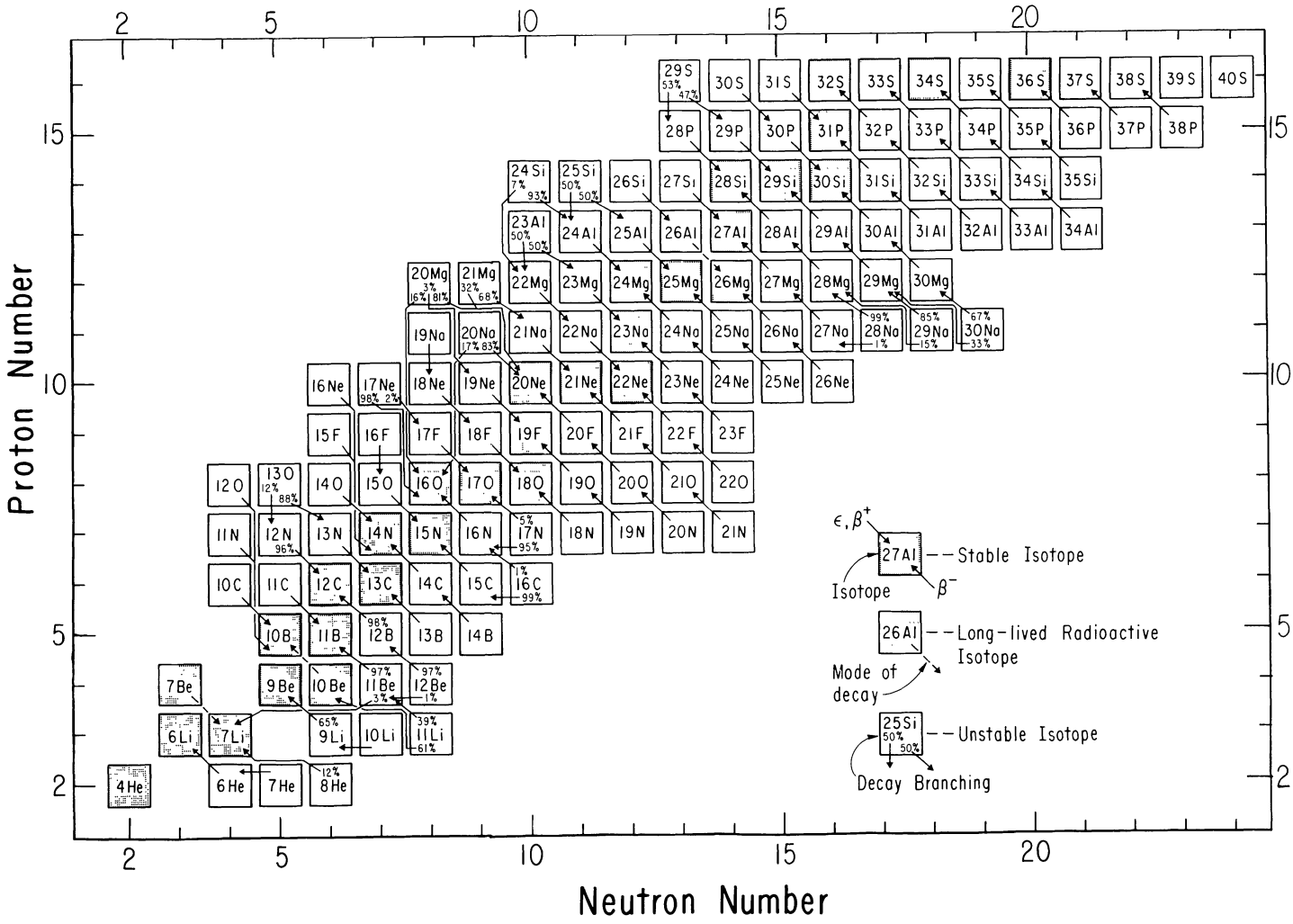

FIG. 14.—Cosmic-ray progenitors for the elements helium through sulfur

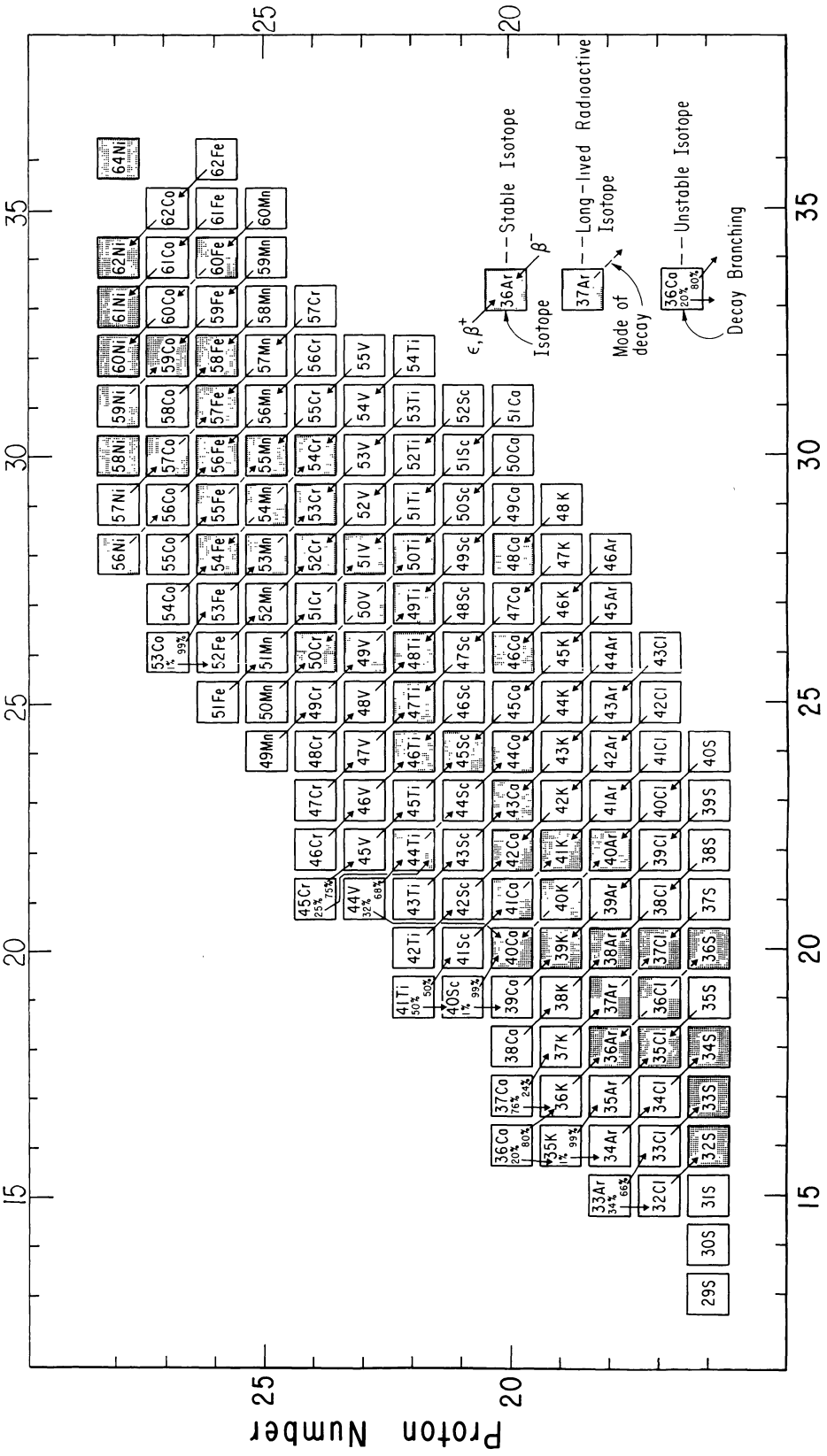

FIG. 15.—Cosmic-ray progenitors for the elements sulfur through nickel

TABLE 2

RADIOACTIVE SPECIES

NUCLEUS	DECAY	DAUGHTER	HALF-LIFE (years) Laboratory	HALF-LIFE (years) Cosmic Ray	NOTES
^{7}Be	ε	^{7}Li	0.146	0.307	1,2
^{10}Be.....	β^-	^{10}B	1.5×10^{6}	1.6×10^{6}	
^{26}Al	β^+	^{26}Mg	7.4×10^{5}	8.8×10^{5}	3
^{36}Cl	β^-	^{36}Ar	3.07×10^{5}	3.07×10^{5}	3
^{36}Cl	β^+	^{36}S	...	1.8×10^{12}	3,4
^{37}Ar	ε	^{37}Cl	0.099	0.209	1,2
^{40}K	β^-	^{40}Ca	1.28×10^{9}	1.43×10^{9}	3,4
^{40}K	β^+	^{40}Ar	...	1.24×10^{12}	3,4
^{41}Ca	ε	^{41}K	8×10^{4}	2.2×10^{5}	1
^{44}Ti	ε	^{44}Ca	48	100	1,2
^{49}V	ε	^{49}Ti	0.904	1.90	1,2
^{50}V	ε	^{50}Ti	4×10^{16}	5.25×10^{16}	4
^{50}V	β^-	^{50}Cr	...	1.33×10^{17}	4
^{51}Cr.....	ε	^{51}V	0.0762	0.160	1,2
^{53}Mn.....	ε	^{53}Cr	3.7×10^{6}	7.7×10^{6}	1
^{54}Mn.....	β^+	^{54}Cr	...	$\sim10^{9}$	4
^{54}Mn.....	ε	^{54}Cr	0.83	1.75	1,2
^{54}Mn.....	β^-	^{54}Fe	2×10^{6}	$\sim2\times10^{6}$	
^{55}Fe.....	ε	^{55}Mn	2.6	5.47	1,2
^{60}Fe.....	β^-	(^{60}Co)^{60}Ni	1×10^{5}	1×10^{5}	
^{57}Co	ε	^{57}Fe	...	1.55	1,2
^{56}Ni.....	ε	(^{56}Co)^{56}Fe	0.017	0.0358	1,2
^{56}Ni.....	β^+	(^{56}Co)^{56}Fe	2×10^{5}	$\sim2\times10^{5}$	
^{59}Ni.....	ε	^{59}Co	8×10^{4}	1.7×10^{5}	1

NOTES–(1) Electron shells and screening effects. (2) Treatment of X* state unnecessary. (3) Assuming electron capture branch is inactive in cosmic rays. (4) Can be omitted from consideration as a decay, if desired.

in the decay schemes of the progenitors (for example, Vieira, Gough, and Cerny 1979) have been included and are indicated in Figures 14 and 15.

Table 2 lists all of the radioactive isotopes included as species to be propagated. The possible decay modes and stable cosmic-ray daughters are indicated along with the half-lives. The column labeled "Laboratory" gives the half-life measured or calculated (Casse 1973*a*, *b*; Wilson 1978) for decay in the laboratory. The column headed "Cosmic Ray" gives the expected half-life for fully stripped nuclei in the cosmic-ray beam. The differences arise (1) from small electron capture branches which are assumed to be inactive (compared with the faster β decay) in the cosmic rays, (2) from the fact that in the laboratory there are two S shall electrons to participate in electron capture, and (3) from screening effects (Wilson 1978). Note 4 to Table 2 indicates those decays whose half-lives are long enough to be effectively inoperative for the cosmic-ray propagation problem.

For isotopes that are observed to decay in the laboratory only by electron capture, it is necessary to estimate the half-life of any energeticaly allowed (but not observed in terrestrial experiments) β decay. This was done using the atomic mass table of Wapstra and Gove (1971) with branching ratios from Gove and Martin (1971). For ^{59}Ni any positron decay would have an extremely long lifetime and can be neglected. For ^{54}Mn and ^{56}Ni, we adopt the estimates of Casse (1973*a*, *b*) with the understanding (Wilson 1978) that these half-lives may be in error by as much as a factor of 5! Clearly, experimental measurements of these half-lives are very much needed.

III. TOTAL INELASTIC CROSS SECTIONS

For each isotope considered in the calculations, it is necessary to have values of the total inelastic or mass-changing ($\Delta A \geq 1$) cross section at all of the energies of interest. Traditionally, these cross sections have been calculated from the energy-independent overlap model (Bradt and Peters 1950; Daniel and Durgaprasad 1962; Silberberg and Tsao 1977*b*; Hagen 1976; Stone and Wiedenbeck 1979) with different forms for the overlap correction parameter. Alternatively, some groups have used formulae proposed by Kirkby and Link (1966) or Renberg *et al.* (1972), which contain a weak energy dependence. The most serious problem with these approaches is the neglect of the actual energy dependence of the cross section, which is important for any discussion of the energy variation of the cosmic-ray data (Garcia-Munoz, Simpson, and Wefel 1980; Guzik *et al.* 1980).

The energy dependence of proton-nucleus total inelastic cross sections arises naturally as a result of the energy dependence in the individual nucleon-nucleon cross sections. Interest in the study of total and total inelastic or reaction cross sections has been renewed in the past few years by the increasing amount of nucleus-nucleus cross section data emerging from heavy-ion accelerator experiments. A number of recent analyses using Glauber theory and/or the optical model have been successful in reproducing the shape of proton-nucleus and nucleus-nucleus cross section results over limited energy intervals. Karol (1975) used a semiclassical

optical model approach involving averaged nucleon-nucleon cross sections and nuclear density distributions obtained from electron scattering experiments. He was able to reproduce the shape of nucleon-nucleus or nucleus-nucleus total reaction cross sections for kinetic energies above 300 MeV per nucleon, but the absolute value of the calculated cross sections was larger than the experimental value (Heckman *et al.* 1978). Similar calculations have been reported by Ray (1979), Ernst (1979), DeVries and Peng (1979), and Schwaller *et al.* (1979). However, Karol (1975) provided a useful scaling formula which allows the total reaction cross section at any energy to be determined from a known cross section measured at a particular energy.

The failure of Karol's (1975) method below ~ 300 MeV per nucleon can be traced to his semiclassical approach which neglected much of the physics of the interaction process. Such an approach is justified at high energy but rapidly breaks down at lower energies. Wilson and Townsend (1981) investigated nuclear scattering in a complete optical model using representations for all two-body scatterings. The results give a reasonable fit to the data at high energies but could not be extrapolated to lower energies. DeVries and Peng (1980; see also Peng, DeVries, and DiGiacomo 1982) analyzed low-energy nucleus-nucleus data and concluded that there was "no evidence for an energy independent, geometric total reaction cross section." For nucleus-nucleus total reaction cross sections, the most complete calculations are those of DiGiacomo, DeVries, and Peng (1980), who incorporated the effects of (1) the Coulomb and real nuclear potentials in determining the trajectory of the incident nucleon through the target nucleus, (2) the Fermi momentum of the nucleons in the nucleus, and (3) the Pauli exclusion principle in the nucleon-nucleon scattering. This complex computer calculation was able to reproduce the energy dependence of the nucleon-nucleus total reaction cross section between ~ 30 and ~ 300 MeV per nucleon.

For cosmic-ray propagation studies of the energy dependence of the propagation process, it is necessary to include the real energy dependence in the total inelastic cross sections. For the higher energies we have adopted the energy scaling formula of Karol (1975) scaled from equation (4) of Kirkby and Link (1966) evaluated at 145 MeV per nucleon. The latter equation gives a good representation to the detailed set of total reaction cross section data at ~ 100 MeV per nucleon. A small correction factor was incorporated for the light elements, since the use of equation (4) led to an underestimate of the cross sections for Li and Be (see discussion by Kirkby and Link 1966). The (p, p) and (p, n) total cross sections needed in the Karol (1975) formula were compiled from numerous sources (Amaldi and Schubert 1980; Giacomelli and Jacob 1979; Carroll *et al.* 1976; Galbraith *et al.* 1965; Bellettini *et al.* 1965; Foley *et al.* 1967; Schwaller *et al.* 1979; Giacomelli 1969, 1974; Ashmore *et al.* 1960; Amaldi *et al.* 1977; Kloet *et al.* 1977; Denisov *et al.* 1971; Hansen *et al.* 1970; Particle Data Group 1980) covering the laboratory energy range 1 MeV to 2 TeV and were fitted to smooth curves. For higher energies the energy-dependent extrapolations given by Giacomelli and Jacob (1979) were employed.

For low energies it was not possible to reproduce the detailed calculations of DiGiacomo, DeVries, and Peng (1980). Instead, an empirical correction term was applied which reduced the calculated cross section as a function of energy ($\propto E^{0.11}$) for energies below about 300 MeV per nucleon. This empirical term, representing a compromise between an exact formulation and calculational simplicity, gives a good representation of the data down to about 50 MeV per nucleon, which is sufficiently low for data described in this paper.

In order to compare the calculated cross sections with experimental data, values of proton-nucleus and neutron-nucleus total reaction, total inelastic, total absorption, and mass-changing cross sections were compiled from the literature. These are shown in Figure 16 for the target elements beryllium, carbon, aluminum, and iron, for which the most comprehensive set of measurements has been found. Additional data for oxygen, ^{40}Ca, nickel, and copper show a form similar to that for the elements in Figure 16. The solid curves show the result of our total inelastic cross section calculations, as described above, and are in good agreement with the collected experimental data down to about 40 MeV per nucleon. Note that neutron-nucleus data in Figure 16 are represented as squares with different shadings, and all other symbols refer to proton-nucleus results. One point to mention with respect to Figure 16 is the scatter in some of the experimental measurements and the large uncertainty limits on many of the points. Clearly, further high-precision measurements are needed to establish these curves firmly.

The data points in Figure 16 are derived principally from measurements of total reaction cross sections. For the cosmic-ray problem, the relevant parameter is the total mass–changing cross section. The difference, if any, is in the cross section for "inelastic but intact" interactions in which the target does not lose a nucleon. One measure of the importance of such effects can be obtained by comparing the mass-changing cross sections measured with a heavy-ion beam (Brautigam *et al.* 1981; Jaros *et al.* 1978; Heckman *et al.* 1978; Westfall *et al.* 1979*b*; Lindstrom *et al.* 1975*b*) with total reaction cross sections measured at similar energies. Such a comparison is possible only at 1–2 GeV per nucleon and shows that the two types of cross sections are in good agreement, with the maximum effect being $\sim 5\%$ at iron. At lower energies there have been several calculations of this "quasi-elastic" cross section (Acquardo *et al.* 1981; Frahn 1978) which imply that it is $\leq 10\%$ of the total reaction cross section at energies of 50–100 MeV per nucleon. Thus, total reaction cross section data represent a good approximation to the total mass–changing cross section for cosmic-ray propagation studies.

A semiempirical equation designed to fit proton-nucleus total reaction cross section data has been presented recently by Letaw, Silberberg, and Tsao (1983). Their equations reproduce the energy variation observed for these cross sections to a precision comparable to the results reported here, but do not involve the use of nucleon-nucleon cross section data.

For cosmic-ray interactions with interstellar helium we use the same formalism described above except that the cross sections are scaled from the fit given by Westfall *et al.* (1979*b*) evaluated at 1 GeV per nucleon. This gives calculated cross sections in agreement with the measurements of Jaros *et al.* (1978) and between the measurements of Millburn *et al.* (1954) and Abdrahmanov *et al.* (1980). There are few experimental data available for helium-nucleus total reaction cross sections, and a more complete comparison between calculations and theory will require more experimental measurements.

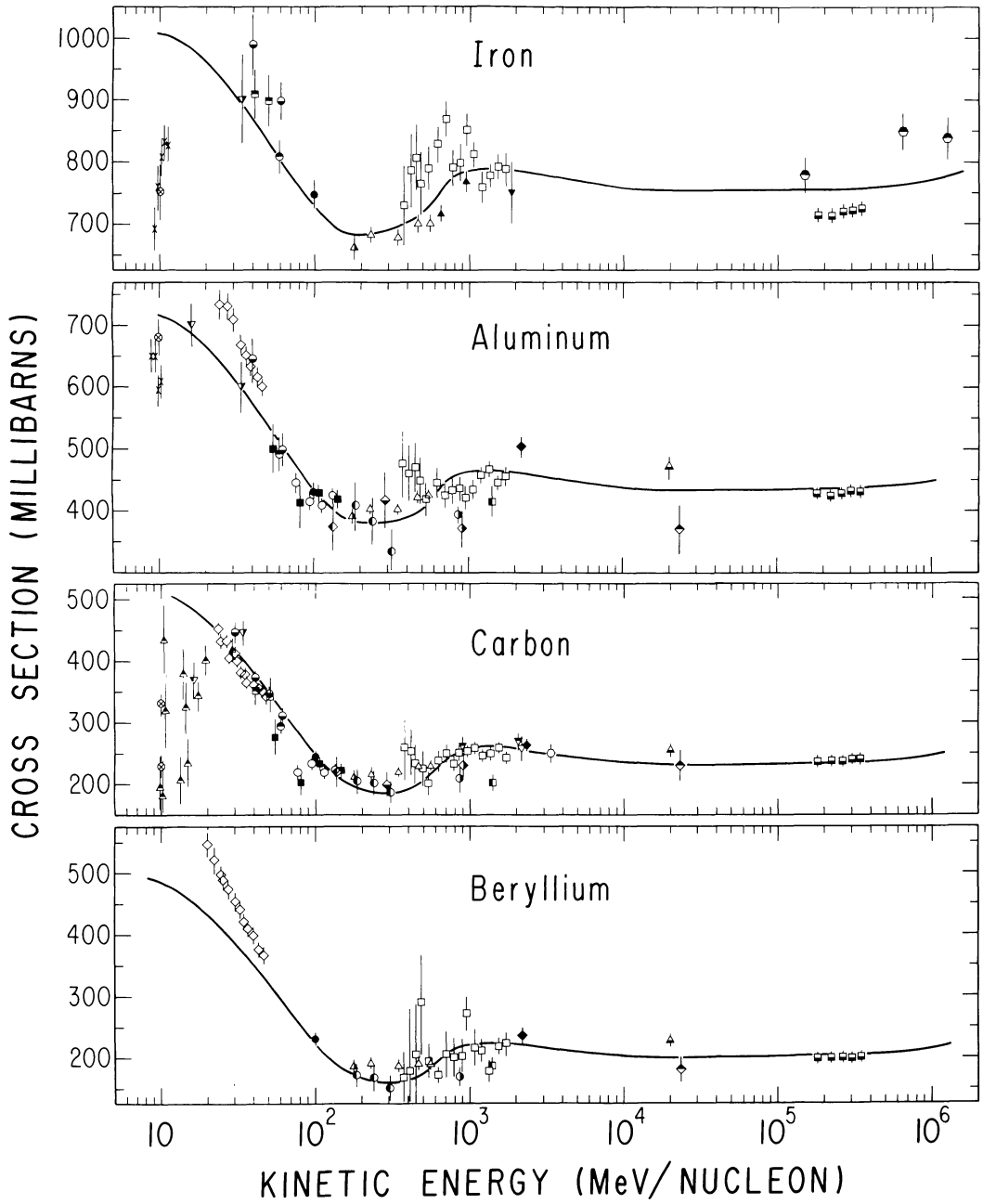

FIG. 16.—Total inelastic (reaction) cross sections for proton- and neutron-induced reactions compared with the predictions of the formula described in the text for Be, C, Al, and Fe. Data points for protons are as follows:

- ⊗ Wilkins and Igo (1963)
- ◐ Kirschbaum (1953)
- ◑ Chen, Leavitt, and Shapiro (1955)
- ◆ Longo and Moyer (1962)
- △ Renberg *et al.* (1972)
- ▲ Bellettini *et al.* (1966)
- ● Kirkby and Link (1966)
- ▲ Johansson, Svanberg, and Sundberg (1961)
- ◇ McGill *et al.* (1974)
- ◆ Ashmore *et al.* (1960)
- ▲ Makino, Waddell, and Eisberg (1964)
- ▼ Gooding (1959)
- ○ Goloskie and Strauch (1962)
- ▼ Pollock and Schrank (1965)
- ◆ Millburn *et al.* (1954)
- ◆ Booth *et al.* (1957)
- ▽ Heckman *et al.* (1978)
- ◆ Cassels and Lawson (1954)
- ◒ Menet *et al.* (1971)
- ▽ Jaros *et al.* (1978)
- ⬡ Abdrahmanov *et al.* (1980)
- x Bearpark, Graham, and Jones (1965)
- ▼ Westfall *et al.* (1979*b*)
- ▲ Brautigam *et al.* (1981)
- ◓ Macfall *et al.* (1979)

For neutrons, data points are as follows:

- ◒ Roberts *et al.* (1979)
- ◧ Coor *et al.* (1955)
- □ Schimmerling *et al.* (1973)
- ◒ Zanelli *et al.* (1981)
- ■ Voss and Wilson (1956)
- ▲ Dicello and Igo (1970)
- ◓ Menet *et al.* (1969)

Considering the individual measurements in Figure 16 and the calculated curve, the proton total inelastic cross sections calculated by our formalism appear to be accurate to $\leq 10\%$ over the energy region of interest. For the He-nucleus cross sections the uncertainty is larger, being at least 20%–30%. Fortunately, helium is a relatively minor constituent of the interstellar medium, so that the uncertainty in the helium-nucleus total inelastic cross sections has only a minor effect on the result of the propagation calculations.

IV. PARTIAL PRODUCTION CROSS SECTIONS

For each isotopic species included in the propagation calculation, it is necessary to determine the production cross section for the species in question (plus all of its progenitors; see Appendix § II) from nuclear interactions of all heavier species. Unfortunately, such a set of cross sections has not been measured experimentally. However, the regularities in the known cross sections can be combined with nuclear structure considerations to predict values for unmeasured cross sections (Rudstam 1955). Silberberg and Tsao (1973*b*, 1977*a*, *b*, *c*; Tsao and Silberberg 1979) have developed a set of semiempirical formulae which permit the calculation of $\sigma_{i,j}$ for proton-nucleus interactions for energies above about 100 MeV per nucleon and for all isotopes up to the actinide region. Below nickel, the predictions of these formulae have been checked extensively against the emerging body of experimental cross section results—and the formulae modified where necessary—and against Monte Carlo calculations of the nuclear interaction process. The agreement with experimental data, generally, is found to be within about 20%–30% for products near the valley of β stability and not far removed in mass from the target nucleus, and 30% (to a factor of 2–3) for other products. Fortunately, for the production of secondary species in the cosmic-ray problem, it is the former cross sections which make the most important contribution.

The semiempirical equations are an evolving technique for calculating cross sections, changing as new experimental data become available. The particular code used to calculate the cross sections for this investigation was extensively cross-checked with the current calculations of Silberberg and Tsao and with the results of other workers in this area. Agreement for all of the major cross sections to $\leq 2\%$ and for the minor cross sections to ± 1 millibarn was obtained, giving confidence that the present results are in accord with the current, "best" semiempirical estimates.

The semiempirical formulae provide an indispensable tool for propagation studies, but the primary reliance for cross sections should be on the experimentally measured values. For a number of years we have been compiling experimental cross section data and using this, wherever possible, in place of the semiempirical calculations (see, for example, Garcia-Munoz *et al.* 1979). In this approach, a complete matrix of cross section values (a separate matrix for each point in the cross section energy grid) is first calculated using the semiempirical formulae. A file of experimental cross section values, as a function of energy, is then read, and these values are substituted for the semiempirical values in the matrices. This gives a cross section file consisting of both experimentally measured and semiempirically calculated partial cross section results. As new measurements become available, they are compared with the existing body of data/calculations, and new or modified entries made, if appropriate, in the experimental cross section file. In this manner, the partial cross section file for use in the propagation calculations can be kept current with both the changing semiempirical formulae and the evolving experimental data set.

The results discussed in this paper use the light elements (e.g., B, C) and the sub-Fe elements (e.g., Sc, V) in secondary-to-primary ratios (B/C, Sc/Fe, V/Fe) as tracers of the propagation process. For boron isotope production, interactions of carbon and oxygen are the most important sources. Figure 3 shows the collected experimental data for the production of ^{10}B and ^{11}B (plus their progenitors) in proton-carbon interactions. The excitation functions given by the semiempirical equations are shown as the solid lines, and the dashed curves give the "experimental" excitation functions adopted for these calculations. For the production of ^{11}B, there is only a small difference between the calculated and the adopted excitation functions, but for ^{10}B the two curves give very different results below about 500 MeV per nucleon. At very low energies (<100 MeV per nucleon) the experimental data determine the shape of the excitation function quite well. Figure 17 shows the equivalent situation for proton-oxygen interactions. Here there is a smaller amount of experimental data, and the semiempirical relations give a reasonably good fit to the data at high energy. At low energy the dashed curves are employed. The difficulty with the data of Figure 17 is the large error bars on the measurements, which would allow the excitation function to be drawn about 20% higher or lower than shown. The situation in Figure 16 is somewhat better, owing to the larger number of experimental measurements, but there is still a residual uncertainty of $\sim 15\%$. More precise experimental measurements, especially below 1 GeV per nucleon, are much needed.

The most widely studied element, from the point of view of cross section measurements, is beryllium, because of the interest in using radioactive ^{10}Be as a cosmic-ray chronometer and because ^{7}Be, decaying in the laboratory by electron capture (see Fig. 14), forms a spallation product relatively easy to measure and use as a reaction normalization standard. A large portion of the experimental cross section data for the beryllium isotopes is due to the Orsay group, summarized by Raisbeck and Yiou (1975*b*). In addition, data are available for targets of ^{10,11}B (Radin, Gradsztajn, and Smith 1979), ^{12,13}C (Lindstrom *et al.* 1975*a*; Fontes 1975; Roche *et al.* 1976; Davids, Laumer, and Austin 1970; Westfall *et al.* 1978; Radin, Gradsztajn, and Smith 1979; Williams and Fullmer 1967; Oberg *et al.* 1975; see also data compilation by Silberberg and Tsao 1973*a*), ^{14}N (Laumer *et al.* 1973; Jacobs *et al.* 1974; Radin, Gradsztajn, and Smith 1979; Raisbeck and Yiou 1974), ^{16}O (Raisbeck and Yiou 1975*a* and corrections 1977; Albouy *et al.* 1962; Valentin *et al.* 1963; Lindstrom *et al.* 1975*a*; Moyle *et al.* 1979; Heydegger *et al.* 1976; Silberberg and Tsao 1973*a*), ^{27}Al, ^{24}Mg, and ^{28}Si (Heydegger *et al.* 1976; Westfall *et al.* 1978; Raisbeck and Yiou 1974, 1977; Silberberg and Tsao 1973*a*), and, finally, iron and nickel (see compilation by Silberberg and Tsao 1973*a*). The analysis of these collected data has led to experimental excitation functions often differing from the curves predicted by the semiempirical formulae. Table 3 gives our

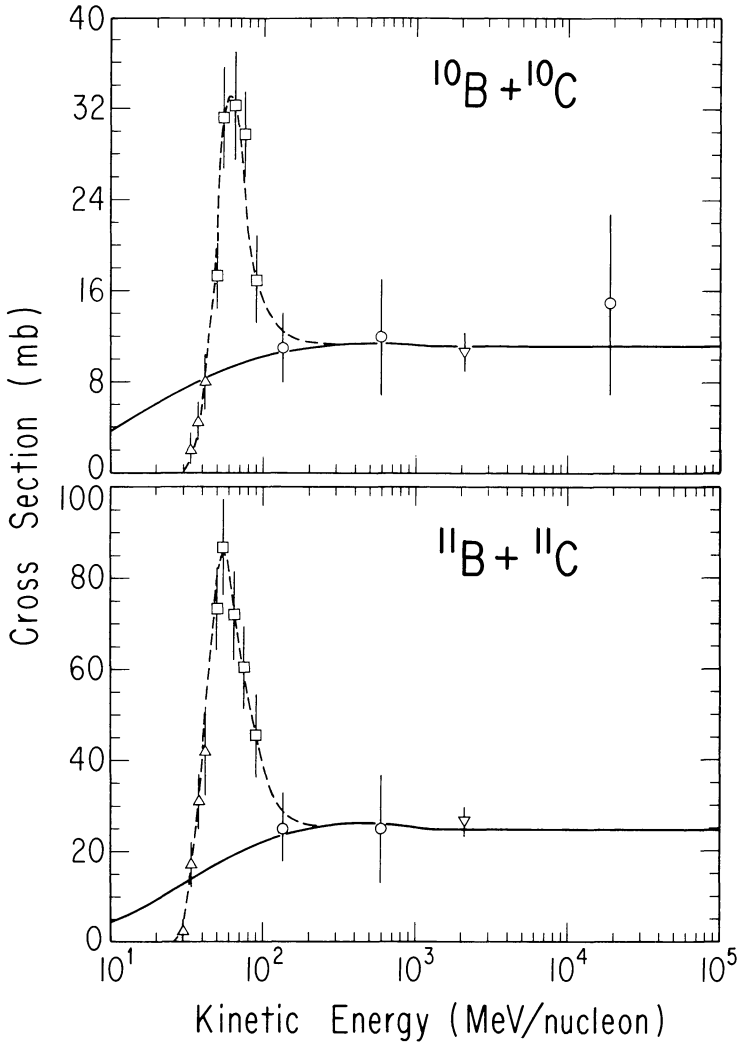

FIG. 17.—Partial production cross section for the isotopes of boron (plus progenitors) from $p + ^{16}O$ interactions. Data points are from the following: *circles*, Raisbeck and Yiou (1975*b*); *inverted triangles*, Lindstrom *et al.* (1975*a*); *triangles*, Laumer, Austin, and Panggabean (1974); *squares*, Moyle *et al.* (1979). The solid curve is the result of the semiempirical calculations (Silberberg and Tsao 1973*b*), and the dashed curve shows the excitation function adopted in this paper.

"experimental" values of the partial production cross sections for the beryllium isotopes from the important targets of the CNO group. Additional information for other targets is available.

Although the cross sections for beryllium are more completely measured than for boron, both the quantity and the quality of the cosmic-ray beryllium data are far inferior to the boron measurements (cf. Figs. 2*a* and 8*b*). Therefore, the analysis in this paper is based mainly on the B/C ratio, with the Be/C data used as a test of the results.

For the study of the shape of the path-length distribution, in particular the contribution of short path lengths (Garcia-Munoz *et al.* 1981*b*), it is necessary to employ a secondary-to-primary ratio in the vicinity of iron. Ideal for this purpose are the ratios Sc/Fe and V/Fe, since both Sc and V are essentially secondary nuclei and their isotopes are largely unaffected by long-lived radioactive species. Figure 18 shows the available experimental data for the production of the isotopes of vanadium in proton-iron interactions, and Figure 19 gives similar data for the production of ^{45}Sc. For ^{49}V production the data show considerable scatter, giving an overall uncertainty of about 30%, and the semiempirical formulae give a good representation of the data points. For $^{50,51}V$ the semiempirical curve appears high above 1 GeV per nucleon and is replaced with the dashed curve. Below 600 MeV per nucleon there are no experimental data, and the semiempirical curves must be employed. A similar situation exists for ^{45}Sc, the only stable isotope of scandium, and the dashed curve is employed at high energy.

Plots similar to Figures 18 and 19 have been generated for the isotopes of manganese, chromium, and titanium, and the results are used in the computation of the sub-Fe/Fe ratio. This latter ratio is not a true secondary-to-primary ratio, since Mn, Cr, and Ti may have nonnegligible source components.

The foregoing discussion has dealt only with proton-nucleus interactions, but in passing through the interstellar medium the cosmic rays encounter both hydrogen and helium. Cross sections for helium-nucleus interactions are calculated in a manner

TABLE 3

EXPERIMENTAL PARTIAL CROSS SECTIONS (millibarns) FOR THE PRODUCTION OF THE Be ISOTOPES

ENERGY (MeV per nucleon)	$^{12}C + p \rightarrow$			$^{14}N + p \rightarrow$	$^{16}O + p \rightarrow$		
	^{7}Be	^{9}Be	^{10}Be	^{7}Be	^{7}Be	^{9}Be	^{10}Be
50	20.90	2.15	0.43	5.30	13.40	3.40	2.27
60	18.80	2.40	0.53	4.60	14.00	9.70	2.08
70	16.90	2.70	0.64	4.20	13.50	8.80	1.94
80	15.20	2.90	0.72	4.05	12.30	7.00	1.85
90	14.20	3.05	0.82	4.15	10.70	6.10	1.80
100	13.30	3.20	0.90	4.35	9.10	5.10	1.76
150	10.50	3.70	1.30	6.30	5.90	3.75	1.67
200	10.00	4.05	1.62	7.30	6.00	3.81	1.66
300	10.23	4.48	2.12	8.37	6.75	4.19	1.68
400	10.45	4.75	2.45	8.83	7.60	4.37	1.78
500	10.60	5.00	2.70	9.15	8.30	4.45	1.82
600	10.70	5.15	2.85	9.30	8.85	4.45	1.85
700	10.65	5.30	2.94	9.43	9.20	4.45	1.87
800	10.60	5.40	3.05	9.50	9.40	4.45	1.89
900	10.60	5.45	3.15	9.55	9.53	4.45	1.90
1000	10.50	5.50	3.20	9.60	9.65	4.45	1.90
1500	10.00	5.70	3.32	9.70	9.70	4.45	1.92
2000	9.80	5.80	3.35	9.70	9.70	4.45	1.92
3000	9.60	5.85	3.35	9.70	9.70	4.45	1.92
4000	9.45	5.90	3.35	9.70	9.70	4.45	1.92
5000	9.30	5.90	3.35	9.70	9.70	4.45	1.92
10000	9.10	5.90	3.35	9.70	9.70	4.45	1.92

similar to the proton case using semiempirical relations developed to allow scaling from proton-induced to alpha particle–induced cross section values (Silberberg and Tsao 1977*d*). Experimental data for helium-nucleus cross sections are relatively rare except for the work of the Orsay group (Raisbeck and Yiou 1975*a*, *b*, 1977; Fontes 1975; Yiou, Raisbeck, and Quechon 1977; Raisbeck *et al.* 1979). The remaining experimental measurements are concentrated at low kinetic energies, < 50 MeV per nucleon (Jung *et al.* 1969; Baixeras-Aiguabella *et al.* 1970; Fulmer and Goldberg 1975; Rudy *et al.* 1972; Jacobs *et al.* 1974; Glascock *et al.* 1979; Hornyak *et al.* 1979), and determine the low-energy end of the excitation curve. The helium-nucleus experimental data were compiled, and experimental excitation curves were determined where possible. Finally, the hydrogen and helium cross sections were combined to obtain the cross sections per atom of interstellar medium, which are the cross sections actually employed in the propagation calculations.

The importance of the fusion of two alpha particles to the production of cosmic-ray ^{7}Li, ^{7}Be, and ^{6}Li has long been disputed. The cross sections from early work (Reeves, Fowler, and Hoyle 1970; Meneguzzi, Audouze, and Reeves 1971; Mitler 1972; Kozlovsky and Ramaty 1974) were based upon the principle of detailed balance, applied at energies below about 20 MeV per nucleon, and upon theoretical extrapolations for higher energies. These analyses concluded that ^{7}Li and ^{7}Be, being mirror nuclei, should have the same cross section, and the ^{6}Li cross section should be below the ^{7}Li value until all cross sections reach a constant value of ~ 1 millibarn above about 400 MeV per nucleon. More recent work (Glagola *et al.* 1978) has shown that, at least for the interval 20–40 MeV per nucleon, ^{7}Li and ^{7}Be do indeed have identical cross sections. Measurements of $^{4}He + {}^{4}He \rightarrow {}^{7}Be$ by Yiou, Raisbeck, and Quechon (1977) at 100–250 MeV per nucleon gave a constant value of only 0.01 millibarns. We adopt an excitation function for both mass 7 isotopes having a constant value of 0.01 millibarns above 200 MeV per nucleon and rising smoothly to pass through the Glagola *et al.* (1978) results. At low energies, Glagola *et al.* (1978) show that the ^{6}Li cross section is larger than the ^{7}Li value, contrary to the early assumptions. No high-energy measurements are available, and there are arguments both for $^{6}Li > {}^{7}Li$ (Montmerle 1977) and for $^{6}Li < {}^{7}Li$ (Yiou, Raisbeck, and Quechon 1977). Therefore, we assume that at high energies the excitation functions for ^{6}Li and ^{7}Li production in alpha-alpha interactions are the same.

V. ELECTRON CAPTURE AND LOSS

Isotopes that decay by electron capture present a unique set of problems. These are nearly all secondary isotopes produced by the spallation of other species. At cosmic-ray energies the parent nuclei are completely stripped of electrons, and the daughter isotopes are formed with no orbital electrons attached. Thus, electron capture decay is forbidden unless the nucleus can capture an electron from the interstellar medium. If such an electron is captured, then decay can proceed following the cosmic-ray half-lives given in Table 2, which lists all of the electron capture isotopes important in the propagation of cosmic rays below nickel.

In order to treat these electron capture species effectively, each long-lived isotope was included twice in the code, first as a fully stripped nucleus and again as a nucleus with one electron attached (e.g., ^{7}Be and $^{7}Be^{*}$, the latter having an attached electron). Both the normal and the electron-attached states are assigned the same total inelastic cross section and the same β^{+} or β^{-} decay

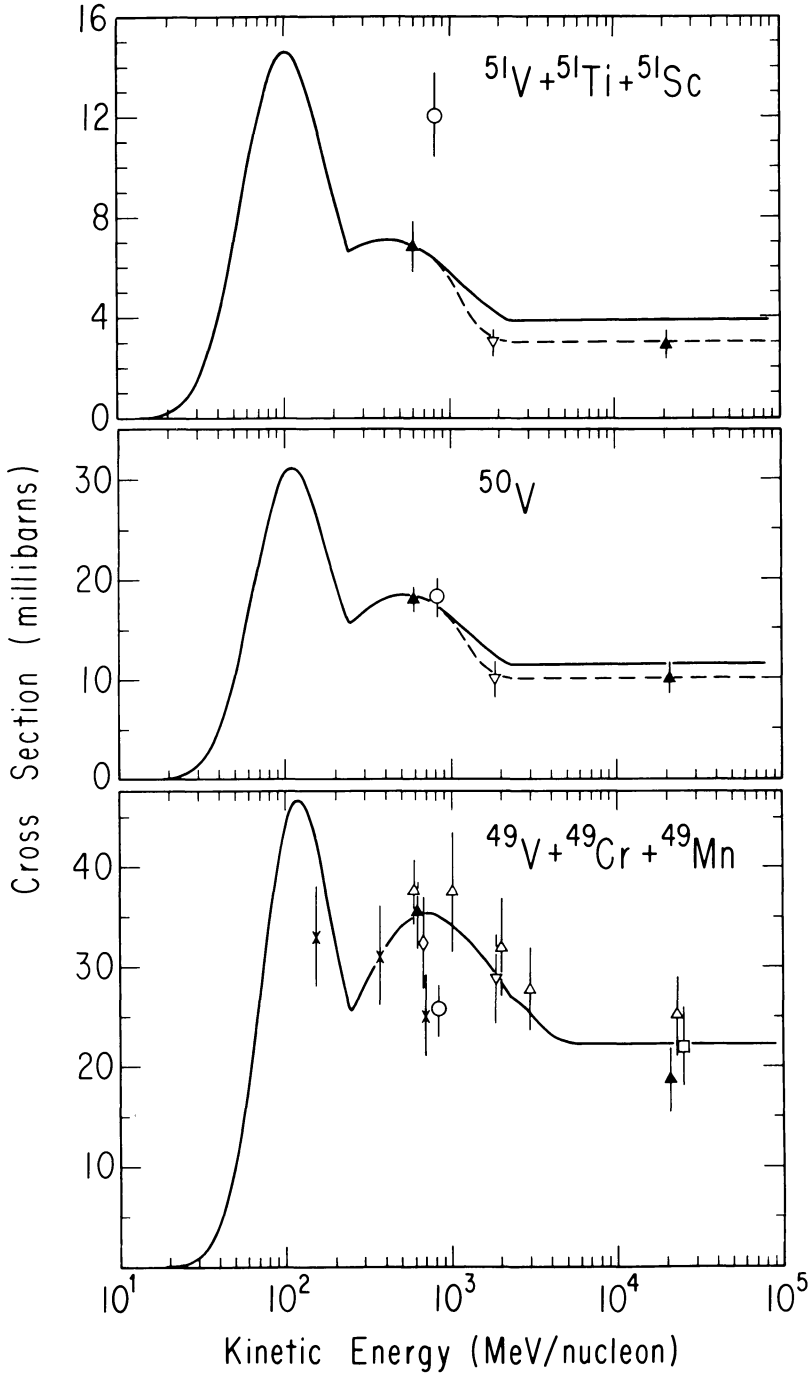

FIG. 18.—Partial production cross section for the isotopes of vanadium (plus progenitors) from $p + ^{56}Fe$ interactions. The solid curve is the prediction of the semiempirical calculations (Silberberg and Tsao 1973*b*), and the dashed curve gives the excitation function adopted in this paper. Data points are from the following: *filled triangles*, Perron (1976); *open triangles*, Raisbeck *et al.* (1979); *open squares*, Estrup (1963); *inverted filled triangles*, Westfall *et al.* (1979*b*); *open circles*, Brautigam *et al.* (1981); *open diamonds*, Lavrukhina *et al.* (1963); *crosses*, compilation by Silberberg and Tsao (1973*a*).

lifetime (if applicable). However, production by spallation of heavier species goes only to the normal state. The electron-attached state is produced when a nucleus of the normal isotope captures an electron from the interstellar medium. The electron-attached state species has the additional possibility of decaying via electron capture decay. If the half-life of the electron-attached state against electron capture decay is much less than the propagation time through a typical step Δx in path length, and the probability of electron stripping is negligible for the step, then essentially all of these atoms in the electron-attached state decay immediately upon formation. For these particular isotopes it is not necessary to propagate the electron-attached state separately (see note 2 to Table 2), but rather the cross section for capturing an electron by the normal state is treated as an additional radioactive decay for the normal isotope.

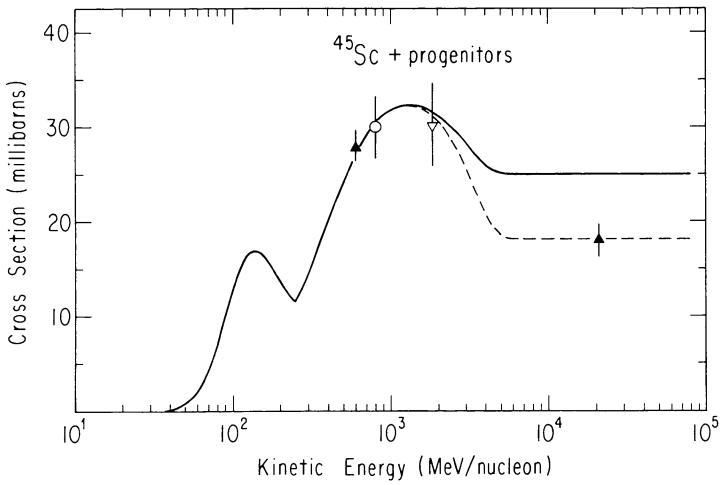

FIG. 19.—Partial production cross section for the isotope ^{45}Sc (plus progenitors) from $p + ^{56}$Fe interactions. Curves and data points are as described in Fig. 18.

The cross sections for capture and stripping of electrons by nuclei have been measured in detail only at very low energies. Recently, however, some data have become available at higher energies (Raisbeck and Yiou 1971) and for heavy-ion beams (Crawford 1979; Raisbeck *et al.* 1977). The theoretical formalism for describing the capture and loss of electrons was developed for low-velocity ions (Bohr 1948; Oppenheimer 1928; Brinkman and Kramers 1930), and the application of these formulae at higher energies in the cosmic-ray problem requires some modifications to the formalism (see reviews by Raisbeck 1974; Pratt, Ron, and Tseng 1973). In addition, comparison with the recent experimental measurements has confirmed many of the modifications.

The electron capture cross section is composed of two parts, radiative and nonradiative electron capture. The nonradiative case is treated in the Oppenheimer-Brinkman-Kramers (OBK) approximation, suitably extrapolated to high energies (Wilson 1977, 1978; Crawford 1979) and including corrections for capture into excited states and for electron screening in the atoms of the propagation medium. The resulting formalism is in reasonably good agreement with the experimental data.

In many applications, radiative capture is more important than the nonradiative process (low-Z ions at low energy), and radiative capture can be treated accurately by detailed balance from the inverse photoionization process (Raisbeck and Yiou 1971). The high-energy photoionization cross section has been discussed by Pratt, Ron, and Tseng (1973), who suggest modifications to the simple first-order Born approximation calculation. These modifications have been described by Wilson (1978) and have been shown by Crawford (1979) to give a good fit to the recent experimental data.

The largest change in the formalism was needed for the stripping (electron loss) cross section originally calculated by Bohr (1948). This cross section is important, since, after the capture of an electron, it is the stripping cross section which controls return to the normal state. The Bohr formalism was found consistently to underestimate this cross section compared with experiment. The deficiency can be remedied by including the effects of distant collisions (Fowler *et al.* 1970; Wilson 1978), which brings the calculated cross sections into agreement with the data (see discussion in Crawford 1979).

For the calculations performed here, we have adopted the formulations presented by Wilson (1978) and Crawford (1979) after comparison with the analysis of Pratt, Ron, and Tseng (1973). Our formulae reproduce the calculations of Crawford (1979) and Raisbeck and Yiou (1971) to better than 0.3%.

VI. IONIZATION ENERGY LOSS

The energy loss of charged particles by ionization during traversal of the interstellar medium is an extremely important effect, especially at lower energies. This energy loss usually acts as an additional particle loss term, since, for a negative-power-law cosmic-ray energy spectrum, fewer particles arrive from higher energies than depart for lower energies. The effect of energy loss on secondary-to-primary ratios is most easily seen in the "leaky box" formalism (Gloeckler and Jokipii 1969), considering one secondary and one primary particle. In this case the secondary-to-primary ratio, S/P, is given by

$$\frac{\mathrm{S}}{\mathrm{P}} = \frac{\sigma_{ij}}{\bar{A}/\lambda_e N_0 + \sigma_j}, \tag{A3}$$

where N_0 is Avogadro's number, $\bar{A}$ is the mean atomic weight of an atom of the interstellar medium, σ_{ij} is the partial production cross section for the secondary from the primary, σ_j is the total inelastic cross section of the secondary, and λ_e is the mean escape length. Equation (A3) is for the case of no energy loss, and inclusion of ionization results in the addition of another term, σ', to

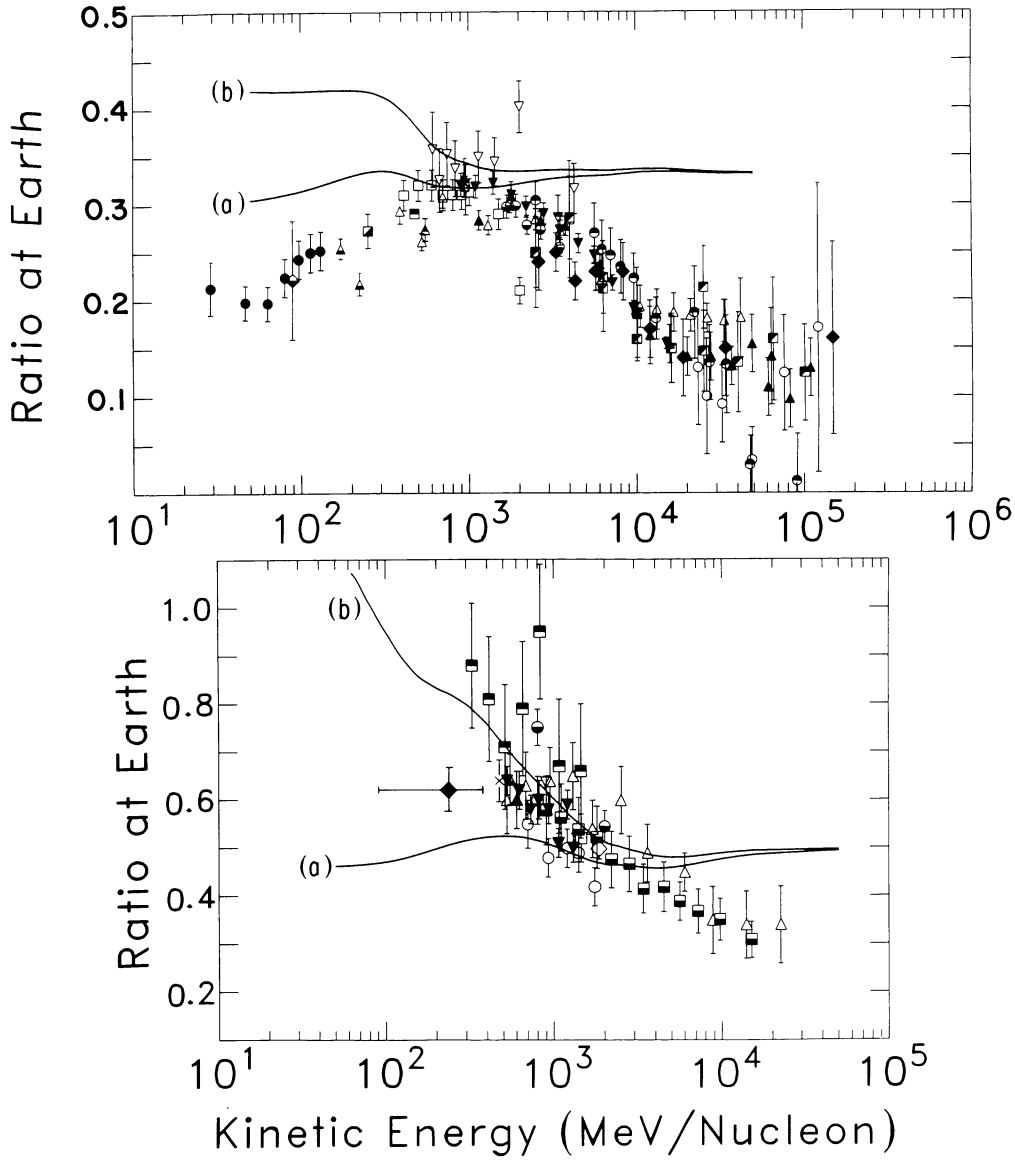

FIG. 20.—B/C (*top*) and sub-Fe/Fe (*bottom*) ratios as a function of energy. Data points are as described in Fig. 2. Curves *a* show the result of calculations with energy loss compared with curves *b* for which no energy loss was included. An exponential PLD with a constant value of $X_0 = 9.25$ g cm^{-2} was assumed, and the results include solar modulation at a level of $\phi = 490$ MV.

the denominator of the equation. The net effect is to reduce the size of the calculated secondary-to-primary ratio. Since σ' scales as Z^2 while σ_j is approximately proportional to $A^{2/3}$, and λ_e is effectively constant with particle species, the relative effect of the energy loss increases for heavier, higher charge isotopes.

Figure 20 shows the results of two separate runs of the code, (*a*) with ionization energy loss and (*b*) without energy loss. The differences, especially at low energy, are striking, with the sub-Fe/Fe ratio showing a larger effect than the B/C ratio. The curves in Figure 20 are for an energy-independent exponential path length distribution with a constant mean $X_0 = 9.25$ g cm^{-2}, and include solar modulation, which reduces the size of the effect at low energies. At high energy, about 1 GeV per nucleon, the energy loss still has an effect, $\sim 3\%$ for B/C and $\sim 10\%$ in the sub-Fe/Fe ratio.

To calculate the energy loss, the proton stopping power tables of Barkas and Berger (1967) for hydrogen and helium were employed, along with the effective-charge formulation of Pierce and Blann (1968). For energies greater than those given in the table (~ 5 GeV), the analytic formula of Ahlen (1978) was used, incorporating the density-effect correction of Sternheimer and Peierls (1971). The calculations were checked against the measurements and calculations of Cobb, Allison, and Bunch (1976) and were found to give a good fit to the data reported by Allison *et al.* (1976). It is expected that, at very high energies, the present formulation should give ionization energy loss values accurate to $< 15\%$.

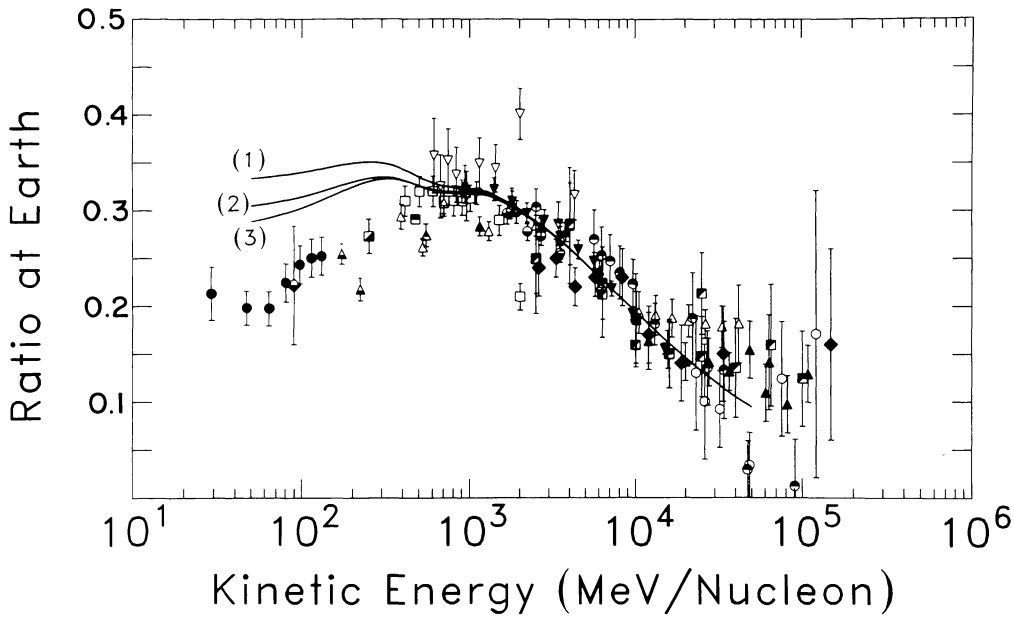

FIG. 21.—B/C ratio as a function of energy. Data points are as in Fig. 2. The curves show results for an exponential PLD with a mean that is constant below 1 GeV per nucleon and falls as $E^{-0.6}$ for energies above 1 GeV per nucleon. Solar modulation for $\phi = 490$ MV is included. For a source energy spectrum of the form $(T + T_0)^{-\gamma}$, curves 1 and 2 give results for $T_0 = 931$ MeV per nucleon, $\gamma = 2.3$, and for $T_0 = 400$ MeV per nucleon, $\gamma = 2.6$, respectively. Curve 3 gives the results for a power-law source spectrum in rigidity with index 2.6.

VII. THE INTERSTELLAR MEDIUM

For these calculations we assume an interstellar medium composed of hydrogen and helium with 6.9% helium by number, giving an atomic weight for the average atom of $A = 1.197$. Following Garcia-Munoz, Mason, and Simpson (1977*a*; see also Wiedenbeck and Greiner 1980; Garcia-Munoz, Simpson, and Wefel 1981) and their analysis of propagation for the radioactive isotope ^{10}Be, we assume a uniform density for the interstellar medium of 0.2 atoms cm^{-3}. This may imply a confinement region involving a Galactic halo (Parker 1976) or a cloud-intercloud medium (McKee and Ostriker 1977), but such interpretations have no effect on the results of these calculations. We do assume, however, that the propagation medium is composed of cold gas of uniform average density. The consequences of relaxing this assumption will be discussed elsewhere.

VIII. THE COSMIC-RAY SOURCE

The calculations require initial conditions at the cosmic-ray source consisting of relative source abundances and a source energy spectrum. Both of these are assumed to be representative of a "typical" cosmic-ray source, and no differences from source to source in composition or energy spectrum are considered.

For the source composition we use the "average" source abundances determined by Dwyer *et al.* (1981; see also summary by Mewaldt 1981; Simpson 1983) from a consideration of both high- and low-energy data and a selection of different propagation models. These abundances are in agreement ($\pm 20\%$) with the abundances determined by other groups from other data sets. For the B/C ratio, the most important source abundance ratio is O/C, for which there is little variation allowed by the experimental data. Of less importance is the ^{14}N/O ratio and the ratio of oxygen to the major primary elements, Ne, Mg, Si, S, Ar, Ca, and Fe. Small changes in these source ratios give a negligible change in the calculated B/C ratio. For the sub-Fe/Fe ratio and the Sc/Fe and V/Fe elemental ratios, the important source abundances are the Mn/Fe, Cr/Fe, and Ti/Fe ratios. We have used two values for these ratios, either zero, which assumes the sub-Fe elements to be purely secondary species, or solar system abundances relative to iron (Cameron 1981). In the latter case, the first ionization potentials of Mn, Cr, and Ti are almost identical with the ionization potential of iron, so that there should be little differential enhancement for these elements (Casse and Goret 1978). The exact values of the Mn/Fe, Cr/Fe, and Ti/Fe source ratios make an important difference in the calculated sub-Fe/Fe ratio, as described in the text, but have only a small effect on the calculated Sc/Fe and V/Fe ratio, since these latter ratios are, more nearly, pure secondary-to-primary ratios.

The cosmic-ray energy spectrum at the source is a more controversial parameter. Many analyses (see, for example, Protheroe, Ormes, and Comstock 1981) assume a power law in total energy per nucleon, while other groups use a power law in rigidity (e.g., Engelmann *et al.* 1981) or a more general form. We have adopted the form $(T + T_0)^{-\gamma}$ for the source energy spectrum, with T the kinetic energy per nucleon and T_0 and γ constants which can be changed for different calculations. Garcia-Munoz, Mason, and Simpson (1977*b*) have shown that values of $T_0 = 400$ MeV per nucleon and $\gamma = 2.6$ give a good fit, after propagation and solar modulation, to the measured proton and helium spectra below 1 GeV per nucleon. This form of the spectrum is intermediate between a rigidity and a total energy spectrum, and has been adopted for the analysis reported here.

Figure 21 shows a comparison of calculations using the different source spectra. For these calculations the PLD varied with energy as $E^{-0.6}$ above 1 GeV per nucleon, but had a constant value of $x_0 = 9.25$ g cm^{-2} below ~ 1 GeV per nucleon. Solar modulation was included in the calculations. Curve 3 shows the results of a rigidity spectrum with $\gamma = 2.6$; curve 2 shows our standard case for $T_0 = 400$ MeV per nucleon, $\gamma = 2.6$; and curve 1 shows results for $T_0 = 931$ MeV per nucleon (total energy spectrum) with $\gamma = 2.3$. The rigidity spectrum (curve 3) at 100 MeV per nucleon gives results about 5% below the spectrum (curve 2) used in this paper, and the total energy spectrum is about 10% higher. The largest effect in going from curve 2 to curve 1 is in changing the value of T_0, not the value of γ. The available evidence on the overall shape of the cosmic-ray spectrum argues against a spectrum in total energy and favors a rigidity spectrum or something in between. In any case, the conclusion to be drawn from Figure 21 is that the exact choice of the parameters to use in the source energy spectrum makes only a small difference in the calculated B/C ratio and does not change conclusions on the shape of the PLD. The uncertainty introduced by the exact choice of the source spectrum is smaller than the other errors in the problem (i.e., the cross section uncertainties), as discussed in the text.

REFERENCES

Abdrahmanov, E. O. *et al.* 1980, *Zs. Phys.*, *C*, **5**, 1.
Acquardo, J. C., Hussein, M. S., Pereira, D., and Sala, O. 1981, *Phys. Letters B*, **100**, 381.
Ahlen, S. P. 1978, *Phys. Rev. A*, **17**, 1236.
Ajzenberg-Selove, F. 1977, *Nucl. Phys. A*, **281**, 1.
_____. 1978, *Nucl. Phys. A*, **300**, 1.
_____. 1979, *Nucl. Phys. A*, **320**, 1.
_____. 1980, *Nucl. Phys. A*, **336**, 1.
_____. 1981, *Nucl. Phys. A*, **360**, 1.
Albouy, M. G., Cohen, J. P., Gusakow, M., Poffe, M. N., Sergolle, H., and Valentin, L. 1962, *Phys. Letters*, **2**, 306.
Alburger, D. E., Millener, D. J., and Wilkinson, D. H. 1981, *Phys. Rev. C*, **23**, 473.
Allison, W. W. M., Brooks, C. B., Bunch, J. N., Pleming, R. W., and Yamamoto, R. K. 1976, *Nucl. Instr. Meth.*, **133**, 325.
Amaldi, U., *et al.* 1977, *Phys. Letters B*, **66**, 390.
Amaldi, U., and Schubert, K. R. 1980, *Nucl. Phys. B*, **166**, 301.
Artukh, A. G., Avdeichikov, V. V., Chelnokov, L. P., Gridnev, G. F., Mikheev, V. L., Vakatov, V. I., Volkov, V. V., and Wilczynski, J. 1970*a*, *Phys. Letters B*, **32**, 43.
Artukh, A. G., Avdeichikov, V. V., Gridnev, G. F., Mikheev, V. L., Volkov, V. V., and Wilczynski, J. 1970*b*, *Phys. Letters B*, **31**, 129.
_____. 1971, *Nucl. Phys. A*, **176**, 284.
Artukh, A. G., Gridnev, G. F., Mikheev, V. L., and Volkov, V. V. 1969, *Nucl. Phys. A*, **137**, 348.
Ashmore, A., Cocconi, G., Diddens, A. N., and Wetherell, A. M. 1960, *Phys. Rev. Letters*, **5**, 576.
Auger, P., *et al.* 1979, *Zs. Phys.*, *A*, **289**, 255.
Axford, W. I. 1981, in *IAU Symposium 94, Origin of Cosmic Rays*, ed. G. Setti, G. Spada, and A. W. Wolfendale (Dordrecht: Reidel), p. 339.
Axford, W. I., Leer, E., and Skadron, G. 1977, *Proc. 15th Internat. Cosmic Ray Conf.* (Plovdiv), **11**, 132.
Aysto, J., Cable, M. D., Parry, R. F., Wouters, J. M., Moltz, D. M., and Cerny, J. 1981, *Phys. Rev. C*, **23**, 879.
Baixeras-Aiguabella, C., Jung, M., Jacquot, C., Girardin, L., and Schmitt, R. 1970, *Phys. Rev. C*, **2**, 1194.
Balasubrahmanyan, V. K., Boldt, E., and Palmeira, R. A. R. 1965, *Phys. Rev. B*, **140**, 1157.
Barkas, W. H., and Berger, M. J. 1967, in *Penetration of Charged Particles in Matter* (NAS–NRC Pub., No. 1133), p. 103.
Bearpark, K., Graham, W. R., and Jones, G. 1965, *Nucl. Phys.*, **73**, 206.
Bell, A. R. 1978, *M.N.R.A.S.*, **182**, 147.
Bellettini, G., Cocconi, G., Diddens, A. N., Lillethun, E., Matthiae, G., Scanlon, J. P., and Wetherell, A. M. 1966, *Nucl. Phys.*, **79**, 609.
Bellettini, G., *et al.* 1965, *Phys. Letters*, **14**, 164.
Benegas, J. C., Israel, M. H., Klarmann, J., and Maehl, R. C. 1975, *Proc. 14th Internat. Cosmic Ray Conf.* (Munich), **1**, 251.
Benenson, W., Kashy, E., Ledebuhr, A. G., Pardo, R. C., Robertson, R. G. H., and Robinson, L. W. 1978, *Phys. Rev. C*, **17**, 1939.
Binns, W. R., Fixsen, D. J., Garrard, T. L., Israel, M. H., Klarmann, J., Stone, E. C., and Waddington, C. J. 1984 *Adv. Space Res.*, **4** (Nos. 2–3), 25.
Binns, W. R. Israel, M. H., Klarmann, J., Scarlett, W. R., Stone, E. C., and Waddington, C. J. 1981, *Nucl. Instr. Meth.*, **185**, 415.
Blake, J. B., Hainebach, K. L., Schramm, D. N., and Anglin, J. D. 1978, *Ap. J.*, **221**, 694.
Blandford, R. D., and Ostriker, J. P. 1978, *Ap. J. (Letters)*, **221**, L29.
_____. 1980, *Ap. J.*, **237**, 793.
Bogatin, V. I., Ganza, E. A., Lozhkin, O. V., Murin, Yu. A., and Oplavin, V. S. 1980, *Soviet J. Nucl. Phys.*, **32**, 14 (*Yad. Fiz.*, **32**, 27).
Bohr, N. 1948, *Kgl. Danske Videnskab. Selskab, Mat.-Fys. Medd.*, Vol. **18**, No. 8.
Booth, N. E., Ledley, B., Walker, D., and White, D. H. 1957, *Proc. Phys. Soc. London*, **A**, **70**, 209.
Bradt, H. L., and Peters, B. 1948, *Phys. Rev.*, **74**, 1828.
Bradt, H. L., and Peters, B. 1950, *Phys. Rev.*, **77**, 54.
Brautigam, D. A., Chappell, J. H., Kish, J. C., Simpson, G. A., and Webber, W. R. 1981, *Proc. 17th Internat. Cosmic Ray Conf.* (Paris), **2**, 177.
Bretthorst, G. L., and Margolis, S. H. 1985, *Proc. 19th Internat. Cosmic Ray Conf.* (La Jolla), **3**, 58.
Brinkman, H. C., and Kramers, H. A. 1930, *Proc. Acad. Sci. Amsterdam*, **33**, 973.
Buffington, A., Orth, C. D., and Mast, J. S. 1978, *Ap. J.*, **226**, 355.
Butler, G. W., Perry, D. G., Remsberg, L. P., Poskanzer, A. M., Natowitz, J. B., and Plasil, F. 1977, *Phys. Rev. Letters*, **38**, 1380.
Caldwell, J. H., and Meyer, P. 1977, *Proc. 15th Internat. Cosmic Ray Conf. (Plovdiv)*, **1**, 243.
Cameron, A. G. W. 1981, in *Essays in Nuclear Astrophysics*, ed. C. A. Barnes, D. D. Clayton, and D. N. Schramm (Cambridge: Cambridge University Press), p. 23.
Carroll, A. S., *et al.* 1976, *Phys. Letters B*, **61**, 303.
Casse, M. 1973*a*, *Ap. J.*, **180**, 623.
_____. 1973*b*, *Proc. 13th Internat. Cosmic Ray Conf.* (Denver), **1**, 546.
Casse, M., and Goret, P. 1978, *Ap. J.*, **221**, 703.
Cassels, J. M., and Lawson, J. D. 1954, *Proc. Phys. Soc. London*, *A*, **67**, 125.
Cesarsky, C. J. 1980, *Ann. Rev. Astr. Ap.*, **18**, 289.
Chappell, J. H. and Webber, W. R. 1981, *Proc. 17th Internat. Cosmic Ray Conf.* (Paris), **2**, 59.
Chen, F. F., Leavitt, P., and Shapiro, A. M. 1955, *Phys. Rev.*, **99**, 857.
Cobb, J. H., Allison, W. W. M., and Bunch, J. N. 1976, *Nucl. Instr. Meth.*, **133**, 315.
Comstock, G. M. 1969, *Ap. J.*, **155**, 619.
Comstock, G. M., Fan, C. Y., and Simpson, J. A. 1966, *Ap. J.*, **146**, 51.
Coor, T., Hill, D. A., Hornyak, W. F., Smith, L. W., and Snow, G. 1955, *Phys. Rev.*, **98**, 1369.
Cowsik, R. 1980, *Ap. J.*, **241**, 1195.
Cowsik, R., Pal, Y., Tandon, S. N., and Verma, R. P. 1967, *Phys. Rev.*, **158**, 1238.
_____. 1968, *Canadian J. Phys.*, **46**, S646.
Cowsik, R., and Wilson, L. W. 1973, *Proc. 13th Internat. Conf. Cosmic Rays* (Denver), **1**, 500.
_____. 1975, *Proc. 14th Internat. Cosmic Ray Conf.* (Munich), **2**, 659.
Crawford, H. J. 1979, Ph.D. thesis, University of California, Berkeley (Rept. LBL-8807, unpublished).
Daniel, R. R., and Durgaprasad, N. 1962, *Nuovo Cimento* (Suppl.), **23**, 82.
Davids, C. N., Laumer, H., and Austin, S. M. 1970, *Phys. Rev. C*, **1**, 270.
Davis, L. 1960, *Proc. 6th Internat. Cosmic Ray Conf.* (Moscow), **3**, 220.
Denisov, S. P., *et al.* 1971, *Phys. Letters B*, **36**, 528.
Detrax, C., *et al.* 1979, *Phys. Rev. C*, **19**, 164.
DeVries, R. M., and Peng, J. C. 1979, *Phys. Rev. Letters*, **43**, 1373.
_____. 1980, *Phys. Rev. C*, **22**, 1055.
Dicello, J. F., and Igo, G. 1970, *Phys. Rev. C*, **2**, 488.
DiGiacomo, N. J., DeVries, R. M., and Peng, J. C. 1980, *Phys. Rev. Letters*, **45**, 527.
Dwyer, R. 1978, *Ap. J.*, **224**, 691.
Dwyer, R. D., Garcia-Munoz, M., Guzik, T. G., Meyer, P., Simpson, J. A., and Wefel, J. P. 1981, *Proc. 17th Internat. Cosmic Ray Conf.* (Paris), **9**, 222.
Dwyer, R., and Meyer, P. 1981, *Proc. 17th Internat. Cosmic Ray Conf.* (Paris), **2**, 54.
Eichler, D. 1980, *Ap. J.*, **237**, 809.
Endt, P. M., and van der Leun, C. 1978, *Nucl. Phys. A*, **310**, 1.
Engelmann, J. J., *et al.* 1981, *Proc. 17th Internat. Cosmic Ray Conf.* (Paris), **9**, 97.
Ernst, D. J. 1979, *Phys. Rev. C*, **19**, 896.
Eskola, K., Riihonen, M., Vierinen, K., Honkanen, J., Kortelahti, M., and Valli, K. 1980, *Nucl. Phys. A*, **341**, 365.

Estrup, P. J. 1963, *Geochim. Cosmochim. Acta*, **27**, 891.
Evenson, P., Garcia-Munoz, M., Meyer, P., Pyle, K. R., and Simpson, J. A. 1983, *Ap. J. (Letters)*, **275**, L15.
Ewan, G. T., Hagberg, E., Hardy, J. C., Jonson, B., Matteson, S., Tidemand-Petersson, P., and Towner, I. S. 1980, *Nucl. Phys A*, **343**, 109.
Fan, C. Y., Gloeckler, G., and Simpson, J. A. 1965, *Proc. 9th Internat. Cosmic Ray Conf.* (London), **1**, 109.
_____. 1966, *Phys. Rev. Letters*, **17**, 329.
Fan, C. Y., Meyer, P., and Simpson, J. A. 1960, *Phys. Rev. Letters*, **5**, 272.
Ferrando, P., Goret, P., and Soutoul, A. 1985, *Proc. 19th Internat. Cosmic Ray Conf.* (La Jolla), **3**, 61.
Fichtel, C. E., and Reames, D. V. 1968, *Phys. Rev.*, **175**, 1564.
Fintz, P., Guillaume, G., Jundt, F., Ordonez, I., Gallmann, A., and Alburger, D. E. 1976, *Nucl. Phys. A*, **259**, 493.
Fisher, A. J., Hagen, F. A., Maehl, R. C., Ormes, J. F., and Arens, J. F. 1976, *Ap. J.*, **205**, 938.
Fisk, L. A. 1971, *J. Geophys. Res.*, **76**, 221.
_____. 1979, in *Solar System Plasma Physics*, Vol. **1**, ed. E. N. Parker, C. F. Kennel, and L. J. Lanzerotti (Amsterdam: North-Holland), p. 179.
Foley, K. J., Jones, R. S., Lindenbaum, S. J., Love, W. A., Ozaki, S., Platner, E. D., Quarles, C. A., and Willen, E. H. 1967, *Phys. Rev. Letters*, **19**, 857.
Fontes, P. 1975, Ph.D. thesis, University of Paris.
_____. 1977, *Phys. Rev. C*, **15**, 2159.
Fowler, P. H., Clapham, V. M., Cowan, V. G., Kidd, J. M., and Moses, R. T. 1970, *Proc. Roy. Soc. London*, *A*, **318**, 1.
Fowler, P. H., Mashedek, M. R. W., Moses, R. T., Walker, R. N. F., Worley, A., and Gay, A. M. 1985*a*, *Proc. 19th Internat. Cosmic Ray Conf.* (La Jolla), **2**, 115.
_____. 1985*b*, *Proc. 19th Internat. Cosmic Ray Conf.* (La Jolla), **2**, 119.
Frahn, W. E. 1978, *Nucl. Phys. A*, **302**, 301.
Fransson, C., and Epstein, R. I. 1980, *Ap. J.*, **242**, 411.
Freedman, I., Giler, M., Kearsey, S., and Osborne, J. L. 1980, *Ast. Ap.*, **82**, 110.
Freedman, S. J., Gagliardi, C. A., Oothoudt, M. A., Nero, A. V., Robertson, R. G. H., Zutavern, F. J., Adelberger, E. G., and McDonald, A. B. 1978, *Phys. Rev. C*, **17**, 2071.
Freier, P. S. 1981, *Proc. 17th Internat. Cosmic Ray Conf.* (Paris), **2**, 182.
Freier, P. S., Lofgren, E. J., Oppenheimer, F., Bradt, H. L., and Peters, B. 1948, *Phys. Rev.*, **74**, 213.
Fulmer, C. B., and Goldberg, D. A. 1975, *Phys. Rev. C*, **11**, 50.
Galbraith, W., Jenkins, E. W., Kycia, T. F., Leontic, B. A., Phillips, R. H., Read, A. L., and Rubinstein, R. 1965, *Phys. Rev. B*, **138**, 913.
Garcia-Munoz, M., Guzik, T. G., Margolis, S. H., Simpson, J. A., and Wefel, J. P. 1981*a*, *Proc. 17th Internat. Cosmic Ray Conf.* (Paris), **9**, 195.
Garcia-Munoz, M., Guzik, T. G., Simpson, J. A., and Wefel, J. P. 1981*b*, *Proc. 17th Internat. Cosmic Ray Conf.* (Paris), **2**, 192.
_____. 1983, *Proc. 18th Internat. Cosmic Ray Conf.* (Bangalore), **2**, 210.
_____. 1984, *Ap. J. (Letters)*, **280**, L13.
Garcia-Munoz, M., Juliusson, E., Mason, G. M., Meyer, P., and Simpson, J. A. 1975, *Ap. J.*, **197**, 489.
Garcia-Munoz, M., Margolis, S. H., Simpson, J. A., and Wefel, J. P. 1979, *Proc. 16th Internat. Cosmic Ray Conf. (Kyoto)*, **1**, 310.
Garcia-Munoz, M., Mason, G. M., and Simpson, J. A. 1977*a*, *Ap. J.*, **217**, 859.
_____. 1977*b*, *Proc. 15th Internat. Cosmic Ray Conf.* (Plovdiv), **1**, 301.
Garcia-Munoz, M., Meyer, P., Pyle, K. R., Simpson, J. A., and Evenson, P. A. 1986, *J. Geophys. Res.*, **81**, 2858.
Garcia-Munoz, M., and Simpson, J. A. 1970, *Acta. Phys. Acad. Sci. Hungaricae*, **29**, Suppl. 1, 325.
_____. 1979, *Proc. 16th Internat. Cosmic Ray Conf.* (Kyoto), **1**, 270.
Garcia-Munoz, M., Simpson, J. A., and Wefel, J. P. 1980, in *Proc. Conf. on Cosmic Ray Astrophysics and Low-Energy Gamma Ray Astronomy* (University of Minnesota, unpublished).
_____. 1981, *Proc. 17th Internat. Cosmic Ray Conf.* (Paris), **2**, 72.
Giacomelli, G. 1969, CERN Rept. CERN-HERA 69-3 unpublished.
_____. 1974, *Phys. Rept.*, **23**, 1.
Giacomelli, G., and Jacob, M. 1979, *Phys. Rept.*, **55**, 1.
Ginzburg, V. L., and Syrovatskii, S. I. 1964, *The Origin of Cosmic Rays*, trans. H. S. W. Massey, ed. D. ter Haar (New York: Macmillan), p. 426.
Glagola, B. G., Mathews, G. J., Breuer, H. F., Viola, V. E., Roos, P. G., Nadasen, A., and Austin, S. M. 1978, *Phys. Rev. Letters*, **41**, 1698.
Glascock, M. D., Hornyak, W. F., Chang, C. C. and Quickle, R. J. 1979, *Phys. Rev. C*, **19**, 1577.
Gleeson, L. J., and Axford, W. I. 1968, *Ap. J.*, **154**, 1011.
Gloeckler, G., and Jokipii, J. R. 1969, *Phys. Rev. Letters*, **22**, 1448.
Goloskie, R., and Strauch, K. 1962, *Nucl. Phys.*, **29**, 474.
Gooding, T. J. 1959, *Nucl. Phys.*, **12**, 241.
Gove, N. B., and Martin, M. J. 1971, *Atomic Data Nucl. Data Tables*, **10**, 206.
Gronemeyer, S. A., Meyer-Schutzmeister, L., Elwyn, A. J., and Hardie, G. 1980, *Phys. Rev. C*, **21**, 1290.
Guzik, T. G., Margolis, S. H., Garcia-Munoz, M., Simpson, J. A., and Wefel, J. P. 1980, in *Proc. Conf. on Cosmic Ray Astrophysics and Low-Energy Gamma Ray Astronomy* (University of Minnesota, unpublished).
Hagen, F. A. 1976, Ph.D. thesis, University of Maryland.
Hagen, F. A., Fisher, A. J., and Ormes, J. F. 1977, *Ap. J.*, **212**, 262.
Hansen, J. D., Morrison, D. R. O., Tovey, N., and Flaminio, E. 1970, CERN Rept. CERN-HERA 70-2, unpublished.
Hardy, J. C., *et al.* 1980, *Phys. Letters B*, **91**, 207.
Hayakawa, S., Ito, K., and Terashima, Y. 1958, *Progr. Theoret. Phys. Suppl.*, **6**, 1.
Heckman, H. H., Greiner, D. E., Lindstrom, P. J., and Bieser, F. S. 1972, *Phys. Rev. Letters*, **28**, 926.
Heckman, H. H., Greiner, D. E., Lindstrom, P. J., and Shwe, H. 1978, *Phys. Rev. C*, **17**, 1735.
Heydegger, H. R., Turkevich, A. L., Van Ginneken, A., and Walpole, P. H. 1976, *Phys. Rev. C*, **14**, 1506.
Holmes, J. A. 1974, *M.N.R.A.S.*, **166**, 155.
Hornyak, W. F., Glascock, M. D., Chang, C. C. and Wu, J. R. 1979, *Phys. Rev. C*, **19**, 1595.
Hsieh, K. C. 1970, *Ap. J.*, **159**, 61.
Ipavich, F. M. 1975, *Ap. J.*, **196**, 107.
Israel, M. H., Klarmann, J., Love, P. L., and Tueller, J. 1979, *Proc. 16th Internat. Cosmic Ray Conf.* (Kyoto), **1**, 323.
Jacobs, W. W., Bodansky, D., Chamberlin, D., and Oberg, D. L. 1974, *Phys. Rev. C*, **9**, 2134.
Jaros, J., *et al.* 1978, *Phys. Rev. C*, **18**, 2273.
Johansson, A., Svanberg, U., and Sundberg, O. 1961, *Ark. Fys.*, **19**, 527.
Johnson, H. E., and Axford, W. I. 1971, *Ap. J.*, **165**, 381.
Jokipii, J. R. 1971, *Rev. Geophys. Space Phys.*, **9**, 27.
_____. 1976, *Ap. J.*, **208**, 900.
Jokipii, J. R., and Higdon, J. C. 1979, *Ap. J.*, **228**, 293.
Jones, F. C. 1979*a*, *Proc. 16th Internat. Cosmic Ray Conf.* (Kyoto), **2**, 173.
_____. 1979*b*, *Ap. J.*, **229**, 747.
Juliusson, E. 1974, *Ap. J.*, **191**, 331.
Juliusson, E., Meyer, P., and Muller, D. 1972, *Phys. Rev. Letters*, **29**, 445.
Julliot, C., Koch, L., and Petrou, N. 1975, *Proc. 14th Internat. Cosmic Ray Conf.* (Munich), **12**, 4118.
Jung, M., Jacquot, C., Baixeras-Aiguabella, C., Schmitt, R., Braun, H., and Girardin, L. 1969, *Phys. Rev.*, **188**, 1517.
Karol, P. J. 1975, *Phys. Rev. C*, **11**, 1203.
Kekelis, G. J., Zisman, M. S., Scott, D. K., Jahn, R., Vieira, D. J., Cerny, J., and Ajzenberg-Selove, F. 1978, *Phys. Rev. C*, **17**, 1929.
Kirkby, P., and Link, W. T. 1966, *Canadian J. Phys.*, **44**, 1847.
Kirschbaum, A. J. 1953, Ph.D. thesis, University of California (Rept. UCRL-1967, unpublished).
Klarmann, J., Margolis, S. H., Stone, E. C., Waddington, C. J., Binns, W. R., Garrard, T. L., Israel, M. H., and Kertzman, M. P. 1985, *Proc. 19th Internat. Cosmic Ray Conf.* (La Jolla), **2**, 127.
Kloet, W. M., Silbar, R. R., Aaron, R., and Amado, R. D. 1977, *Phys. Rev. Letters*, **39**, 1643.
Koch, L., *et al.* 1981*a*, *Astr. Ap. Letters*, **102**, L9.
Koch, L., Perron, C., Goret, P., Cesarsky, C. J., Juliusson, E., Soutoul, A., and Rasmussen, I. L. 1981*b*, *Proc. 17th Internat. Cosmic Ray Conf.* (Paris), **2**, 18.
Kota, J., and Owens, A. J. 1980, *Ap. J.*, **237**, 814.
Kozlovsky, B., and Ramaty, R. 1974, *Astr. Ap.*, **34**, 477.
Lau, K. H., Mewaldt, R. A., and Stone, E. C. 1985, *Proc. 19th Internat. Cosmic Ray Conf.* (La Jolla), **3**, 91.
Laumer, H., Austin, S. M., and Panggabean, L. M. 1974, *Phys. Rev. C*, **10**, 1045.
Laumer, H., Austin, S. M., Panggabean, L. M., and Davids, C. N. 1973, *Phys. Rev. C*, **8**, 483.
Lavrukhina, A. K., Revina, L. D., Malyshev, V. V., and Satarova, L. M. 1963, *Soviet Phys.—JETP*, **17**, 960.
Lederer, C. M., and Shirley, V. S., eds. 1978, *Table of Isotopes* (7th ed.; New York: Wiley), p. 200.
Lerche, I., and Schlickeiser, R. 1985, *Astr. Ap.*, **151**, 408.
Letaw, J. R., Silberberg, R., and Tsao, C. H. 1983, *Ap. J. Suppl.*, **51**, 271.
_____. 1984, *Ap. J. Suppl.*, **56**, 369.
_____. 1985, *Proc. 19th Internat. Cosmic Ray Conf.* (La Jolla), **3**, 42.
Lezniak, J. A. 1979, *Ap. Space Sci.*, **63**, 279.
Lezniak, J. A., and Webber, W. R. 1978*a*, *Ap. J.*, **223**, 676.
_____. 1978*b*, *Ap. Space Sci.*, **63**, 1.
Lindstrom, P. J. Greiner, D. E., Heckman, H. H., and Cork, B. 1975*a*, Rept. LBL-3650, unpublished.

Lindstrom, P. J., Greiner, D. E., Heckman, H. H., Cork, B., and Bieser, F. S. 1975*b*, *Proc. 14th Internat. Cosmic Ray Conf.* (Munich), **7**, 2315.
Longo, M. J., and Moyer, B. J. 1962, *Phys. Rev.*, **125**, 701.
Lund, N., Rasmussen, I. L., Peters, B., and Westergaard, N. J. 1975, *Proc. 14th Internat. Cosmic Ray Conf.* (Munich), **1**, 257.
Macfall, J. R., Ellsworth, R. W., Ito, A. S., Siohan, F., Streitmatter, R. E., Tonwar, S. C., Viswanath, P. R., and Yodh, G. B. 1979, *Nucl. Phys. B*, **151**, 213.
Maehl, R. C., Ormes, J. F., Fisher, A. J., and Hagen, F. A. 1977, *Ap. Space Sci.*, **47**, 163.
Makino, M. Q., Waddell, C. N., and Eisberg, R. M. 1964, *Nucl. Phys.*, **50**, 145.
Margolis, S. H. 1986, *Ap. J.*, **300**, 20.
McGill, W. F., *et al.* 1974, *Phys. Rev. C*, **10**, 2237.
McKee, C. F., and Ostriker, J. P. 1977, *Ap. J.*, **218**, 148.
Meneguzzi, M., Audouze, J., and Reeves, H. 1971, *Astr. Ap.*, **15**, 337.
Menet, J. J. H., Gross, E. E., Malanify, J. J., and Zucker, A. 1969, *Phys. Rev. Letters*, **22**, 1128.
_____. 1971, *Phys. Rev. C*, **4**, 1114.
Mewaldt, R. A. 1981, *Proc. 17th Internat. Cosmic Ray Conf.* (Paris), **13**, 49.
_____. 1983, *Rev. Geophys. Space Phys.* **21**, 295.
Mewaldt, R. A., Spalding, J. D., Stone, E. C., and Vogt, R. E. 1981, *Ap. J. (Letters)*, **251**, L27.
Millburn, G. P., Birnbaum, W., Crandall, W. E., and Schecter, L. 1954, *Phys. Rev.* **95**, 1268.
Mitler, H. E. 1972, *Ap. Space Sci.*, **17**, 186.
Montmerle, T. 1977, *Ap. J*, **216**, 177.
Morfill, G., Meyer, P., and Lust, R. 1985, *Proc. 19th Internat. Cosmic Ray Conf.* (La Jolla), **3**, 50.
Moyle, R. A., Glagola, B. G., Mathews, G. J., and Viola, V. E., Jr. 1979, *Phys Rev. C*, **19**, 631.
Norman, E. B., Davids, C. N., and Moss, C. E. 1978, *Phys. Rev. C*, **18**, 102.
Oberg, D. L., Bodansky, D., Chamberlin, D., and Jacobs, W. W. 1975, *Phys. Rev. C*, **11**, 410.
Olive, K. A., and Schramm, D. N. 1982, *Ap. J.*, **257**, 276.
Oppenheimer, J. R. 1928, *Phys. Rev.*, **51**, 349.
Ormes, J. F. 1981, private communication.
Ormes, J. F., and Freier, P. S. 1978, *Ap. J.*, **222**, 471.
Ormes, J. F., and Protheroe, R. J. 1983, *Ap. J.*, **272**, 756.
Orth, C. D., Buffington, A., Smoot, G. F., and Mast, T. 1978, *Ap. J.*, **226**, 1147.
Parker, E. N. 1965, *Planet. Space Sci.*, **13**, 9.
_____. 1969, *Space Sci. Rev.*, **9**, 651.
_____. 1976, in *The Structure and Content of the Galaxy and Galactic Gamma Rays* (NASA/GSFC Rept., No. X-662-76-154), p. 320.
Particle Data Group. 1980, Rev. Mod. Phys., **52**, 1.
Peng, J. C., DeVries, R. M., and DiGiacomo, N. J. 1982, *Phys. Letters B*, **98**, 244.
Perron, C. 1976, *Phys. Rev. C*, **14**, 1108.
Perron, C., *et al.* 1981, *Proc. 17th Internat. Cosmic Ray Conf.* (Paris), **9**, 118.
Perron, C., and Koch, L. 1981, *Proc. 17th Internat. Cosmic Ray Conf.* (Paris), **2**, 27.
Pierce, T. E., and Blann, M. 1968, *Phys. Rev.*, **173**, 290.
Pollock, R. E., and Schrank, G. 1965, *Phys. Rev.*, **140**, 575.
Poskanzer, A. M., Butler, G. W., Hyde, E. K., Cerny, J., Landis, D. A., and Goulding, F. S. 1968, *Phys. Letters B*, **27**, 414.
Poskanzer, A. M., Cosper, S. W., Hyde, E. K., and Cerny, J. 1966, *Phys. Rev. Letters*, **17**, 1271.
Pratt, R. H., Ron, A., and Tseng, H. K. 1973, *Rev. Mod. Phys.*, **45**, 273.
Protheroe, R. J., Ormes, J. F., and Comstock, G. M. 1981, *Ap. J.*, **247**, 362.
Radin, J. R., Gradsztajn, E., and Smith, A. R. 1979, *Phys. Rev. C*, **20**, 787.
Raisbeck, G. M. 1974, in *Second High Energy Heavy Ion Summer Study*, ed. L. S. Schroeder (Rept. LBL-3675; Berkeley: Lawrence Berkeley Laboratory), p. 333.
Raisbeck, G. M., Crawford, H. J., Lindstrom, P. J., Greiner, D. E., Bieser, F. S., and Heckman, H. H. 1977, *Proc. 15th Internat. Cosmic Ray Conf.* (Plovdiv), **2**, 67.
Raisbeck, G. M., Lestringuez, J., Salaun, S., Vlieks, A., Bourles, D., and Yiou, F. 1979, *Proc. 16th Internat. Cosmic Ray Conf.* (Kyoto), **2**, 207.
Raisbeck, G. M., and Yiou, F. 1971, *Phys. Rev. A*, **4**, 1848.
_____. 1974, *Phys. Rev. C*, **9**, 1385.
_____. 1975*a*, *Phys. Rev. C*, **12**, 915.
_____. 1975*b*, in *Spallation Nuclear Reactions and Their Applications*, ed. B. S. P. Shen and M. Merker (Dordrecht: Reidel), p. 83.
_____. 1977, *Proc. 15th Internat. Cosmic Ray Conf.* (Plovdiv), **2**, 203.
Ray, L. 1979, *Phys. Rev. C*, **20**, 1857.
Reeves, H. 1981, in *IAU Symposium 94, Origin of Cosmic Rays*, ed. G. Setti, G. Spada, and A. W. Wolfendale (Dordrecht: Reidel), p. 23.
Reeves, H., Fowler, W. A., and Hoyle, F. 1970, *Nature*, **226**, 727.
Renberg, P. U., Measday, D. F., Pepin, M., Schwaller, P., Favier, B., and Richard-Serre, C. 1972, *Nucl. Phys. A*, **183**, 81.
Richtmyer, R. D., and Morton, K. W. 1967, *Difference Methods for Initial-Value Problems* (New York: Interscience).
Roberts, T. J., Gustafson, H. R., Jones, L. W., Longo, M. J., and Whalley, M. R. 1979, *Nucl. Phys. B*, **159**, 56.
Roche, C. T., Clark, R. G., Matthews, G. J., and Viola, V. E. 1976, *Phys. Rev. C*, **14**, 410.
Roeckl, E., Dittner, P. F., Detraz, C., Klapisch, R., Thibault, C., and Rigaud, C. 1974, *Phys. Rev. C*, **10**, 1181.
Rudstam, G. 1955, *Phil. Mag.*, **46**, 344.
Rudy, C., Vandenbosch, R., Russo, P., and Braithwaite, W. J. 1972, *Nucl. Phys. A*, **188**, 430.
Scarlett, W. R., Freier, P. S., and Waddington, C. J. 1978, *Ap. Space Sci.*, **59**, 301.
Schimmerling, W., Devlin, T. J., Johnson, W. W., Vosburgh, K. G., and Mischke, R. E. 1973, *Phys. Rev. C*, **7**, 248.
Schwaller, P., Pepin, M., Favier, B., Richard-Serre, C., Measday, D. F., and Renberg, P. U. 1979, *Nucl. Phys. A*, **316**, 317.
Shapiro, M. M., and Silberberg, R. 1970, *Ann. Rev. Nucl. Sci.*, **20**, 323.
Silberberg, R., and Tsao, C. H. 1973*a*, NRL Rept. No. 7593, unpublished.
_____. 1973*b*, *Ap. J. Suppl.*, **25**, 315.
_____. 1977*a*, *Ap. J. Suppl.*, **35**, 129.
_____. 1977*b*, *Proc. 15th Internat. Cosmic Ray Conf.* (Plovdiv), **2**, 84.
_____. 1977*c*, *Ap. J. Suppl.*, **35**, 137.
_____. 1977*d*, *Proc. 15th Internat. Cosmic Ray Conf.* (Plovdiv), **2**, 89.
Silberberg, R., Tsao, C. H., Letaw, J. R., and Shapiro, M. M. 1983, *Phys. Rev. Letters*, **51**, 1217.
_____. 1985, *Proc. 19th Internat. Cosmic Ray Conf.* (La Jolla), **3**, 238.
Simon, M. 1977, *Astr. Ap.*, **61**, 833.
Simon, M., Heinrich, W., and Mathis, K. D. 1985, *Proc. 19th Internat. Cosmic Ray Conf.* (La Jolla), **3**, 230.
_____. 1986, *Ap. J.*, **300**, 32.
Simon, M., Speigelhauer, H., Schmidt, W. K. H., Siohan, F., Ormes, J. F., Balasubrahmanyan, V. K., and Arens, J. F. 1980, *Ap. J.*, **239**, 712.
Simpson, J. A. 1983, *Ann. Rev. Nucl. Particle Sci.*, **33**, 323.
Smith, L. H., Buffington, A., Smoot, G. F., Alvarez, L. W., and Wahlig, M. A. 1973, *Ap. J.*, **180**, 987.
Soutoul, A., Engelmann, J. J., Ferrando, P., Koch-Miramond, L., Masse, P., and Webber, W. R. 1985, *Proc. 19th Internat. Cosmic Ray Conf.* (La Jolla), **2**, 8.
Sternheimer, R. M., and Peierls, R. F. 1971, *Phys. Rev. B*, **3**, 3681.
Stone, E. C., and Wiedenbeck, M. E. 1979, *Ap. J.*, **231**, 606.
Symons, T. J. M., *et al.* 1979, *Phys. Rev. Letters*, **42**, 40.
Thomas, T. D., Raisbeck, G. M., Boestling, P., Garvey, G. T., and Lynch, R. P. 1968, *Phys. Letters B*, **27**, 504.
Tsao, C. H., and Silberberg, R. 1979, *Proc. 16th Internat. Cosmic Ray Conf.* (Kyoto), **2**, 202.
Urch, I. H., and Gleeson, L. J. 1972, *Ap. Space Sci.*, **17**, 426.
Valentin, L., Albouy, G., Cohen, J. P., and Gusakow, M. 1963, *Phys. Letters*, **7**, 163.
Vieira, D. J., Gough, R. A., and Cerny, J. 1979, *Phys. Rev. C*, **19**, 177.
Volk, H. J. 1983, *Space Sci. Rev.*, **36**, 3.
Voss, R. G. P., and Wilson, R. 1956, *Proc. Roy. Soc. London, A*, **236**, 41.
Wapstra, A. H., and Gove, A. H. 1971, *Atomic Data Nucl. Data Tables*, **10**, 205.
Webber, W. R. 1982, *Ap. J.*, **252**, 386.
_____. 1985, in *Workshop on Cosmic Ray and High Energy Gamma Ray Experiments for the Space Station Era*, ed. W. V. Jones and J. P. Wefel (Baton Rouge: Center for Continuing Education), p. 283.
Webber, W. R., Brautigam, D. A., Kish, J. C., and Schrier, D. 1983, *Proc. 18th Internat. Cosmic Ray Conf.* (Bangalore), **2**, 198.
Webber, W. R., Damle, S. V., and Kish, J. 1972, *Ap. Space Sci.*, **15**, 245.
Webber, W. R., Gupta, M., Koch-Miramond, L., and Masse, P. 1985, *Proc. 19th Internat. Cosmic Ray Conf.* (La Jolla), **3**, 42.
Webber, W. R., and Kish, J. C. 1985, *Proc. 19th Internat. Cosmic Ray Conf.* (La Jolla), **3**, 87.
Webber, W. R., Kish, J. C., and Simpson, G. A. 1979, *Proc. 16th Internat. Cosmic Ray Conf.* (Kyoto), **1**, 430.
Webber, W. R., Lezniak, J. A., Kish, J., and Simpson, G. A. 1977, *Ap. Letters*, **18**, 125.
Wefel, J. P. 1981, in *IAU Symposium 94, Origin of Cosmic Rays*, ed. G. Setti, G. Spada, and A. W. Wolfendale (Dordrecht: Reidel), p. 39.
Westergaard, N. J. 1979, *Ap. J.*, **233**, 374.
Westfall, G. D., Sextro, R. G., Poskanzer, A. M., Zebelman, A. M., Butler, G. W., and Hyde, E. K. 1978, *Phys. Rev. C*, **17**, 1368.
Westfall, G. D., *et al.* 1979*a*, *Phys. Rev. Letters*, **43**, 1859.

Westfall, G. D., Wilson, L. W., Lindstrom, P. J., Crawford, H. J., Greiner, D. E., and Heckman, H. H. 1979*b*, *Phys. Rev. C*, **19**, 1309.
Wiedenbeck, M. E. 1981, private communication.
Wiedenbeck, M. E., and Greiner, D. E. 1980, *Ap. J. (Letters)*, **239**, L139.
Wilkins, B. D., and Igo, G. 1963, *Phys. Rev.*, **129**, 2198.
Williams, I. R., and Fullmer, C. B. 1967, *Phys. Rev.*, **154**, 1005.
Wilson, J. W., and Townsend, L. W. 1981, *Canadian J. Phys.*, **59**, 1569.
Wilson, L. W. 1977, *Proc. 15th Internat. Cosmic Ray Conf.* (Plovdiv), **2**, 274.
_____. 1978, Ph.D. thesis, University of California, Berkeley (Rept. LBL-7723, unpublished).
Yiou, F., Raisbeck, G. M., and Quechon, H. 1977, *Proc. 15th Internat. Cosmic Ray Conf.* (Plovdiv), **2**, 72.
Young, J. S., Freier, P. S., Waddington, C. J., Brewster, N. R., and Fickle, R. K. 1981, *Ap. J.*, **246**, 1014.
Zanelli, C. I., Urone, P. P., Romero, J. L., Brady, F. P., Johnson, M. L., Needham, G. A., Ullman, J. L., and Johnson, D. L. 1981, *Phys. Rev. C*, **23**, 1015.

M. GARCIA-MUNOZ and J. A. SIMPSON: Laboratory for Astrophysics and Space Research, Enrico Fermi Institute, University of Chicago, 933 East 56th Street, Chicago, IL 60637

T. GREGORY GUZIK and JOHN P. WEFEL: Department of Physics and Astronomy, Louisiana State University, Baton Rouge, LA 70803-4001

STEVEN H. MARGOLIS: Mailstop M1/102, Aerospace Corporation, P.O. Box 92957, Los Angeles, CA 90009